MECHANISMS FOR PESTICIDE-INDUCED CARDIOTOXICITY IN FISH: AN ELECTROPHYSIOLOGICAL STUDY USING THE ZEBRAFISH (*Danio rerio*) AS A MODEL

A Thesis
Submitted to the Graduate Faculty
in Partial Fulfilment of the Requirements for the Degree of

MASTER OF SCIENCE

Department of Companion Animals

Faculty of Veterinary Medicine

University of Prince Edward Island

Jonathan Lichtenberger

Charlottetown, P.E.I.

March 29th, 2017

THESIS/DISSERTATION NON-EXCLUSIVE LICENSE

Family Name: Lichtenberger	Given Name, Middle Name (if applicable): Jonathan
Full Name of University: University of Prince Edward Island	
Faculty, Department, School: Companion Animals, Faculty of Veterinary Medicine	
Degree for which thesis/dissertation was presented: Master of Science	Date Degree Awarded: March 29th, 2017
Thesis/dissertation Title: MECHANISMS FOR PESTICIDE-INDUCED CARDIOTOXICITY IN FISH: AN ELECTROPHYSIOLOGICAL STUDY USING THE ZEBRAFISH (*Danio rerio*) AS A MODEL	
Date of Birth : February18th,1986 It is **optional** to supply your date of birth. If you choose to do so please note that the information will be included in the bibliographic record for your thesis/dissertation.	

In consideration of my University making my thesis/dissertation available to interested persons, I, Jonathan Lichtenberger

hereby grant a non-exclusive, for the full term of copyright protection, license to my University, The university of Prince Edward Island:

(a) to archive, preserve, produce, reproduce, publish, communicate, convert into any format, and to make available in print or online by telecommunication to the public for non-commercial purposes;
(b) to sub-license to Library and Archives Canada any of the acts mentioned in paragraph (a).

I undertake to submit my thesis/dissertation, through my University, to Library and Archives Canada. Any abstract submitted with the thesis/dissertation will be considered to form part of the thesis/dissertation.

I represent that my thesis/dissertation is my original work, does not infringe any rights of others, including privacy rights, and that I have the right to make the grant conferred by this non-exclusive license.

If third party copyrighted material was included in my thesis/dissertation for which, under the terms of the *Copyright Act*, written permission from the copyright owners is required I have obtained such permission from the copyright owners to do the acts mentioned in paragraph (a) above for the full term of copyright protection

I retain copyright ownership and moral rights in my thesis/dissertation, and may deal with the copyright in my thesis/dissertation, in any way consistent with rights granted by me to my University in this non-exclusive license.

I further promise to inform any person to whom I may hereafter assign or license my copyright in my thesis/dissertation of the rights granted by me to my University in this non-exclusive license.

Signature	**Date**

University of Prince Edward Island

Faculty of Veterinary Medicine

Charlottetown

CERTIFICATION OF THESIS WORK

We, the undersigned, certify that Dr. Jonathan Lichtenberger, candidate for the degree of Master of Science has presented his/her thesis with the following title

MECHANISMS FOR PESTICIDE-INDUCED CARDIOTOXICITY IN FISH: AN ELECTROPHYSIOLOGICAL STUDY USING THE ZEBRAFISH (*Danio rerio*) AS A MODEL

that the thesis is acceptable in form and content, and that a satisfactory knowledge of the field covered by the thesis was demonstrated by the candidate through an oral examination held on March 29th .

Examiners

Dr. Tracy Doucette (External)

Dr. Hans Gelens (Chair)

Dr. Robert Gilmour (Co-supervisor)

Dr. Shiori Arai

Dr. Don Stevens

ABSTRACT

Fish kills are a common phenomenon in Prince Edward Island (Canada) and their cause often remains unexplained. I hypothesized that fish exposure to selected environmental toxicants leads to increased mortality and morbidity by depressing cardiac function, precipitated by suppression of cardiac electrical activity and rhythm disturbances. These rhythm disturbances could result from toxicant-induced changes in the function of specific cardiac ion channels.

Recently, the zebrafish heart has been shown to hold promise as a suitable model to study cardiac cellular electrophysiology. The purpose of the present study was to evaluate the effects of selected environmental toxicants on cardiac action potential morphology. More specifically, the present work focused on evaluating the effects on atrial action potential in adult zebrafish of: 1) acetylcholine (1-10 μM); 2) a documented acetylcholinesterase inhibitor, physostigmine (50 μM); 3) pesticides with acetylcholinesterase inhibition properties that are commonly used in Prince Edward Island (mancozeb and phorate). Zebrafish hearts were isolated under anesthesia and action potentials were recorded *in vitro* using a standard single microelectrode technique. Action potential morphology was then assessed by measuring parameters including action potential duration (APD) and action potential amplitude (APA).

Results revealed that *in vitro* exposures to high concentrations of acetylcholine and physostigmine led to suppression of cardiac electrical activity by significantly reducing APD and APA, a phenomenon known as cholinergic non-excitability.

Experiments evaluating the effects of commercial pesticides (mancozeb and phorate) did not reveal similar effects.

This study supports the possibility that environmental toxicants containing acetylcholinesterase inhibitors may participate in fish kills by suppressing cardiac electrical activity. However, the specific pesticides mancozeb and phorate did not demonstrate such dramatic cardiotoxic effects, even at high concentrations.

ACKNOWLEDGEMENTS

I wish to acknowledge my supervisors, Dr. Robert Gilmour and Dr. Etienne Côté, for their unconditional encouragements, expertise and intellectual guidance during my Master's research project and cardiology residency. I wish to express to you all my admiration and gratitude.

I also wish to acknowledge the members of my supervisory committee, Dr. Cate Creighton, Dr. Don Stevens and Dr. Van Den Heuvel for their guidance, valuable suggestions, and constructive criticisms thourought my project.

I would like to extend my sincere appreciation to Barry Connell, Monique Saleh, Francis Ortega, Madeleine Brûlé and Tyler Dexter for their technical help. Thank you to Dr. Elizabeth Cherry for her precious expertise during the analysis of my raw data using Matlab, as well as to Dr. Henrik Stryhn for his guidance during the statistical analysis of my data.

This project was made possible by financial support from the Natural Sciences and Engineering Research Council of Canada.

I also wish to acknowledge my past mentors, Dr. Valérie Chetboul and Dr. David Sisson, without whom none of this would have been possible.

Thank you to Elaine Reveler for her sympathetic ear.

Merci à mes parents, Mauricette et Alain, ainsi qu'à Alexandre pour m'avoir permis d'aller toujours plus loin. Merci aux fidèles Cayenne (deuxième thèse!), Jalna et Mina. Je vous aime tous/toutes très fort.

À mes amis, un peu partout sur cette planète. Mille mercis.

TABLE OF CONTENTS

LIST OF FIGURES

LIST OF TABLES

LIST OF ABBREVIATIONS

ACh: acetylcholine
AChE: acetylcholinesterase
AChEI: acetylcholinesterase inhibitor
AcT: acetylated tubulin
ANOVA: analysis of variance
APA: action potential amplitude
APD: action potential duration
Ba^{2+}: barium ion
Ca^{2+}: calcium ion
CCAC: Canadian Council on Animal Care
ChaT: choline acetyltransferase
cTn: cardiac troponin
cTnC: cardiac troponin C
cTnI: cardiac troponin I
cTnT: cardiac troponin T
hpf: hours post fertilization
Hu: human neuronal protein
I_{Ca}: calcium current
I_{CaL}: L-type calcium current
I_{CaT}: T-type calcium current
I_f or I_h: pacemaker current
$I_{K,ACh}$: acetylcholine-sensitive inward rectifier potassium current
$I_{K,ATP}$: ATP-sensitive inward rectifier potassium current
I_{K1}: inward rectifier potassium current
I_{Kr}: rapid delayed rectifier potassium current
I_{Ks}: slow delayed rectifier potassium current
I_{Na}: sodium current
K^+: potassium ion
M_2R: muscarinic cholinergic type 2 receptor
Na^+: sodium ion
NCX: Na^+- Ca^{2+} exchanger
Ni^{2+}: nickel ion
PAH: polycyclic aromatic hydrocarbon
PBDE: polybrominated diphenyl ether
PEI: Prince Edward Island, Canada
SERCA: ATP-dependant Ca^{2+} uptake pump of the sarcoplasmic reticulum
TMS: tricainemethanosulfonate
VAChT: vesicular acetylcholine transporter

1. General introduction

On average, there has been more than one documented fish kill per year in Prince Edward Island (PEI), Canada, over the past 50 years (DCLE 2011a, 2011b, 2015d, 2015e; Johnston and Cheverie 1980; Macphail 2013). This increasing concern with fish kills in PEI is associated with an increase in the use of environmental toxicants, including agricultural pesticides (DCLE 2015a, 2015b). A causal relationship between the use of pesticides and fish kills has been challenging to demonstrate, and necropsies performed on dead fish are often unremarkable. In this project, I hypothesized that fish exposure to selected environmental toxicants leads to increased mortality and morbidity by depressing cardiac hemodynamic function precipitated by cardiac rhythm disturbances. These rhythm disturbances likely result from toxicant-induced changes in the function of specific ion channels.

The rationale for this project derives from several recent studies that have demonstrated that exposure to several environmental toxicants leads to abnormal cardiac development and/or abnormal cardiac function. These environmental toxicants include dioxins (Antkiewicz et al. 2006; Scott et al. 2011; Plavicki et al. 2013; Brown et al. 2015, 2016a), polybrominated diphenyl ethers (PBDEs) (Lema et al. 2007), crude oil constituents such as polycyclic aromatic hydrocarbons (PAHs) (Incardona et al. 2004; Incardona et al. 2005; Incardona et al. 2009; Hicken et al. 2011; Jung et al. 2013; Brette et al. 2014; Incardona et al. 2014; Raimondo et al. 2014; Brown et al. 2015; Edmunds et al. 2015; Gerger and Weber 2015; Incardona et al. 2015; Brown et al. 2016a), or pesticides containing acetylcholinesterase inhibitors (AChEIs) (Lin et al. 2007; Jee et al. 2009;

Tryfonos et al. 2009; Simoneschi et al. 2014; Watson et al. 2014; Du et al. 2015; Pamanji et al. 2015). More specifically, heart rhythm disorders ranging from bradyarrhythmias to tachyarrhythmias have the potential to decrease cardiac output, which at best could have consequences on growth rates or swimming speed and at worst could lead to fish mortality (Gerger and Weber 2015). The electrophysiological mechanisms responsible for these rhythm disturbances rarely have been explored. Given the substantial impact of environmental toxicants on fish health and possibly on the economics of the fishing industry, identifying these mechanisms could lead to improved preventive strategies and regulations.

In order to contribute to a better understanding of this problem, I investigated the effects of selective environmental toxicants, including the commonly used AChEIs, on cardiac action potential morphology using standard microelectrode techniques in adult zebrafish (*Dano rerio*). The first part of my thesis will focus on providing an overview on fish kills in PEI, followed by an assessment of the possible cardiac dysfunctions caused by environmental toxicants in fish, before exploring the cardiac specificities of zebrafish used as models.

2. Background and literature review

2.1. Fish kills in Prince Edward Island (Canada)

2.1.1. History of fish kills in Prince Edward Island

Fish kills are defined as localized mass die-offs of fish that can occur in marine, estuarine, or fresh waters (Meyer and Barclay 1990). The first reported fish kill in PEI occurred in 1962 after accidental spillage of the agricultural fungicide nabam (disodium ethylene bisdithiocarbamate) and the insecticide endrin, a chlorinated hydrocarbon, into Mill River (Saunders 1969). Extensive mortalities, including a total of at least 8000 fish, were observed among brook trout (*Salvelinus fontinalis*) and juvenile Atlantic salmon (*Salmo salar*). Since that time, fish kills have become a chronic issue throughout the province of PEI, with 51 fish kills reported between 1962 and 2011 (Figure 1) (DCLE 2011a, 2011b, 2015d, 2015e; Johnston and Cheverie 1980; Macphail 2013).

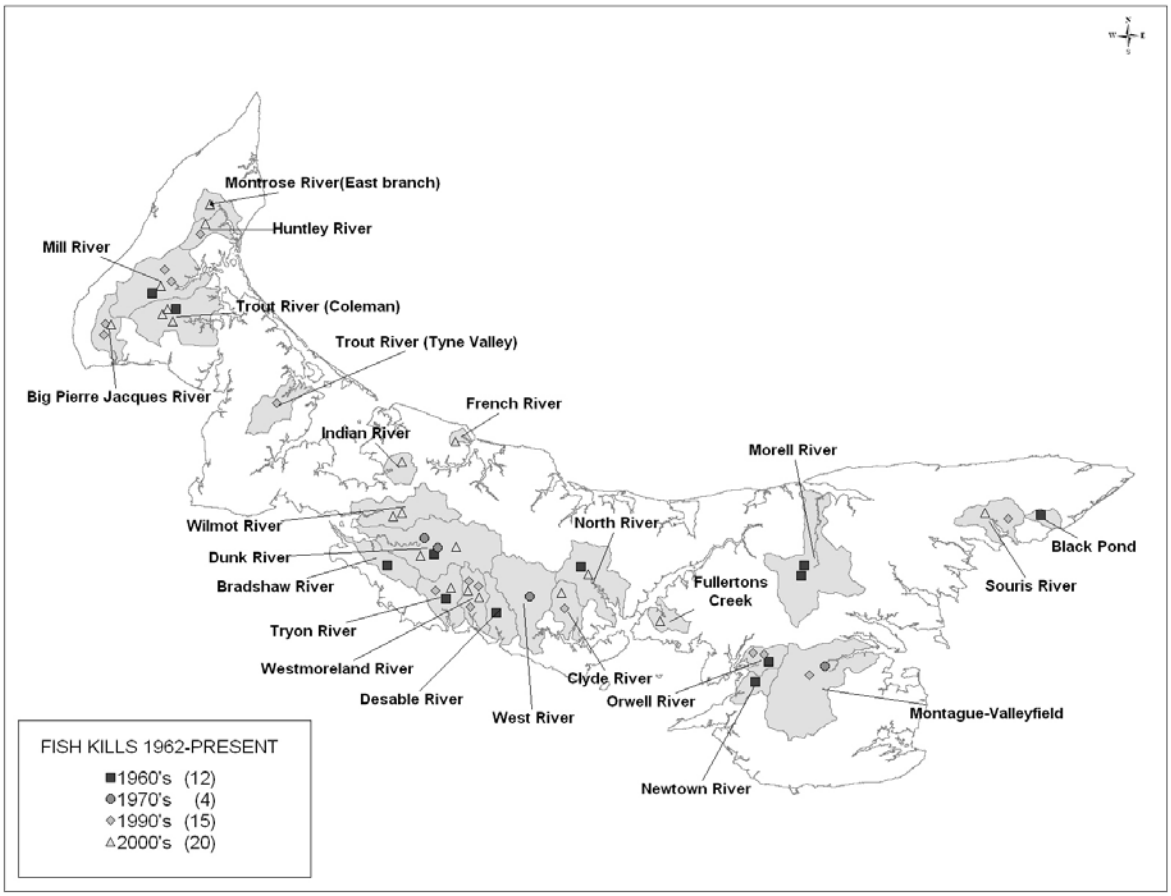

Figure 1. Map of reported fish kills in Prince Edward Island from 1962 to 2011 (DCLE 2011a).

Fish kills typically occur between June and September, with a peak between July 19th and July 25th (DCLE 2011b; Macphail 2013). The two worst years for reported fish kills were 1999 and 2002 with eight fish kills per season (DCLE 2011b; Macphail 2013). Fish kills often occur in cultivated watersheds where pesticide applications are likely, and following rainfalls, suggesting pesticide wash-off as a likely cause (Mutch 2002; Birt 2007; Gordon et al. 2011; Bauer et al. 2013; Dunn et al. 2011).

2.1.2. Impact on fish populations

It has been demonstrated that different species of fish have variable responses to toxicant exposure (Post and Leasure 1974; Gormley et al. 2005; Guignion et al. 2010), which can lead to changes in fish communities over time (Gormley et al. 2005, Bauer et al. 2013). For example, Gormley et al. (2005) showed that brook trout (*Salvelinus fontinalis*) suffered higher mortality than rainbow trout (*Oncorhynchus mykiss*) immediately after runoff events involving the pesticide azinphos-methyl, an organophosphate, on the Wilmot River, PEI, in 2002. Similarly, within the same species, susceptibility to certain toxicants can vary with fish life stages (Van Leeuwen et al. 1985; Gormley et al. 2005). During the 2002 Wilmot River events, young-of-the-year fish were more susceptible than older age classes. Most interestingly, new sampling performed a year after the events, revealed fish communities that were still skewed in terms of the proportions of species and the proportions of age classes (Gormley et al. 2005), highlighting the long-term consequences of fish kills on fish populations.

2.1.3. Public interest and perception of fish kills

There has been an increase in public awareness regarding fish kills over the years, with an increased demand for determining their cause and reducing their occurrence (La and Cooke 2011). Over the past several years, fish kills have been extensively discussed in the media in PEI, including major local newspapers (Figure 2) (McCarthy 2016a, 2016b; Guardian 2016; Yarr 2016).

.

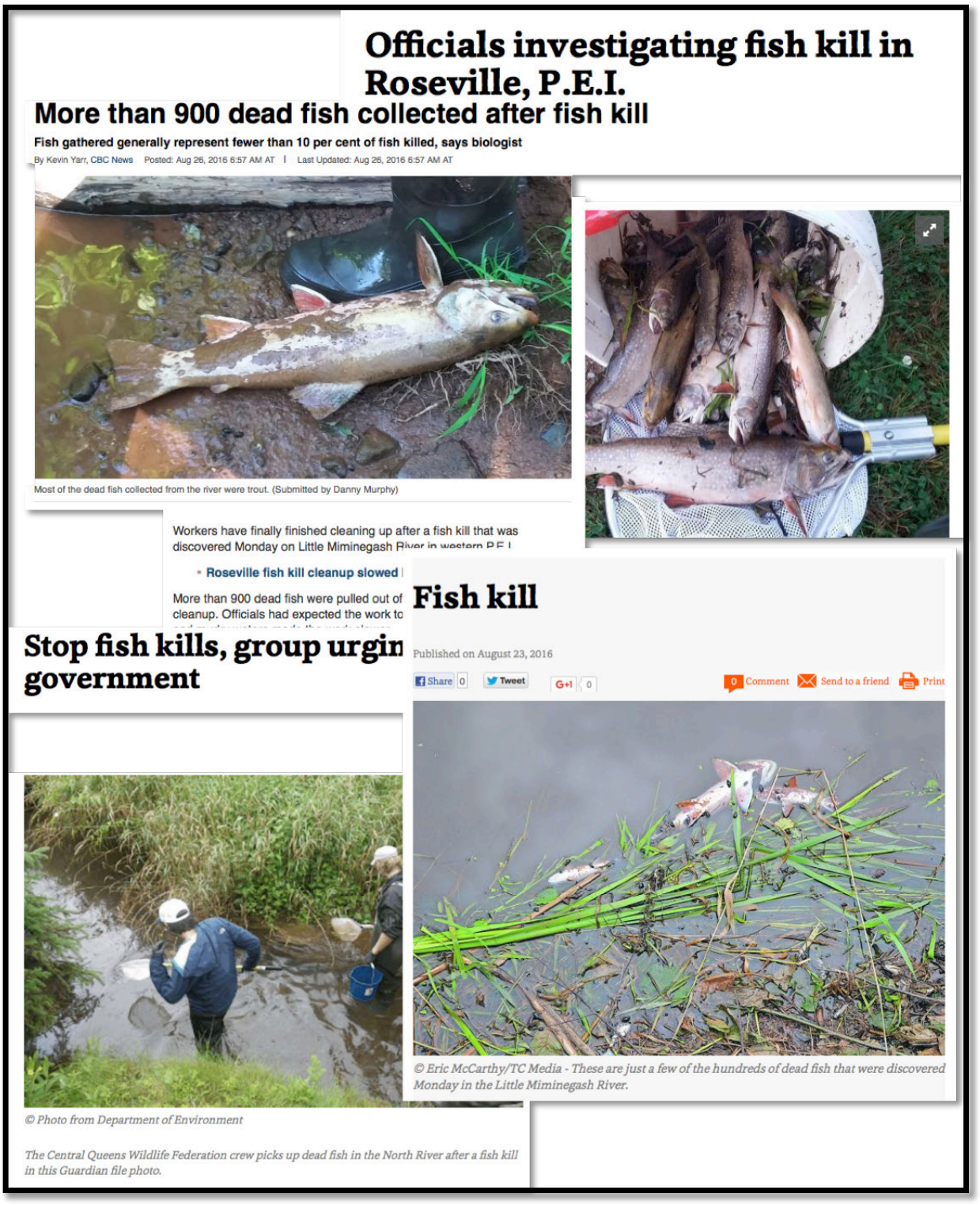

Figure 2. Local newspapers discussing fish kills in Prince Edward Island (McCarthy 2016a, 2016b; Guardian 2016; Yarr 2016).

Fish kills are highly visible to the public and may be signs of detrimental environmental changes (Holck et al. 1993, La and Cooke 2011). Moreover, they may be seen as precursors for future human illnesses. In addition, when it is demonstrated that fish kills have been caused by the release of toxicants such as pesticides, civil and or criminal penalties may be levied against individuals or groups determined to be responsible for the release (Holck et al. 1993). This was the case of a potato farmer in PEI fined $70,000 in connection with a fish kill that occurred in 2011 in a Prince County waterway (Environment Canada 2014). Fish kills may also have political consequences and are increasingly discussed during political campaigns in PEI (NDP PEI 2013). Recently, a petition was mounted by environmental groups to criticize the appointment to the board of Health PEI of two members of the potato industry (Campbell 2016).

2.1.4. The causes of fish kills

Although fish kills sometimes can be attributed to natural phenomena, they are most commonly caused by human modifications and pollution of the environment (Table 1) (La and Cooke 2011). In a study analyzing 170 fish kill events in North American freshwaters and estuaries, the major proximate causes of fish kills were agricultural pollution (19.5%), biotoxins (17.2%), and chemical pollution (7.1%) (La and Cooke 2011). Minor causes were extreme changes in temperatures (5.9%), low dissolved oxygen (5.3%), gas bubble trauma (3.6%), disease (3.6%), exhaustion (2.4%), and acidification (1.2%). Notably, the majority of surveyed fish kills were caused by human activities (67%), while natural events were only responsible for 10% (La and Cooke 2011).

Table 1. Most common causes of fish kills in freshwaters and estuaries (La and Cooke 2011).

Cause	Definition
Agricultural pollution	Pollution that pertains to pesticide, fertilizer and manure, silo and feedlot drainage, animal waste, etc. Can be direct or lead to other problems, such as hypoxia, as a result of biological oxygen demand
Acidification	Acidification by oxidation of sulphide minerals; can be delivered via precipitation (e.g., acid rain)
Biotoxin	Toxic algal and dinoflagellate blooms that are caused by *Karena brevis*, *Pfiestera*, etc.
Disease	Various bacteria, parasites, fungus, and viruses
Exhaustion	Physical exhaustion of fish typically leading to cardiac collapse (e.g., during challenging migration)
Extreme temperature changes	Rapid changes in temperature (e.g., cold shock)
Gas bubble trauma	Gas-supersaturation downstream from dams or other infrastructure or natural barriers
Industrial pollution	Pollution arising from various resource extraction, processing, and manufacturing activities (e.g., mining, food and kindred products, chemicals, metals, petroleum, and paper products)
Low dissolved oxygen (hypoxia)	Low levels of oxygen in the water, usually associated with urban runoff, decay of organic material (i.e., biological oxygen demand), rainfall events, etc.
Municipal pollution	Pollution arising from refuse disposal, water system, swimming pools, power, and sewage systems
Transportation pollution	Pollution that pertains to rail, trucks, barge or boats, and pipeline ruptures
Unknown/undetermined	Fish kill events in which no cause can readily be determined

In PEI, at least 30 out of 51 reported fish kills were likely caused by agricultural pollution (pesticides) between 1962 and 2011 (DCLE 2001b). Potatoes are the single

most common agricultural commodity in PEI in terms of farm cash receipts, and their intensive production may play a role in fish kills. Approximately 89,500 acres of potatoes were planted in 2015 (DAF 2015). Over the last five years farm cash receipts values have ranged from $203 to $257 million (DAF 2015). Intense production systems are used including monoculture row production (Chow et al. 1990), intensive tillage, cultivation along slopes, and limited rotations (Edwards et al. 2000; Jatoe et al. 2008). PEI soil types are particularly suitable for potato production: sandy loams on PEI have moderately high silt content and are well drained. However, these types of soil are also vulnerable to erosion and pesticide wash-offs during heavy rainfalls (Jatoe et al. 2008). In addition, the use of pesticides in agriculture has significantly increased over the 10 past years, with pesticide sales reaching more than a million kilograms in 2013 and 2014 (Figure 3) (DCLE 2015a, 2015b). More than 50 different pesticides are used, including mostly fungicides commonly used on potato crops (Table 2) (DCLE 2015c). AChEIs are commonly used, including carbamates such as mancozeb, or organophosphates such as phorate (DCLE 2015c).

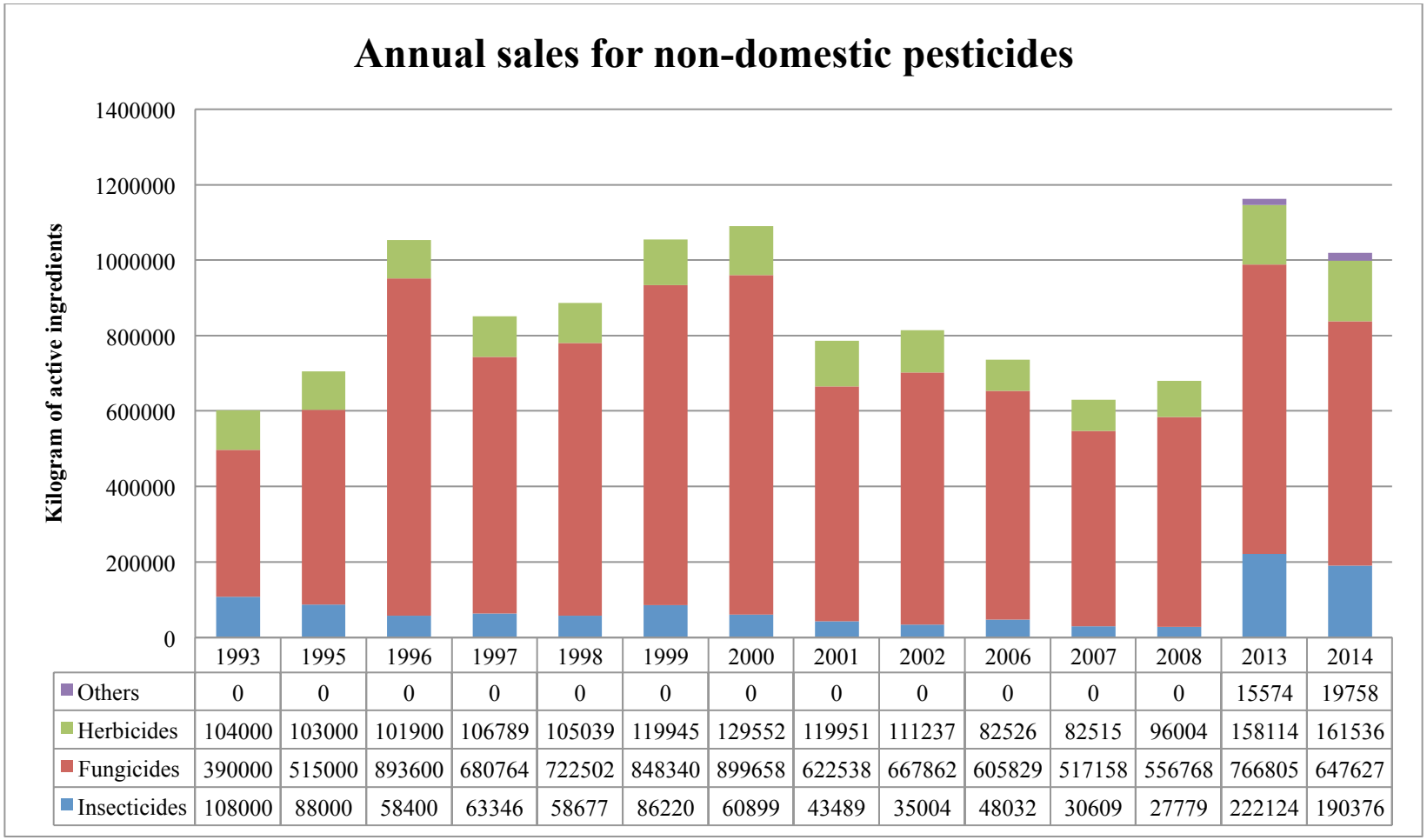

	1993	1995	1996	1997	1998	1999	2000	2001	2002	2006	2007	2008	2013	2014
Others	0	0	0	0	0	0	0	0	0	0	0	0	15574	19758
Herbicides	104000	103000	101900	106789	105039	119945	129552	119951	111237	82526	82515	96004	158114	161536
Fungicides	390000	515000	893600	680764	722502	848340	899658	622538	667862	605829	517158	556768	766805	647627
Insecticides	108000	88000	58400	63346	58677	86220	60899	43489	35004	48032	30609	27779	222124	190376

Figure 3. 1993-2014 sales of non-domestic pesticides in Prince Edward Island (DCLE 2015a, 2015b).
Others: this includes combination products (i.e. insecticide / fungicide), rodenticides, animal and bird repellents, disinfectant, and preservatives. Only reported in 2013 and 2014.

Table 2. 2013-2014 Non-domestic pesticide sales in Prince Edward Island (DCLE 2015c).

Active Ingredient	Amount Sold (kilograms)	
	2013	2014
2,4-D	1 605	1 844
atrazine	2 114	2 870
azoxystrobin	1 229	1 952
boscalid	1 822	1 771
captan	1 640	1 040
carbathiin	1 083	2 319
chlorantraniliprole	1 187	1 382
chlorothalonil	141 457	140 491
chlorpropham	531	1 028
chlorpyrifos	788	741
clethodim	804	834
clothianidin	879	1 322
copper hydroxide	1 647	1 423
cymoxanil	197	536
diazinon	455	247
dimethoate	4 296	2 376
diquat	16 284	22 409
fenamidone	1 179	816
flonicamid	1 202	1 138
fluazifop-p-butyl	813	711
fluazinam	616	1 596
fludioxonil	567	693
glyphosate	52 351	57 696
hexazinone	6 619	7 627
imidacloprid	3 453	3 919
linuron	31 625	27 528
maleic hydrazide	5 122	3 700
mancozeb	424 457	303 957
mandipropamid	748	1 380
MCPA	21 442	18 361
metalaxyl-M and S-isomer	2 014	1 982
metiram	43 565	39 535
s-metolachlor	2 994	2 249
metribuzin	6 284	9 528
mineral oil	175 987	140 961
mono- and di-basic sodium, potassium, and ammonium phosphites	5 810	7 749
mono- and di-potassium phosphite	124 992	124 733
phorate	21 945	27 557

Table 2 *(continued)*. 2013-2014 Non-domestic pesticide sales in Prince Edward Island (DCLE 2015c).

phosmet	8 222	6 796
propiconazole	1 892	1 591
propyzamide	1 621	1 673
pyraclostrobin	2 084	1 981
rimsulfuron	4 600	276
surfactant blend	8 264	12 617
terbacil	1 652	2 025
thiabendazole	865	604
thiophanate-methyl	5 184	5 988
thiram	965	2 060
tribenuron-methyl	1 218	42
trifuralin	1 021	944
all other active ingredients	13 226	14 699
TOTAL	1 162 617	1 019 297

Although many fish kills are suspected to be caused by agricultural pollution, establishing a causal relationship between fish kills and pesticides remains challenging for several reasons (Holck et al. 1993; Muñoz et al. 1994; Mutch 2002; La and Cooke 2011; DCLE 2015d, 2015e): 1) The unpredictable nature of fish kills limits the amount of control that can be exercised over sampling locations, timing and procedures used for investigation. 2) There is often a substantial delay between pesticide wash off into a stream after a rainfall event, and first notice of the resulting impacts on fish (from two hours to as much as a week). 3) Pathology results are often inconclusive due to advanced tissue decomposition or absence of visible lesions. 4) Pesticides can be flushed from the stream water by the time sampling can be initiated (especially with the short length of PEI streams). 5) In cases where one or several pesticides can be identified, the exact mechanism by which they lead to a fish kill is often unknown. 6) Fish kills are often multifactorial in origin (for example, specific conditions including the presence of a pesticide, water oxygen level, or water temperature may have synergistic effects).

2.2. Cardiac effects of environmental toxicants in fish

2.2.1. Common cardiotoxic environmental pollutants in fish

The majority of fish kills are caused by human activities including agricultural, industrial, municipal and transportation-related activities (La and Cooke 2011). Over the recent years, several environmental toxicants have shown to be associated with abnormal cardiac function in fish including dioxins (Antkiewicz et al. 2006; Scott et al. 2011; Plavicki et al. 2013; Brown et al. 2015, 2016a), PBDEs (Lema et al. 2007), crude oil constituants such as PAHs (Incardona et al. 2004; Incardona et al. 2005; Incardona et al. 2009; Hicken et al. 2011; Jung et al. 2013; Brette et al. 2014; Incardona et al. 2014; Raimondo et al. 2014; Brown et al. 2015; Edmunds et al. 2015; Gerger and Weber 2015; Incardona et al. 2015; Brown et al. 2016a), and pesticides including AChEIs (Lin et al. 2007; Jee et al. 2009; Tryfonos et al. 2009; Simoneschi et al. 2014; Watson et al. 2014; Du et al. 2015; Pamanji et al. 2015).

2.2.2. Common cardiac disturbances caused by cardiotoxic environmental pollutants in fish

The exact mechanisms by which pollutants are causing fish kills often remain unknown (La and Cooke 2011). However, based on the existing knowledge, it can be speculated that selected environmental toxicants lead to fish kills by depressing cardiac hemodynamic function, which can be the result of cardiac developmental abnormalities,

cardiac rhythm disturbances, impaired myocardial excitation-contraction coupling, or impaired myocardial contractility or relaxation.

Developmental abnormalities may include altered cardiac looping as seen in zebrafish exposed to dioxins (Antkiewicz et al. 2006), PAHs (Jung et al. 2013) or organophosphates (Pamanji et al. 2014; Du et al. 2015), as well as in mahi mahi (*Coryphaena hippurus*) exposed to PAHs (Edmunds et al. 2015). Abnormal epicardial development has been demonstrated in zebrafish exposed to dioxins, and abnormal myocardial development has been demonstrated in zebrafish exposed to PAHs or organophosphates (Scott et al. 2011; Du et al. 2015; Incardona et al. 2015). For example, the study from Incordona et al. (2015) revealed the development of an abnormally hypertrophic spongy myocardium. These morphological abnormalities are often associated with altered cardiac function manifested as decreased myocardial contractility and/or signs of congestive heart failure. Pericardial edema is often identified as a cardiotoxic effect in fish (Scott et al. 2011; Incardona et al. 2014; Pamanji et al. 2014; Raimondo et al. 2014; Watson et al. 2014; Brown et al. 2015; Edmunds et al. 2015).

Cardiac rhythm disturbances associated with acute exposure to environmental toxicants include asystole, 2nd degree (intermittent) atrioventricular conduction block and supraventricular or ventricular tachyarrhythmias. Ventricular asystole or standstill was reported in zebrafish larvae exposed to 2,3,7,8-tetrachlorodibenzo-*p*-dioxin and manifested as a beating atrium and a complete loss of visible ventricular contraction (Antkiewicz et al. 2006). However, no electrophysiological study was performed to

determine if asystole was caused by complete atrioventricular block with no ventricular escape rhythm or by ventricular inexcitability. Sinus node arrest in the absence of subsidiary pacemaker activity could also explain asystole, but in this case the atrium would also not be contracting. Asystole leads to complete cessation of blood flow to vital organs and subsequent death.

Second-degree atrioventricular block occurs when one or more atrial impulses fail(s) to conduct to the ventricles due to impaired atrioventricular electrical conduction. This type of block leads to decreased cardiac output and potentially insufficient perfusion of vital organs, especially when the fish is active. 2:1 atrioventricular block (every other atrial electrical impulse is being blocked from conducting to the ventricles) was observed in zebrafish embryos exposed to PAHs (Incardona et al. 2004). In this case too, the exact electrophysiological mechanism was not described and diagnosis was suspected based on direct visualization of the heart in zebrafish embryos that are nearly transparent. Lema et al. (2007) also observed 4:1, 5:1 and 8:1 2nd degree atrioventricular block in zebrafish embryos exposed to different concentrations of PBDE.

Tachyarrhythmias, either supraventricular or ventricular, have been observed experimentally in zebrafish embryos exposed to PBDE (Lema et al. 2007), as well as in large predatory pelagic fish after the *Deepwater Horizon* disaster released more than 636 million liters of crude oil into the northern Gulf of Mexico. Tachyarrhythmias also lead to decreased cardiac output secondary to decreased cardiac chamber filling time. Again, the electrophysiological mechanisms of these tachyarrhythmias were not described in most of these studies, but may include abnormal automaticity or early afterdepolarization-induced

triggered activity or re-entry (Gilmour 2015). One study demonstrated that crude oil (PAHs) can cause prolongation of the action potential by blocking the delayed rectifier potassium current I_{Kr} in juvenile bluefin and yellowfin tuna, which predisposes to afterdepolarization-induced triggered activity (Brette et al. 2014).

Bradycardia is often encountered in fish exposed to pesticides containing AChEIs (Lin et al. 2007; Simoneschi et al. 2014; Watson et al. 2014). However, as for other arrhythmias, the electrophysiological mechanisms responsible for bradycardia rarely have been explored. Abramochkin et al. (2012) studied the effects of the organophosphorous AChEI paraoxon, active metabolite of the insecticide parathion, on different electrophysiological parameters, including action potential duration, on isolated atrial and ventricular myocardium preparations of cod. Incubation of isolated atrium with paraoxon caused significant reduction of action potential duration (which can result in decreased contractility) and marked slowing of sinus rhythm. These effects likely cause a serious decrease in cardiac output *in vivo* and, secondarily, death.

One study specifically highlighted the occurrence of altered excitation-contraction coupling due to the reduction of calcium (Ca^{2+}) transients through the sarcolemma and sarcoplasmic reticulum of ventricular cardiomyocytes in juvenile bluefin and yellowfin tuna exposed to crude oil samples obtained from the *Deepwater Horizon* disaster previously mentioned (Brette et al. 2014).

2.2.3. The zebrafish as a model to evaluate the cardiac effects of environmental toxicants

Over the past decade, the zebrafish has been increasingly used as a research model for studies of human cardiac development and electrophysiology, as well as for cardiac toxicological studies (Figure 4) (Arnaout et al. 2007; Ververk and Remme 2012; Bournele and Beis 2016; Brown et al. 2016b; Genge et al. 2016; Sarmah and Marrs 2016). Zebrafish provide several advantages over other vertebrates, such as low cost, small size, easy handling and maintenance, high fecundity, rapid development outside the mother's body, and well-characterized cardiogenesis stages easily visualized through the transparent embryos or larvae (Ververk and Remme 2012; Sarmah and Marrs 2016). Moreover, the zebrafish genome has been fully sequenced, and approximately 71% of human genes have at least one ortholog in the zebrafish genome (Postlethwait et al. 1998; Howe et al. 2013; Vornanen and Hassinen 2016). The zebrafish also has a remarkable cardiac regenerative capacity, which makes it a valuable model to study myocardial regeneration after infarction, the leading cause of death worldwide (Kikuchi 2014; Kikuchi 2015; WHO 2017).

The main disadvantage of the zebrafish as a research model for cardiovascular development and disease is that the heart is extremely small (see section 2.3.1.), making pressure and cardiac output measurements particularly challenging (Genge et al. 2016).

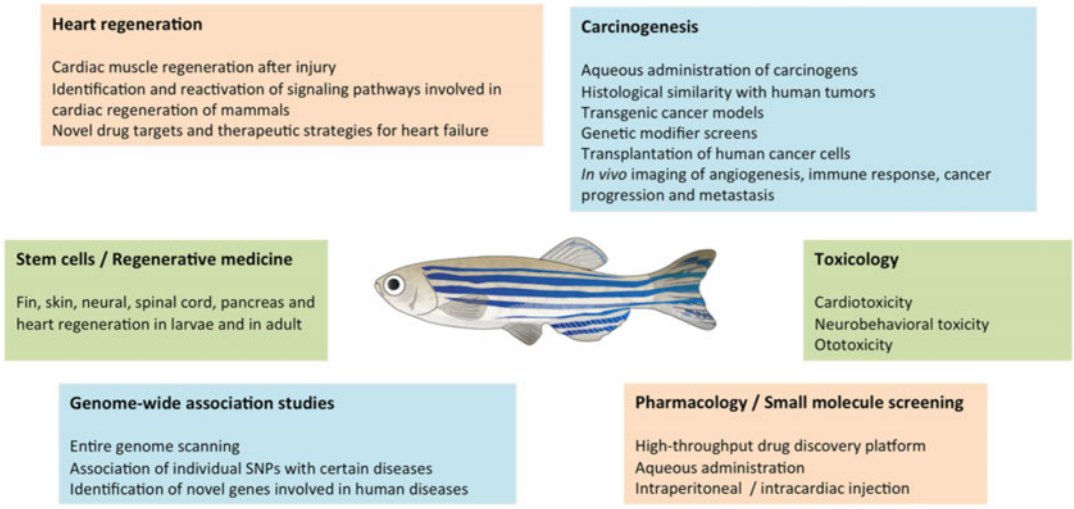

Figure 4. Research areas using zebrafish models (Bournele and Beis 2016). SNP: single-nucleotide polymorphism. With permission of Springer.

Until recently, mice have been predominantly used for the investigation of electrophysiological conditions in humans. However, mice have several limitations for modeling cardiovascular disease, including a fast basal heart rate, a large phase-1 repolarization phase and a short action potential (Ververk and Remme 2012). Despite being coldblooded and having a two-chamber heart morphology, the zebrafish has a heart rate and action potential shape and duration that more closely resemble those of humans (See section 2.3.3.). Over the recent past, the zebrafish has been increasingly used as a model to investigate channelopathies, especially human I_{Kr} channel-related disease, including long QT syndrome (Ververk and Remme 2012).

In toxicology, the zebrafish has been very useful in investigating chemical toxicity during prenatal development; heart rate can be counted and cardiac edema can be easily visualized in transparent developing embryos with a simple dissecting microscope, and more advanced imaging techniques can be used to study cardiac developmental defects

(Sarmah and Marrs 2016). The zebrafish embryo has been used to assess the impact of exposure to environmental pollutants including dioxins, PAHs, PBDEs, AChEIs (see section 2.2.2.), but also exposure to nanoparticles (Chakraborty et al. 2016), alcohol (Dlugos and Rabin 2010; Sarmah and Marrs 2016), recreational drugs such as cocaine (Mersereau et al. 2015), or cigarette smoke (Ellis et al. 2014).

Many fewer studies have used juvenile or adult zebrafish in toxicology, compared with embryos or larvae (Sarmah and Marrs 2016). The effects of cocaine on the heart rate of adult zebrafish have been evaluated using electrocardiography (Mersereau et al. 2015). Recently, Gerger and Weber (2015) determined the acute effects on ventricular rate in adult zebrafish of exposure to the PAH, benzo-*a*-pyrene, by intraperitoneal injection or simple aqueous contact. While electrophysiological data have been obtained in adult zebrafish using standard intracellular microelectrode or patch clamp techniques, no study has been performed to date to evaluate the effects of environmental pollutants on electrophysiological parameters in this species. Thus, there is an opportunity for further research using the adult zebrafish as a model in toxicology.

2.3. The cardiovascular system in zebrafish (*Danio rerio*)

2.3.1. Cardiac anatomy

Cardiac anatomy varies considerably among fish species, depending on body morphology and physiology (Santer 1985). In zebrafish, the heart is located anteroventrally to the thoracic cavity between the operculum and the pectoral girdles (Figure 5) (Hu et al 2001; Farrell and Pieperhoff 2011). The heart is contained in a silver-coloured membranous sac, the pericardium. More specifically, within the pericardium, there are four distinct chambers that comprise the heart: the sinus venosus, the atrium, the ventricle, and an outflow tract, called the bulbus arteriosus (Figure 6). However, the fish heart is often referred to as being two-chambered, with one atrium and one ventricle (Hu et al 2001).

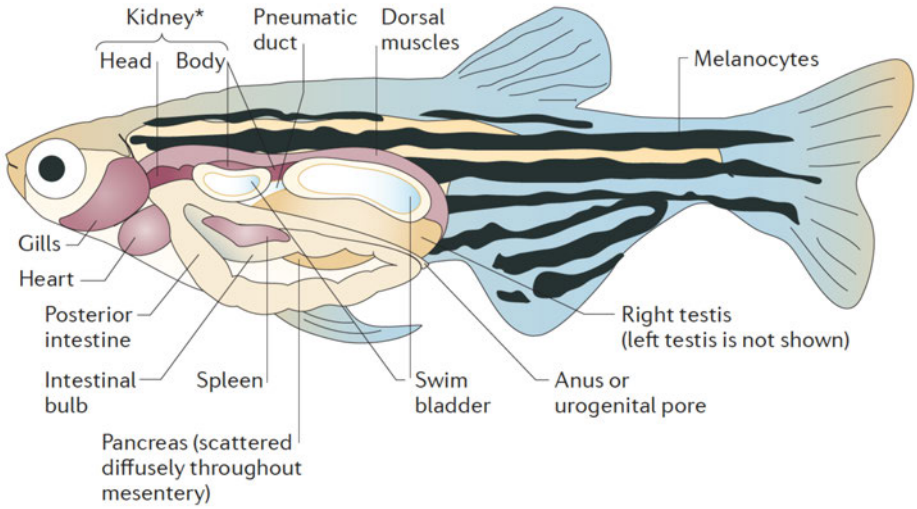

Figure 5. Anatomy of the adult zebrafish (White et al. 2013).
With permission of Macmillan Ltd.

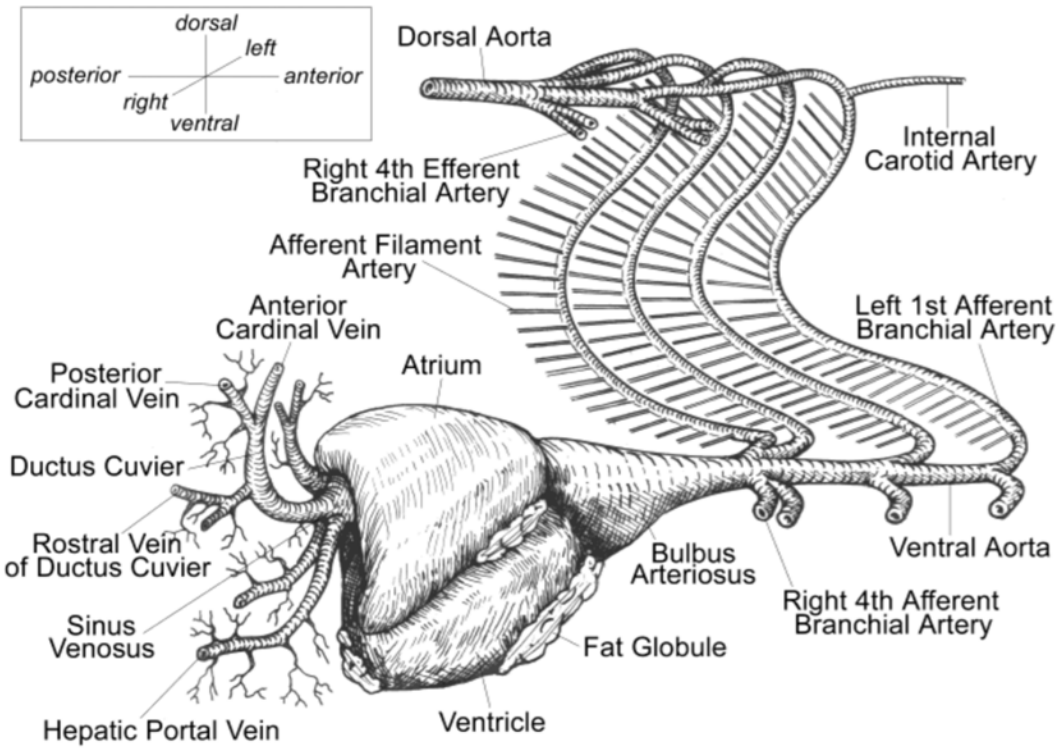

Figure 6. Cardiovascular anatomy of the zebrafish (Hu et al. 2001).
With permission of John Wiley and Sons.

Blood returns to the heart from the ductus of Cuvier (which receives blood from anterior and posterior cardinal veins and lies outside the pericardium), and from hepatic portal veins, which opens directly into the sinus venosus (Hu et al 2001; Farrell and Pieperhoff 2011). The sinus venosus is directly connected to the single-chambered atrium, which lies dorsal to the ventricle, via the sino-atrial canal. The sino-atrial canal has a one-way ostial valve, which prevents blood from back-flowing into the sinus venosus when the atrium contracts (Farrell and Pieperhoff 2011). The atrium is then connected to the single-chambered ventricle via the atrioventricular orifice and valve (Hu et al 2001). The atrioventricular orifice is positioned on the dorsal and anterior portion of the ventricle, adjacent to the bulbus arteriosus. The atrioventricular valve has four distinct leaflets oriented anterior, posterior, left, and right of the atrioventricular orifice. Finally,

the pyramidal ventricle pumps blood through the bulboventricular orifice into a pear-shaped bulbus arteriosus (Hu et al 2001). The bulboventricular valve is located at the anterior portion of the ventricle and has two semilunar valve cusps, one right and one left. The bulbus arteriosus is connected to the ventral aorta, which lies outside the pericardium and provides blood to the gill vasculature (Hu et al 2001; Farrell and Pieperhoff 2011).

The zebrafish heart is relatively small. The length of the ventricle is approximately 1 mm in the adult zebrafish, or 4.28% of the body length (Singleman and Holtzman 2012).

2.3.2. Histology of the zebrafish heart

All cardiac chambers are lined internally with endothelial cells, forming the endocardium. The external surface of the heart has a layer of epithelial cells and connective tissue called the epicardium, which represents the inner part (infolding) of the pericardium. The cardiac muscle (myocardium) lies between the endocardial and epicardial layers.

The atrium of the zebrafish has a thin wall (two to three cell layers) and shows an extensive network of pectinate muscles, which are heavily branched (Figure 7) (Hu et al. 2001). In the ventricle, cardiac muscle is composed of a relatively thin compact layer (three to four cells thick) and an extensive spongy network of muscular trabeculae, which account for the greater proportion of ventricular mass (Figure 7) (Hu et al. 2000, 2001). A network of coronary vessels is present on the epicardial surface of the ventricle and

penetrates the compact layer to terminate at the subtrabecular layer level (Hu et al. 2000, 2001). The trabeculae lack a coronary supply, and likely receive oxygen and nutrients via diffusion from blood present in the ventricular cavity (Hu et al. 2001).

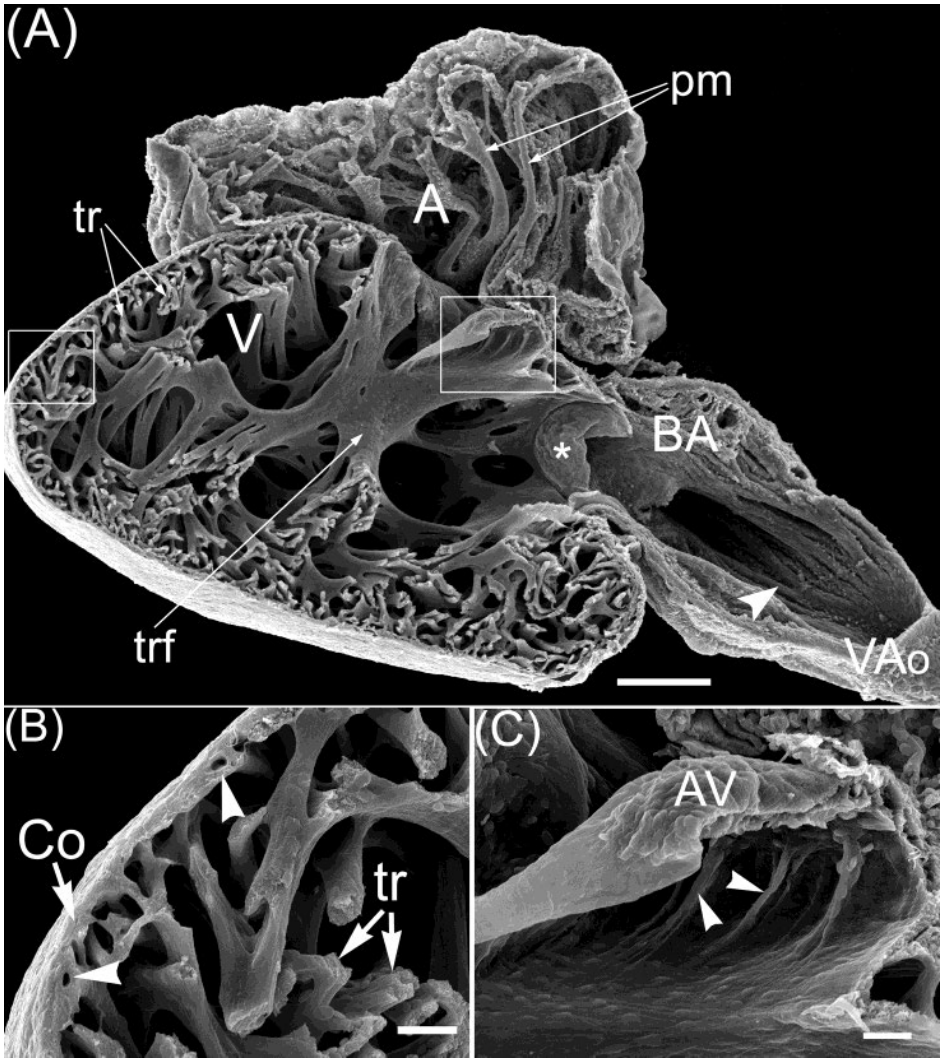

Figure 7. Ultrastructure of the zebrafish heart (from Hu et al. 2001). A: Scanning electron microscopic image of the sagittal section of the left half of a 3 months postfertilization zebrafish heart depicting the atrium (A), ventricle (V), bulbus arteriosus (BA), and a portion of the smooth-walled ventral aorta (VAo). The asterisk indicates the bulboventricular valve. The arrowhead identifies one of the elevated ridges along the inner surface of the bulbar wall. The boxed area on the left side corresponds to B; the right box corresponds to C. tr: trabeculae; trf: trabecular fold; pm: pectinate muscle. B: Arrowheads point to the coronary vessels, which penetrate into the compact layer (Co) of the ventricular wall. tr: trabeculae. C: Arrowheads point to the trabecular bands that act as pillars supporting the leaflet of the atrioventricular valve (AV) to prevent retrograde flow. Scale bar = 100 μm in A, 40 μm in B,C. With permission of John Wiley and Sons.

Cardiomyocytes are relatively small and rod-shaped in zebrafish, with ventricular myocytes being larger than those found in the atrium (Hu et al. 2001). Freshly isolated ventricular myocytes from adult zebrafish are approximately 100 x 5 x 6 μm in size (lengh x width x height; Brette et al. 2008) and are very narrow compared with human ventricular myocytes (Figure 8) (Verkerk and Remme 2012). Myofibrils occupy more than half of the atrial and ventricular myocytes, and are centrally located in the cell, with abundant mitochondria in the periphery (Hu et al. 2001). Sarcoplasmic reticulum is sparse in the zebrafish ventricle, and there is no T-tubule system (Hu et al. 2001).

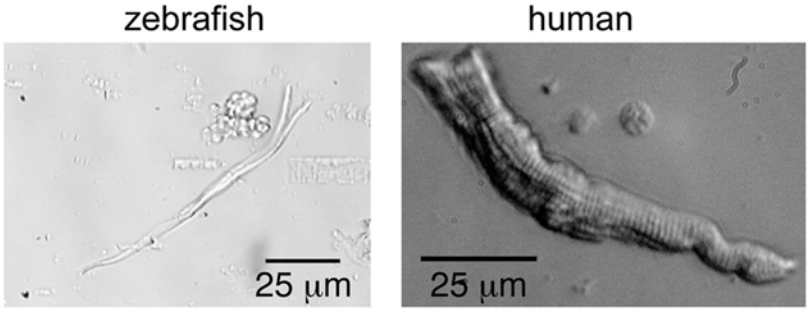

Figure 8. Photographs of atrial myocytes of zebrafish and human (enzymatically isolated) (Verkerk and Remme 2012). Notice the narrow shape of the zebrafish atrial myocyte.

The distensible bulbus arteriosus has three distinct layers: externa (outer layer), media (middle layer) and intima (inner layer) (Figure 9) (Hu et al. 2001). The intima is composed of a subendothelium overlying a thin endothelial layer. The media is composed of seven to ten layers of helically arranged smooth muscle cells surrounded by a fine network of collagen and reticular and elastic fibrils. The externa is composed of the external elastic lamina.

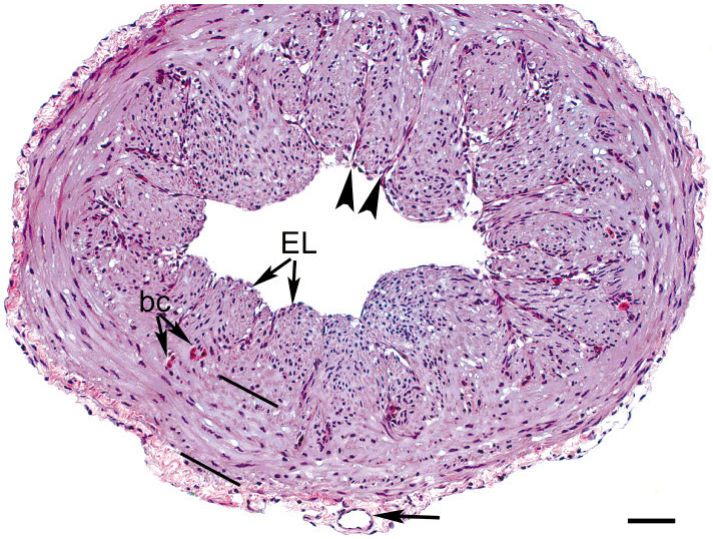

Figure 9. Cross section of the bulbus arteriosus showing the three concentric layers (Hu et al. 2001). The three successive concentric layers of the bulbous arteriosus are marked by line bars. EL: endothelial layer. Arrowheads: ridges separating the luminal surface. bc: nucleated red blood cell. Hematoxylin-eosin staining. Scale bar 20 μm. With permission of John Wiley and Sons.

2.3.3. Cardiac action potentials in zebrafish

Adult zebrafish action potential recordings have been reported for isolated ventricular cardiomyocytes using the patch clamp technique (Brette et al. 2008), as well as for intact atria and ventricles using a standard intracellular microelectrode technique (Nemtsas et al. 2010). These studies showed that the zebrafish adult cardiomyocytes have a resting membrane potential of approximately -70 mV and that all phases (0-4) of the cardiac action potential are present in the zebrafish heart, except the rapid phase-1 repolarization ("spike"). Zebrafish action potentials have a rapid upstroke, followed by a long lasting plateau phase and a rapid terminal repolarization phase (Figure 10). The plateau phase is shorter in atrial than in ventricular tissue. This type of morphology is relatively similar to the one found in large mammals such as humans, except for the absence of phase 1 (Brette et al. 2008; Nemtsas et al. 2010; Verkerk and Remme 2012; Alday et al. 2014, Vornanen and Hassinen 2016). Action potential morphology is typically characterized by its duration at different levels of repolarization such as 50% or 90% (APD 50 or APD 90), its amplitude (APA) and the slope of phase 0, which represents the maximum rate of voltage change (dV/dt_{max}). Average action potential parameters measured with sharp microelectrodes in the intact adult zebrafish heart at a physiologic temperature of 28°C are summarized in Table 3 (Nemtsas et al. 2010). The adult zebrafish spontaneous heart rate (149 ± 8 bpm) is much closer to the human spontaneous heart rate (60-100 bpm) than to the mouse spontaneous heart rate (300-600 bpm) (Nemtsas et al. 2010; Bournele and Beis 2016).

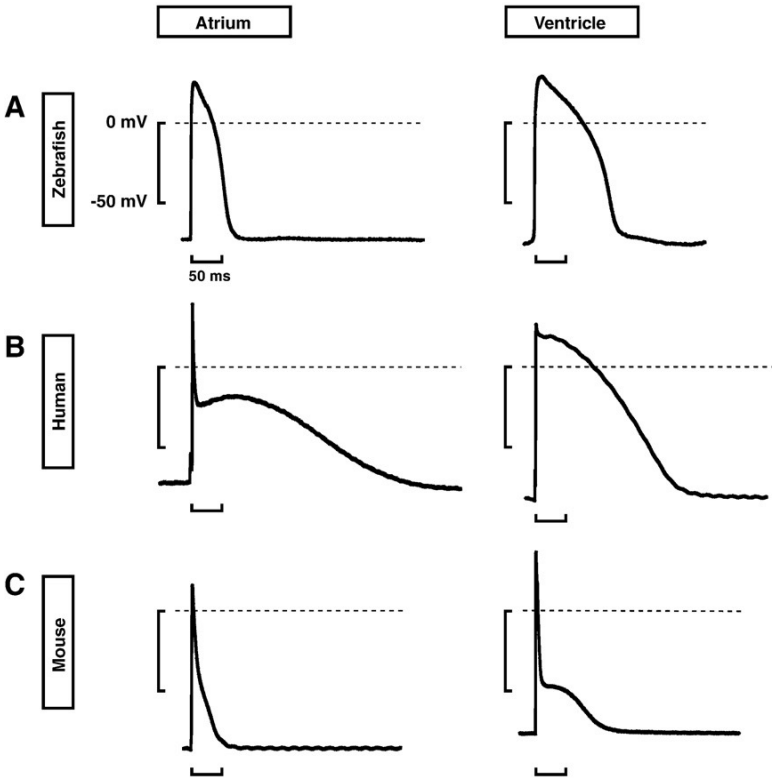

Figure 10. Representative shapes of atrial (left column) and ventricular (right column) cardiac action potentials in the adult zebrafish (A), human (B) and mouse (C) (Nemtsas et al. 2010). Action potentials were recorded from spontaneously beating (149 ± 8 bpm) intact zebrafish hearts at 28 °C, while human and mouse cardiac tissues were stimulated at a frequency of 1 Hz and measured at 37 °C. Zebrafish recordings were obtained from the apical half of the ventricle and from the central area of the atrium. Note that the induced heart rate used for the mouse is substantially lower than the spontaneous heart rate in this species, which influences action potential morphology. With permission of Elsevier.

Table 3. Action potential parameters in atria and ventricles of adult zebrafish as compared with human and mouse (Nemtsas et al. 2010).

	Atrium			**Ventricle**		
	Zebrafish	*Human*	*Mouse*	*Zebrafish*	*Human*	*Mouse*
n (preparations)	16	28	7	16	5	6
APA (mV)	100 ± 2	97 ± 2	104 ± 1	99 ± 2	101 ± 4	95 ± 2
RMP (mV)	-74 ± 2	-74 ± 1	-81 ± 2	-72 ± 2	-77 ± 3	-74 ± 1
dV/d_{tmax} (V/s)	129 ± 9	246 ± 22	239 ± 10	92 ± 5	180 ± 10	166 ± 11
APD 20 (ms)	29 ± 2	9 ± 2	3 ± 0	69 ± 3	98 ± 5	4 ± 1
APD 50 (ms)	46 ± 2	148 ± 8	9 ± 1	110 ± 4	165 ± 12	9 ± 3
AP 90 (ms)	62 ± 2	316 ± 7	42 ± 4	132 ± 4	242 ± 15	82 ± 4

Action potentials were measured with sharp microelectrodes in intact zebrafish hearts, mouse left atrial trabeculae and right ventricular muscle strips, human right atrial appendage trabeculae and right ventricular papillary muscles. Recordings were obtained from the apical half of zebrafish ventricles and the central area of atria. Zebrafish hearts were beating spontaneously at 149 ± 8 bpm and kept at 28 °C, while human and mouse tissues were electrically stimulated at 1 Hz and kept at 37 °C. APA, action potential amplitude; RMP, resting membrane potential; dV/dt_{max}, maximum depolarization velocity; APD 20, APD 50 and APD 90, action potential duration measured at 20%, 50% and 90% of repolarization, respectively. With permission of Elsevier.

In ectothermic fish, the duration of the action potential varies with body temperature within the thermal tolerance range from 6.2°C to 41.7°C (Lopez-Olmeda and Sanchez-Vazquez 2011;Vornanen 2016; Vornanen and Hassinen 2016). For example, at 19°C the duration of the ventricular action potential in zebrafish is similar to the one in humans at 37°C. However, at 37°C the duration of the ventricular action potential in zebrafish only represents one fifth of the human action potential (Vornanen and Hassinen 2016). Action potential recordings have also been reported in embryonic zebrafish through the use of a patch clamp technique (Jou et al. 2010), and voltage sensitive dyes (Panáková et al. 2010; Wythe et al. 2011).

2.3.4. Ion currents contributing to the action potential

2.3.4.1. Sodium currents

As in mammals, the rapid upstroke of the zebrafish cardiac action potential (phase 0) is generated by a fast sodium (Na^+) current (I_{Na}), in the atrium and in the ventricle. The current flows through voltage-gated Na^+ channels, as demonstrated by Nemtsas et al. (2010). Indeed, exposure of the heart to the specific Na^+ channel blocker tetrodotoxin induced a significant reduction in upstroke velocity to 25% in the atrium and 19% in the ventricle (reduced dV/dt_{max}), as well as a reduction in APA. On the other hand, the duration of the action potential was not affected by tetrodotoxin, suggesting that there is no sustained (non-inactivating) I_{Na}. A study using isolated ventricular cardiomyocytes indicated that the density of the Na^+ current in zebrafish was approximately four times

smaller than in mammals (Brette et al. 2008). In zebrafish, two Na^+ channel isoforms, coded by the genes scn5Laa and scn5Lab, were found in larval cardiac tissue (72 hpf) (Novak et al. 2006; Vornanen and Hassinen 2016). These genes are orthologous to the mammalian gene SCN5A, and are required for cardiac development (Chopra et al 2010). In the adult zebrafish, only scn5Lab has been identified (Chopra et al 2010; Vornanen and Hassinen 2016).

2.3.4.2. Calcium currents

Ca^{2+} currents are necessary for the plateau phase (phase 2) of the action potential and they participate in contraction by triggering the interaction between actin and myosin. Two types of Ca^{2+} currents (I_{Ca}) have been demonstrated in adult zebrafish atrial and ventricular cardiomyocytes: the T-type (I_{CaT}) and the L-type (I_{CaL}) currents (Vornanen and Hassinen 2016).

The L-type Ca^{2+} channel blocker nifedipine causes shortening of the action potential duration, and the I_{CaL} activator BayK8644 causes prolongation of the QT interval in a dose-dependant manner, indicating that I_{CaL} is responsible for the plateau phase of the action potential (phase 2) (Nemtsas et al. 2010; Tsai et al. 2011). Patch-clamp recordings demonstrated that I_{CaL} was associated with a fast run-down or decrease during the first few minutes after membrane rupture (Nemtsas et al. 2010). This phenomenon may be explained by the small cell size, which can cause run-down due to loss of important intracellular factors during cell dialysis (Nemtsas et al. 2010).

Alternatively, it may be a characteristic property of zebrafish α_{1C}-channel subunits caused by the C-terminal sequence, which is reported to play an important role in run-down (Kepplinger et al. 2000, Nemtsas et al. 2010). It was also demonstrated that in the zebrafish, ventricular contraction was abolished by mutation in the α_{1C}-channel subunit (Vornanen and Hassinen 2016). This subunit, also named $Ca_v1.2$, is the dominant cardiac isoform in mammals among four subunits (α_{1S}, α_{1C}, α_{1D}, α_{1F}, or $Ca_v1.1$-4), suggesting that it is produced by orthologous genes in mammals and zebrafish (Vornanen and Hassinen 2016). Transcripts of the α_{1D}-channel subunit are also expressed in the hearts of adult zebrafish (Sidi et al. 2004; Vornanen and Hassinen 2016). Notably, there is a significantly larger density of I_{CaL} in zebrafish ventricular cardiomyocytes than in human cardiomyocytes (Zhang et al. 2011; Vornanen and Hassinen 2016).

The expression of T-type Ca^{2+} channels in atrial and ventricular cardiomyocytes in the adult zebrafish was demonstrated by Nemtsas et al. (2010). I_{CaT} was identified using the following criteria: 1) the potential range of activation (usually a low-voltage range), 2) insensitivity to nifedipine, 3) high sensitivity to nickel (Ni^{2+}), and 4) resistance to tetrodotoxin for discrimination from I_{Na}. This substantial expression of T-type Ca^{2+} channels in adult zebrafish is very different from many mammalian hearts, where T-type Ca^{2+} channels are only expressed in the fetal heart and pathologically in the adult (Nemtsas et al. 2010). Two cardiac subunits for T-type Ca^{2+} channels are known in mammals, α_{1G} and α_{1H} (respectively also named $Ca_v3.1$ and $Ca_v3.2$). In zebrafish, T-type Ca^{2+} channels most likely consist of the subunit α_{1G} based on their sensitivity to Ni^{2+} (Nemtsas et al. 2010). However, immunofluorescence findings suggested the presence of α_{1H} subunits (Alday et al. 2014). Some authors speculate that the presence of I_{CaT}

indicates that zebrafish cardiomyocytes in adults have a more immature phenotype than adult mammalian cardiomyocytes (Nemtsas et al. 2010).

2.3.4.3. Potassium currents

- Delayed rectifier potassium currents

In zebrafish cardiomyocytes, only the I_{Kr} current has been clearly demonstrated by using the I_{Kr} blocker E4031, which substantially prolonged APD. This result sugests that the zebrafish heart does display an ether-à-go-go related gene (Nemtsas et al. 2010, Alday et al. 2014, Vornanen and Hassinen 2016). I_{Kr} is the main repolarizing potassium (K^+) current in the atrial and ventricular myocytes, and is active during phase 2 and phase 3 of the cardiac action potential. Some studies suggest that zebrafish possess an ortholog of the mammalian KCNH2 gene called zerg (also called HERG in humans) coding for the pore-forming subunit of the K^+ channel (Langheinrich et al. 2003; Arnaout et al. 2007; Scholtz et al. 2009; Leong et al. 2010). When this orthologous gene was mutated, zebrafish embryos exhibited electrocardiographic changes similar to humans with long QT syndrome LQT2, including increased Q-T interval and atrioventricular block (Langheinrich et al. 2003). Vornanen and Hassinen (2016) suggested that as opposed to mammals, I_{Kr} was mostly produced by erg2 channels, which are encoded by the zebrafish ortholog to the mammalian KCNH6 gene, mainly expressed in the nervous tissue and not in the heart, instead of erg1 channels (KCNH2 gene) mainly expressed in the mammalian heart.

The presence of I_{Ks} in zebrafish cardiomyocytes is still controversial (Verkerk and Remme 2012; Vornanen and Hassinen 2016). Nemtsas et al. (2010) concluded that I_{Ks} had no significant role in repolarization in adult zebrafish cardiomyocytes, because the I_{Ks} blocker HMR 1556 had no effect on membrane outward currents during patch-clamp recordings on isolated cardiomyocytes. In contrast, Tsai et al. (2011) found that the I_{Ks} blocker chromanol 293B prolonged both QT interval and action potential duration in a dose-dependent manner in adult zebrafish cardiomyocytes, suggesting the presence of I_{Ks}. Transcripts orthologous to the mammalian KCNQ1 gene are also expressed in the zebrafish heart (Wu et al. 2014). In mammals, the KCNQ1 gene encodes for the α-subunit ($K_v7.1$), which is part of the K^+ channel responsible for I_{Ks} (Vornanen and Hassinen 2016). Moreover, I_{Ks} has been identified in another species of the zebrafish family (Cyprinidae), *Carassius carassius* (Hassinen et al. 2011). In this case, I_{Ks} was mainly produced by homotetramers of $K_v7.1$ channel without the MinK β-subunit as in mammals. In humans, it was demonstrated that I_{Ks} blockade significantly increases APD only when "repolarization reserve" is attenuated or with sympathetic activation (Jost et al. 2005; Verkerk and Remme 2012). This phenomenon may explain the contrasting results of studies assessing the effect of I_{Ks} blockade on the zebrafish action potential.

- Inward rectifier potassium current

As in mammals, a robust background of the inwardly rectifying K^+ current I_{K1} is present in the atrial and ventricular cardiomyocytes of the zebrafish (Hassinen et al. 2015; Vornanen and Hassinen 2016). This current is also blocked by barium (Ba^{2+}) (Hassinen et al. 2015). I_{K1} mainly participates in the maintenance of the resting membrane potential (phase 4), but also plays a role in early depolarization and late repolarization (phase 3).

However, marked differences were seen in terms of the composition of the channel responsible for I_{K1} compared with mammals. The main channel isoform identified in the zebrafish ventricle is Kir2.4, which represents 92.9 % of the total Kir2 population. In the zebrafish atrium, Kir2.2a and Kir2.4 represent 64.7 % and 29.3 % of the Kir2 transcripts, respectively (Hassinen et al. 2015; Vornanen and Hassinen 2016). In humans, by contrast, Kir2.4 is hardly expressed in cardiomyocytes and Kir2.1, Kir2.2 and Kir2.3 are predominant. These findings may have functional implications, as the zebrafish Kir2.4, for example, is approximately two times more sensitive to Ba^{2+} than its mammalian counterpart (Vornanen and Hassinen 2016).

2.3.4.4. Other ionic currents

- $I_{K,ATP}$: The ATP-sensitive channels Kir6.1, Kir6.2 and Kir6.3 are present in the zebrafish genome, occupying three different chromosomes. Kir6.1 and Kir6.2 are orthologs to Kir6.1 and Kir6.2 of mammals (Zhang et al. 2006; Vornanen and Hassinen 2016). While Zhang et al (2006) presented Kir6.3 as a new member of the inward rectifier K^+ channel family; others consider Kir6.3 as a paralog of Kir6.2 (i.e., Kir6.2b) (Vornanen and Hassinen 2016).
- $I_{K,ACh}$: Acetycholine (ACh) induces a large inwardly rectifying K^+ current in the zebrafish heart (Nemtsas et al. 2010; Vornanen and Hassinen 2016). However, this effect is limited to the atrium and the molecular basis of this current has not been described at this time (Vornanen and Hassinen 2016).
- I_h or I_f: The "pacemaker current" I_h has been identified in the zebrafish heart. The

slow mo mutation reduces I_h and heart rate in embryos and adult zebrafish (Baker et al. 1997; Warren et al. 2001). The transcription factor Isl1 is the first identified molecular marker for pacemaker cells in the zebrafish heart, and its expression in pacemaker cells is conserved from fish to human (Tessadori et al. 2012). Thanks to this marker, it was determined that the functional pacemaker of the zebrafish was likely organized as a ring around the venous pole (Figure 11) (Tessadori et al. 2012). The presence of the hyperpolarization-activated cyclic nucleotide-gated ion channels HCN4, which are characteristic of mammalian pacemaker cells, was also detected in this region of the zebrafish heart (Tessadori et al. 2012; Stoyek et al. 2015).

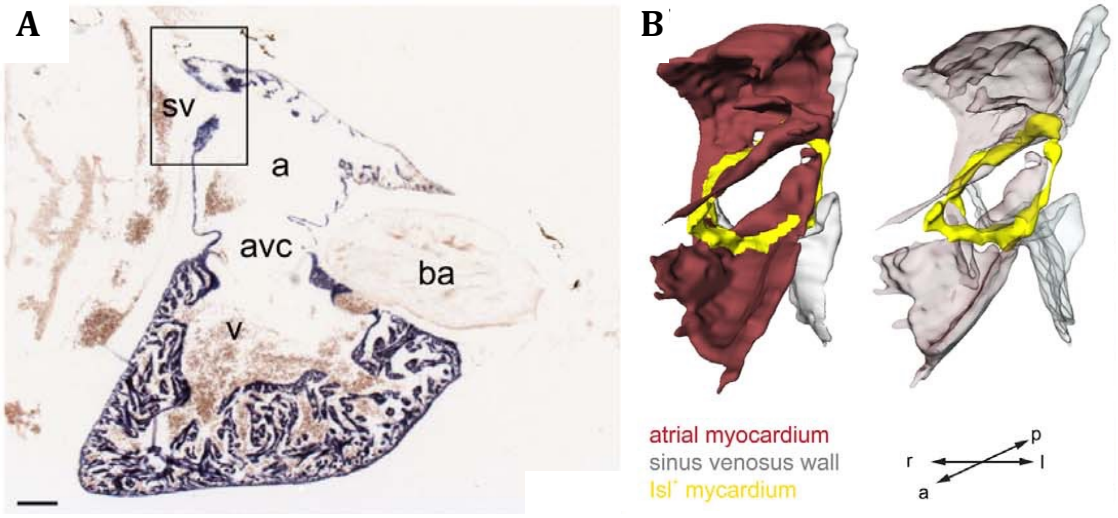

Figure 11. Expression of Isl1 and likely location of the functional pacemaker in the adult zebrafish heart (Tessadori et al. 2012). A: Sagittal section through zebrafish heart labeled with the myocardial marker myl7. sv: sinus venosus; a: atrium; avc: atrioventricular canal; v: ventricle; ba: bulbus arteriosus.The box indicates the region of the sinoatrial junction. B: 3D reconstruction of the sinoatrial junction. Isl1 (yellow) is expressed around the entire sinoatrial junction, forming a ring-like structure.

2.3.5. Excitation-contraction coupling

As in all vertebrate hearts, cardiac contraction in zebrafish is caused by the generation of cross bridges between thick filaments composed of the protein myosin, and thin filaments mainly composed of the protein actin (Gillis 2011). The thin filaments of actin contain two chains that intertwine in a helical pattern, and each actin filament is carried on a twisting backbone of the heavier tropomyosin protein (Opie 2004). Each thick filament of myosin is composed of hundreds of myosin molecules that have a head and a tail. The tails are aligned side by side but the heads emerge in a spiral fashion. Within the cardiomyocytes, thick and thin filaments are arranged in a parallel overlapping patterns within structures called sarcomeres. Necessary to the interaction between actin and myosin are the cardiac troponin (cTn) complexes that occur at regular intervals along tropomyosin (Figure 12). Each cTn complex is composed of three types of proteins: the cardiac troponin C (cTnC, C for Ca^{2+}) responds to the Ca^{2+} released as a result of the action potential during systole, and binds to the inhibitory molecule troponin I (cTnI, I for inhibitor) that otherwise restricts the interaction between actin and myosin heads. When Ca^{2+} is low, as in diastole, cTnI binds to actin to inhibit myosin interaction. Troponin T (cTnT, T for tropomyosin) is involved in distributing the inhibitory effect of the cTn complex, via tropomyosin, to other actin monomers with which it interacts in the absence of Ca^{2+}. In the presence of Ca^{2+}, cTnT removes these inhibitions. Thereby, Ca^{2+} handling has a key role in excitation-contraction coupling.

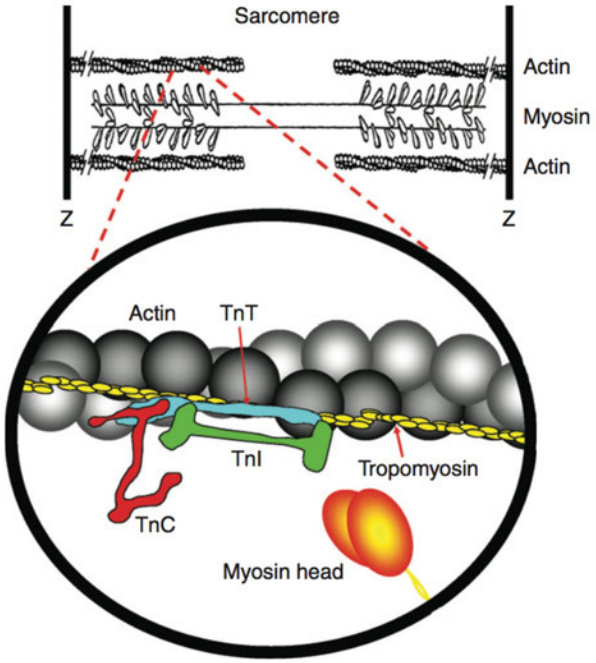

Figure 12. Schematic diagram of the cardiac sarcomere and of the regulatory complex associated with the actin filament responsible for making the contractile reaction activated by calcium (Gordon et al. 2001; Gillis 2011). TnC: troponin C; TnI: troponin I; TnT: troponin T. With permission of Elsevier.

In mammals, the wave of depolarization leads to an influx of extracellular Ca^{2+} through the L-type calcium channels, which triggers the release of more Ca^{2+} from the sarcoplasmic reticulum by the process of Ca^{2+}-induced Ca^{2+} release with activation of the ryanodine receptors (Opie 2004). This process requires a direct interface between the cell membrane and the sarcoplasmic reticulum membrane, which is made possible in mammalian cardiomyoctes by invaginations of the cell membrane called T-tubules. The cytosolic Ca^{2+} then increases and contraction occurs. During relaxation, cytosolic Ca^{2+} decreases thanks to the activity of the ATP-dependent Ca^{2+} uptake pump of the sarcoplasmic reticulum called SERCA, as well as trans-sarcolemmal calcium efflux through the Na^{+}- Ca^{2+} exchanger (NCX) and a sarcolemmal Ca^{2+}-ATPase.

As opposed to the situation in mammals, T-tubules are absent in zebrafish cardiomyocytes (Brette et al. 2008; Bovo et al. 2013; Haustein et al. 2015), and ryanodine receptors are not sensitive to the mechanism of Ca^{2+}-induced Ca^{2+} release (Bovo et al. 2013). As a result, trans-sarcolemmal Ca^{2+} influx has been suggested to be the main contributor to the increase in cytosolic Ca^{2+} (Ca^{2+} transient) during cardiac contraction while Ca^{2+}-induced Ca^{2+} release from the sarcoplasmic reticulum appears to be less important (Figure 13) (Brette et al. 2008; Zhang et al. 2011; Bovo et al. 2013). The absence of T-tubules is compensated by the small diameter of fish cardiomyocytes and the presence of flask-like invaginations of the membrane (caveolae), both of which increase the cell surface-to-volume ratio (Galli 2011). This also would explain the larger density of I_{CaL} in zebrafish ventricular cardiomyocytes compared with large mammals such as humans (Zhang et al. 2011; Vornanen and Hassinen 2016). However, a recent study in zebrafish suggests that sarcoplasmic Ca^{2+} release is more important than previously thought, especially in contractile force generation (Haustein et al. 2015). In contrast to mammals, it also was demonstrated that the force-frequency relationship is strongly negative in the zebrafish heart (Haustein et al. 2015). Mechanisms of relaxation have not been fully determined in zebrafish, but studies suggested that NCX significantly contributes to Ca^{2+} removal (Bovo et al. 2013; Haustein et al. 2015). This also was shown to be the primary pathway to remove cytosolic Ca^{2+} during relaxation in rainbow trout cardiomyocytes (Shiels 2011).

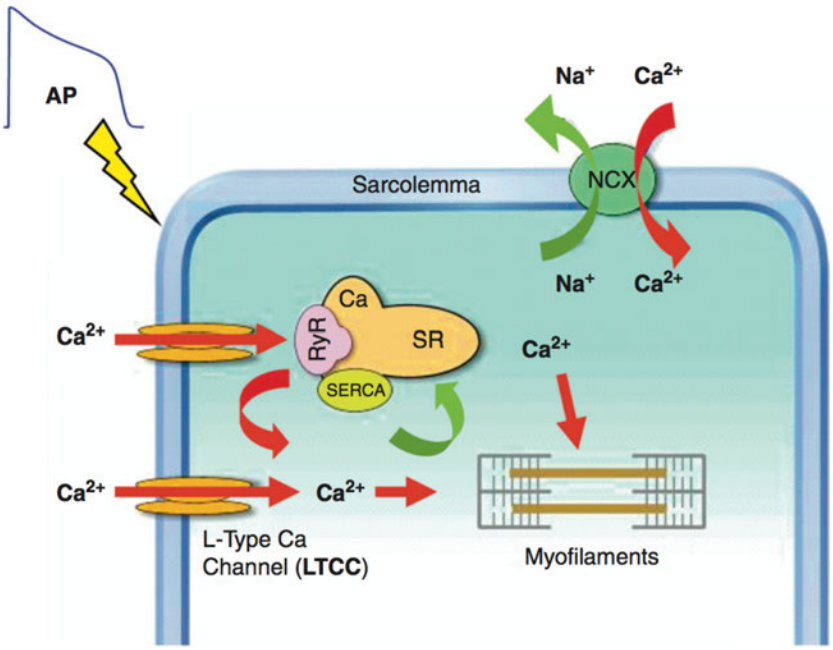

Figure 13. Calcium handling in the fish cardiomyocyte (Shiels 2011). The sarcolemma (SL) is being excited by an action potential (AP), which opens L-type Ca^{2+} channels (LTCC) in the cell membrane allowing Ca influx (red arrows) down its concentration gradient into the cell. Calcium can also enter the cell via reverse-mode Na^{+}–Ca^{2+} exchange (NCX). Calcium influx can trigger calcium release from the sarcoplasmic reticulum (SR) through ryanodine receptors (RyR). Together, these calcium influxes cause a transient rise in calcium that initiates contraction at the myofilaments. Relaxation occurs when calcium is removed from the cytosol (green arrows) either back across the SL via forward-mode NCX or back into the SR via the SR Ca^{2+}-pump (SERCA). With permission of Elsevier.

As for cardiac action potentials, Ca^{2+} handling during excitation-contraction coupling depends on the environmental temperature (Shiels 2011; Vornanen 2016). The amplitude of the rising phase of the Ca^{2+} transient is correlated with the temperature: warm temperatures tend to increase the rate of rise of the Ca^{2+} transient and low temperatures tend to decrease the rate. This observation is partially caused by the L-type Ca^{2+} channels, which show increased kinetics at warm temperatures (Shiels 2011). Certain hormones can also play a role, such as epinephrine, which stimulates Ca^{2+} influx, and can counteract the effect of low temperatures when higher cardiac output is needed. In contrast to L-type Ca^{2+} channels, the activity of NCX is not significantly affected by the environmental temperature. However, the activity of SERCA is very temperature-

dependent and its activity decreases markedly when temperature decreases (Shiels 2011). In this case as well, epinephrine can counteract this depression effect of cold temperatures by activating phospholamban, an accessory protein attached to SERCA (Shiels 2011).

2.3.6. Cardiovascular control: innervation of the zebrafish heart.

As in mammals, cardiac output of zebrafish is regulated based on the body's oxygen and metabolic demands and oxygen supply. The autonomic nervous system is the main controller of cardiac output by regulating heart rate and contractility, and is composed of the cranial limb or parasympathetic limb that causes cardioinhibition, and the spinal limb or sympathetic limb that causes cardioexcitation (Figure 14) (Nilsson 2011; Zaccone et al. 2011; Stoyek et al. 2015). Each pathway is composed of two neurons, the preganglionic and postganglionic neurons.

For the cranial autonomic limb, preganglionic neurons originate in vagal motor nuclei of the brainstem and project in the vagus nerve to synapse on postganglionic neurons in the intracardiac nervous system (Stoyek et al. 2015). Between the pre- and postganglionic neurons, the neurotransmitter ACh is released in the synaptic junction acting at postsynaptic nicotinic receptors. ACh also is released at the synaptic junction between postganglionic neurons and the myocardium, but it binds to muscarinic receptors (Stoyek et al. 2015).

For the spinal autonomic limb, preganglionic neurons originate in spinal cord

nuclei and their axons leave the cord to synapse on somata of postganglionic neurons in the paravertebral ganglia. ACh is released at the preganglionic synaptic junctions acting on nicotinic receptors, and epinephrine or norepinephrine is released at the postganglionic synaptic junction acting on adrenergic receptors (Stoyek et al. 2015). Although the vagus is only parasympathetic at its origin, it receives postganglionic fibres from the sympathetic chain in the head region, creating the vagosympathetic trunk (Zaccone et al. 2011).

In teleost fish, chromaffin cells controlled by preganglionic neurons also cause cardioexcitation by releasing catecholamines into the bloodstream (Figure 14) (Nilsson 2011).

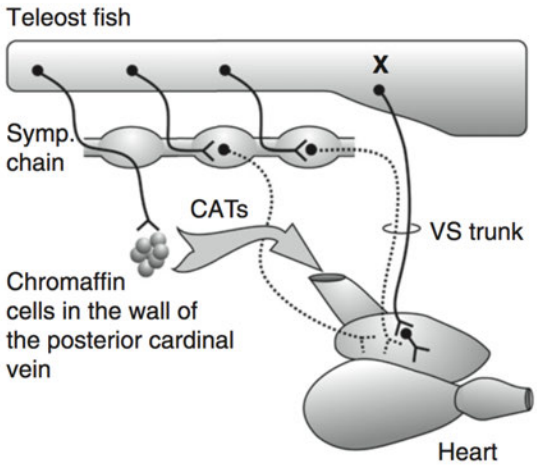

Figure 14. Autonomic cardiac control in teleost fish (Nilsson 2011). CATs: catecholamines; Symp: sympathetic; VS: vagosympathetic; X: vagus. With permission of Elsevier.

The intracardiac nervous system in the zebrafish has been described in detail by Stoyek et al. (2015, *in press*). This work showed that all cardiac chambers were innervated using the pan-neuronal markers AcT and Hu (Figure 15). A major nerve

plexus called the sinoatrial plexus is located at the sinoatrial junction and receives inputs from the cardiac vagosympathetic rami. A few of these rami also project to the atrial wall and the atrioventricular junction. A second nerve plexus also is present at the atrioventricular junction surrounding the valve. The ventricle and bulbus arteriosus also are innervated by axons arising from the venous pole or entering the heart along the aorta.

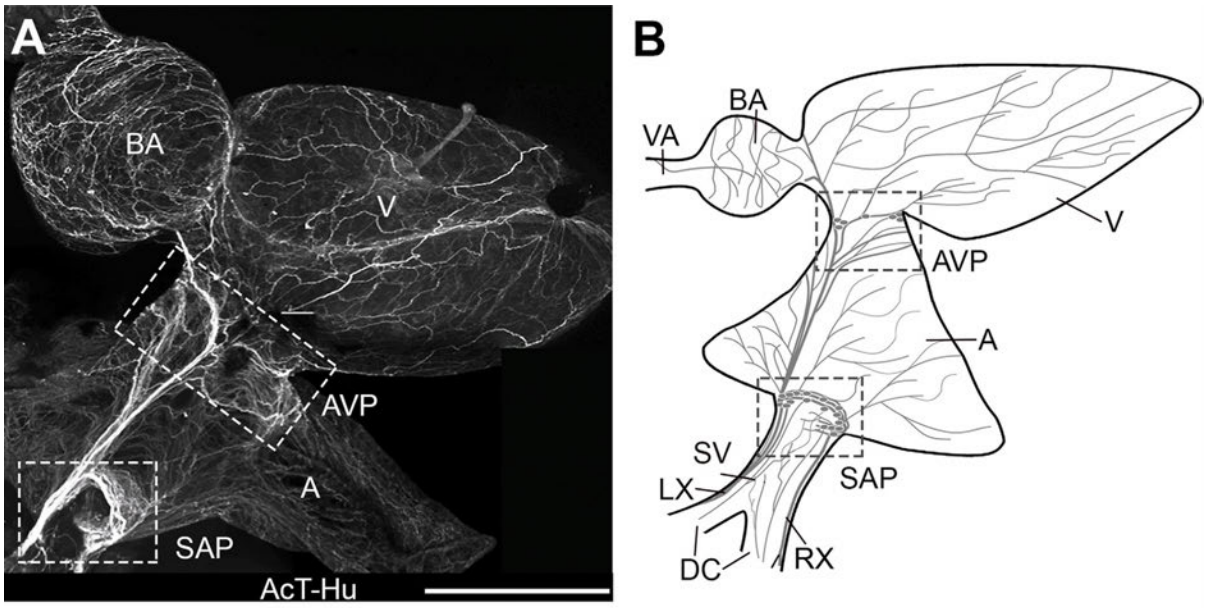

Figure 15. Organization of intracardiac nervous system demonstrated with acetylated tubulin (AcT) and human neuronal protein (Hu) immuhistochemistry (Stoyek et al. 2015). A,B: Whole mount of heart (A) and schematic (B) show an overview of the chambers of the heart and the major elements of cardiac innervation. Blood passes serially from the paired ducts of Cuvier (DC) into the sinus venosus (SV), through the sinoatrial valves and into the atrium (A), then into the ventricle (V), the bulbus arteriosus (BA), and the ventral aorta (VA) to the gills. The lower-boxed areas in A and B correspond to the region containing the sinoatrial valve, where the sinoatrial plexus (SAP) is located. The upper-boxed areas correspond to the region of the atrioventricular plexus (AVP) at the atrioventricular junction. RX, LX: right and left vagosympathetic trunks. With permission of John Wiley and Sons.

Cholinergic innervation was demonstrated using immunoreactivity for choline acetyltransferase (ChaT), an enzyme involved in ACh synthesis, as well as an antibobody against vesicular acetylcholine transporter (VAChT) (Stoyek et al. 2015). The vast

majority of neurons in the sinoatrial region (sinoatrial plexus) showed uptake with ChaT and VAChT and thus were determined to be cholinergic. Muscarinic cholinergic type 2 receptors (M_2R) were also identified using immunohistochemical methods mainly in the sinoatrial and atrioventricular junctions where putative pacemaker cells were determined to be, as well as in the atrial and ventricular myocardium (Stoyek et al. *in press*). The density of M_2R appeared to be significantly higher in the atrial myocardium than in the ventricular myocardium. All these regions also expressed adrenergic β_2 receptors, but the density of this receptor was higher in the ventricular myocardium than in the atrial myocardium (Stoyek et al. *in press*).

In summary, the zebrafish heart has been increasingly used as a model of mammalian, and especially human cardiac function. Zebrafish have similar properties to human hearts with respect to heart rate and action potential duration and morphology, although they differ with respect to the cardiac structure and ultrastructure and the molecular basis of the components of some cardiac ionic currents (Genge et al. 2016). On the whole, zebrafish are an attractive and useful model to study human electrophysiology. For the present study involving fish kills, they also appear to be a representative model for freshwater fish in general.

To test the hypothesis that selected environmental toxicants lead to increased fish morbidity and mortality by precipitating cardiac rhythm disturbances, adult zebrafish hearts were exposed to selected toxicants *in vitro* in order to characterize their effects on action potential morphology.

3. Materials and methods

3.1. Animals

Wild-type zebrafish were obtained from two commercial suppliers (Aquatron Laboratory, Dalhousie University, Halifax, NS and Pet Culture, Charlottetown, PE). They were maintained in separate 20 L glass aquaria (40 x 20 x 25 cm) at a stocking density of maximum 1.5 fish/L. Temperature was maintained at approximately 27 °C by submersible heaters. The water was filtered through multistage external power filters with mechanical, chemical and biological components. Water aeration was provided using air stones. The light cycle was 10 hours on 14 hours off and fish were fed flake food daily (Nutrafin Max, Hagen, Montreal, QC). The mean ± standard deviation fish weight was 1.09 g ± 0.41 (based on a sample of 20 fish from both providers). All fish were maintained and treated according to ethical guidelines of the CCAC; this project was approved by the University of Prince Edward Island Animal Care Committee (Protocol number: 13-020; File number: 6005334).

3.2. Procedures common to all experiments

- Fish euthanasia and heart explantation

Zebrafish were euthanized using a two-step procedure. They were first anesthetized using tricainemethanesulfonate (TMS; 100-150 mg/L of water bath, buffered with sodium bicarbonate using a 1:1 ratio) (Matthews and Varga 2012; Leary et al. 2013; Spears et al. 2014). Secondly, after cessation of opercular movements, their hearts

(including atrium, ventricle and bulbus arteriosus, Figure 16) were rapidly excised under stereomicroscopy following a midline sternotomy and were immediately transferred to a plexiglas chamber, where they were immobilized to the floor of the chamber using a bipolar stimulating electrode and superfused with Tyrode's solution (containing no TMS) at room temperature (approximately 20 °C) at a rate of approximately 30 ml/hour. All hearts were allowed to equilibrate for at least 15 min before intracellular action potentials were recorded (Nemtsas et al. 2010). Tyrode's solution was of the following composition (in mM): NaCl 124, KCl 4, $CaCl_2$ 0.5, $MgCl_2$ 0.7, $NaHCO_3$ 24, $NaHPO_4$ 0.9, and D-glucose 5.5. $CaCl_2$ concentration was reduced in order to decrease contractility and obtain more stable recordings. Although a stimulating electrode was used to immobilize the heart, no stimulation was used for the purpose of the present study.

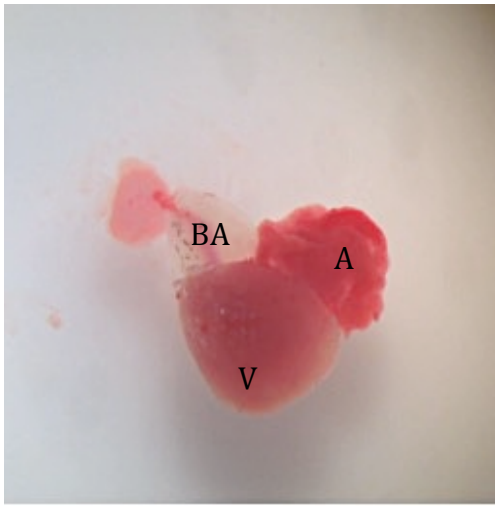

Figure 16. Adult zebrafish heart after explantation from the throracic cavity. The heart measures approximately 1 mm in diameter. A: atrium; V: ventricle; BA: bulbus arteriosus.

- Action potential recordings

The setup is shown in Figure 17. Transmembrane action potentials were recorded with sharp machine-pulled glass capillary electrodes (1 mm diameter borosilicate

capillaries, World Precision Instruments, Saratosa, FL) filled with 3M KCl connected to an amplifier (Duo 773,World Precision Instruments, Saratosa, FL) via a Ag/AgCl wire and a probe (712P, World Precision Instruments, Saratosa, FL). The reference electrode (Ag/AgCl pellet, World Precision Instruments, Saratosa, FL) was immersed in the bath and connected to the amplifier. The amplifier was connected to an oscilloscope (2522A, BK Precision, Yorba Linda, CA) and to a personal computer. Each heart was visualized using a fixed stage upright microscope (Olympus BX51WP, Richmond Hill, ON) placed on a vibration isolation table (Technical Manufacturing Corporation, Peabody MA) in a custom-made Faraday cage, and recordings were obtained from the epicardial surface of the heart. The microelectrode was positioned using a hydraulic micromanipulator (MP285, Sutter Instrument Company, Novato, CA). Action potentials from stable impalements were recorded with a sampling rate of 1 or 10 kHz using a custom written data acquisition program (Real Time Experiment Interface RTXI, rtxi.org) and off-line analysis was performed using custom-written programs written in MATLAB (MathWorks, Natick, MA). Measured parameters included APD 90, APD 50 and APA. For each recording, parameters were measured from 10 consecutive action potentials and were averaged. The solutions used for superfusion were contained in 60 mL syringes and switched manually using three-way stopcocks. All treatments were diluted in Tyrode's solution (same formula as above). When solutions were switched (from plain Tyrode's solution to a treatment), action potential parameters were measured only once a stable morphology could be visualized on the oscilloscope (typically 15-30 min after switching).

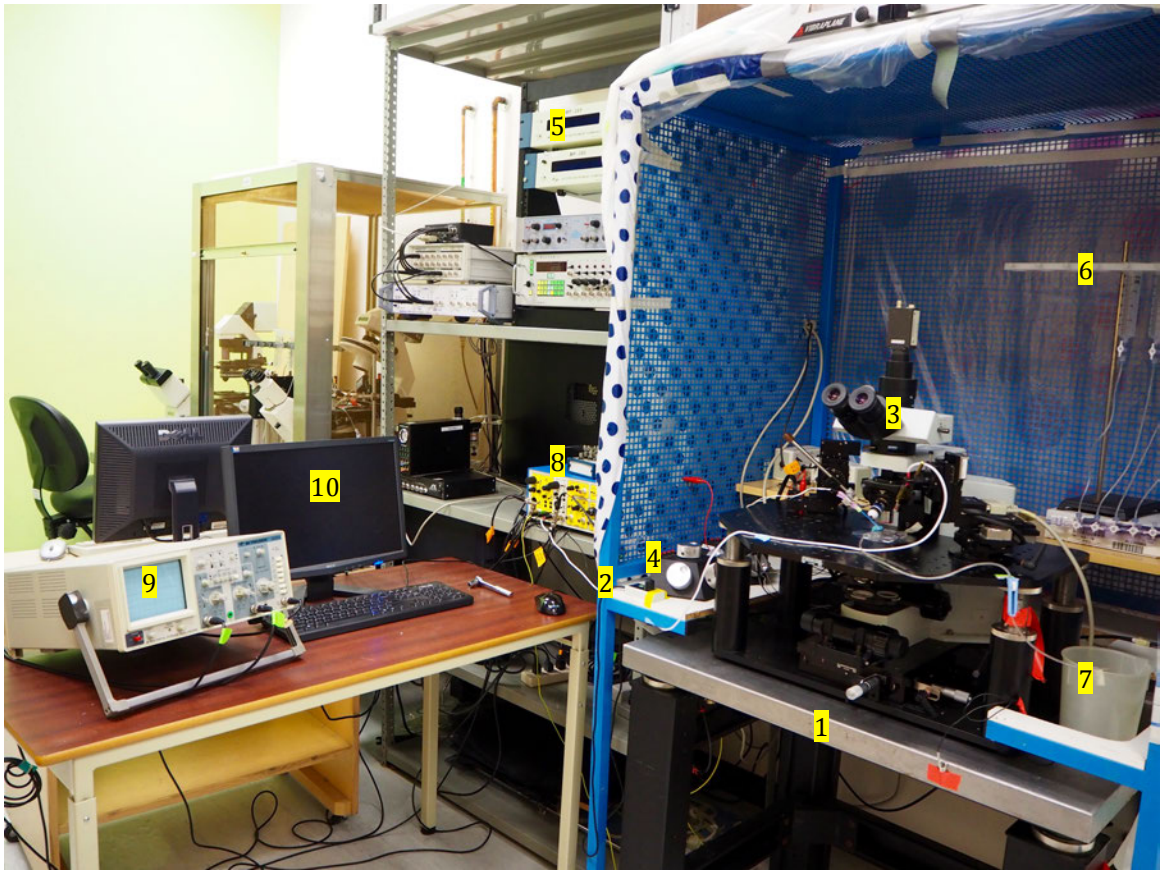

Figure 17. Intracellular action potential recording setup. 1: vibration isolation table; 2: supertable with Faraday cage; 3: microscope; 4: hydraulic micromanipulator; 5: controller unit for hydraulic micromanipulator; 6: superfusion system; 7: waste; 8: amplifier; 9: oscilloscope; 10: personal computer.

3.3. Treatments

All treatments performed are summarized in Table 4. The compounds that were tested are summarized in Table 5.

3.3.1. Choice of toxicants to investigate

The choice of toxicants to investigate was based on the list of agricultural pesticides commonly used in PEI, as well as past fish kills in PEI for which specific pesticides have been identified in run-offs and may have contributed to fish mortality:

- Chlorothalonil (2,4,5,6-tetrachloro-1,3-benzenedicarbonitrile)

Chlorothalonil is a broad-spectrum organochlorine fungicide and mildewicide extensively used on PEI's potato crops (Van Scoy and Tjeerdema 2014; DCLE 2015c). It has been suspected of contributing to several fish kills in PEI over the past 20 years (Mutch 2002; MacPhail 2013). The effect of chlorothalonil on the ventricular action potential morphology was qualitatively assessed using a concentration found in PEI run-off (3.8 nM or 0.2 μg/ml) and with a high concentration (94.0 nM or 5 μg/ml) (Purcell and Giberson 2007). No visible change of action potential morphology was identified with a low concentration and the effect seen with a high concentration (mainly shortening of APD) was similarly seen when hearts were exposed to chlorothalonil's vehicle, acetonitrile, exclusively. Based on these preliminary observations, further experiments with this pesticide were not pursued.

- Acetylcholinesterase inhibitors (AChEIs)

AChEIs such as organophosphates or carbamates are very commonly used as pesticides in agriculture and cause toxic effects due to the accumulation of the neurotransmitter ACh at parasympathic neuroeffector junctions (Roberts and Reigarts 2013). Organophosphates primarily act by phosphorylation of the acetylcholinesterase enzyme (AChE), while carbamates act by carbamylation of AChE (Roberts and Reigarts

2013). The decision to investigate the effect of AChEIs on zebrafish action potential morphology was motivated by the extensive use of this class of pesticide in PEI (DCLE 2015c). Indeed, mancozeb, a dithiocarbamate fungicide, represents the leading pesticide sold in PEI in kilograms per year and was suspected to contribute to several fish kills in PEI (MacPhail 2013; DCLE 2015c). Phorate is the most commonly sold organophosphate (in kilograms per year) in PEI (DCLE 2015c). Moreover, a study from Abramochkin et al. (2008) revealed that exposure of cod atria to high concentrations of ACh caused suppression of electrical activity, an effect called the "cholinergic non-excitability phenomenon". Preliminary qualitative experiments revealed a visible effect on atrial action potential morphology of ACh at a high concentration (10 μM) and further experiments evaluating the effects of ACh, a documented AChEI, physostigmine, and the commonly used pesticides mancozeb and phorate were pursued. Action potential recordings were performed on the atrium, because cholinergic innervation appears more prominent in the atrium than in the ventricle (Newton 2010; Stoyek et al. 2015).

3.3.2. Treatments with acetylcholine (treatments 1a, 1b and 1c)

Because the effect of ACh on the atrial action potential morphology had not been previously investigated in zebrafish, initial experiments consisted of evaluating the effects of a low concentration of ACh (1 μM, n = 5, treatment 1a) as well as a high concentration of ACh (10 μM, n = 6, treatment 1b) on APD 90, APD 50 and APA. The same impalements were maintained throughout these experiments.

The reversible effect of ACh was assessed after exposure to a high concentration of ACh (treatment 1b) while maintaining the same atrial impalements. After recordings were obtained following exposure to ACh 10 μM, all preparations were superfused with Tyrode's solution until the action potential morphology had stabilized (approximately 15-30 min). APD 90, APD 50 and APA, were again measured after ACh was washed-out.

In order to assess whether ACh was acting via muscarinic receptors, another set of experiments was performed (n = 5). Each heart was exposed to a high concentration of ACh (10 μM), followed by atropine (1 μM, antagonist of the muscarinic receptors) + ACh (10 μM) (treatment 1c). Because the same impalement could not be maintained during all experiments of this set, only APD 90 was measured at baseline (Tyrode's solution), after exposure to ACh (10 μM), and after exposure to atropine (1 μM) + ACh (10 μM).

3.3.3. Treatment with physostigmine (treatment 2)

The effect of a documented AChEI, physostigmine (50 μM), was assessed on APD 90, APD 50 and APA in the presence of a low concentration of ACh (1 μM) (n = 6). The same atrial impalements were maintained throughout these experiments. It has been previously documented that physostigmine at a concentration of 50 μM significantly reduces AChE activity in zebrafish embryos (Küster 2005).

3.3.4. Treatment with mancozeb (treatment 3)

The effect of the pesticide mancozeb (18.5 μM or 10 mg/L) was assessed on APD 90, APD 50 and APA in the presence of a low concentration of ACh (1 μM) (n = 6). The same atrial impalements were maintained throughout these experiments.

3.3.5. Treatment with phorate (treatment 4)

The effect of the pesticide phorate (38.4 μM or10 mg/L) was assessed on APD 90, APD 50 and APA in the presence of a low concentration of ACh (1 μM) (n = 6). The same atrial impalements were maintained throughout these experiments.

Table 4: Summary of the different treatment protocols.

Treatment group	Treatment performed	Number of experiments (n)
1a	ACh 1 μM	5
1b	ACh 10 μM, followed by washing with Tyrode's solution	6
1c	ACh 10 μM, followed by atropine 1 μM + ACh 10 μM	4
2	Physostigmine 50 μM + ACh 1 μM	5
3	Mancozeb 18.5 μM (10 mg/L) + ACh 1 μM	6
4	Phorate 38.4 μM (10 mg/L) + ACh 1 μM	6

Table 5: Mechanisms of action, chemical properties, and structures of the tested compounds (INERIS 2017; NCBI 2017).

Molecule	Mechanism of action and chemical properties	Structure
Acetylcholine chloride	- Cholinergic receptor agonist - MW: 181.7 g/mol - Solubility in water: 100 mg/mL	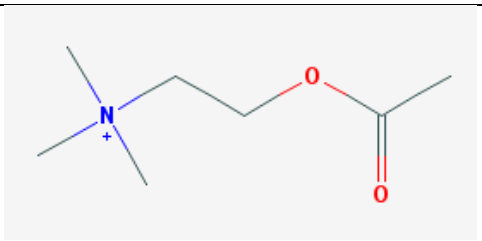 Cl^-
Physostigmine hemisulfate	- Cholinesterase inhibitor (carbamate) - MW: 324.4 g/mol - Solubility in water: 32 g/L	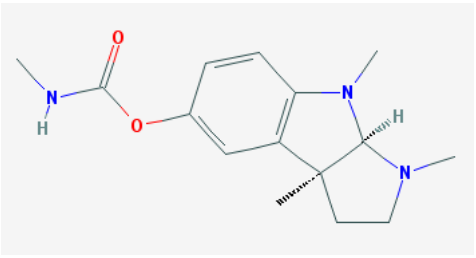 $1/2H_2SO_4$
Mancozeb	- Cholinesterase inhibitor (carbamate) - MW: 541.1 g/mol - Solubility in water: 2-20 mg/L	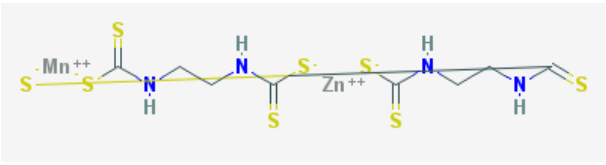
Phorate	- Cholinesterase inhibitor (organophosphate) - MW: 260.4 g/mol - Solubility in water: 50 mg/L	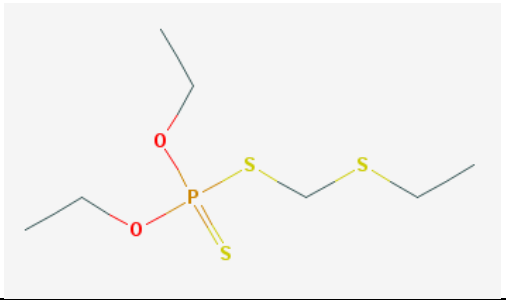

3.4. Statistical Analysis

All statistical analysis was performed using Prism 7 for Mac OS X (GraphPad Software, La Jolla, CA). Each treatment was considered to be an independent set of independent experiments (one fish per experiment). For treatments 1a, 3 and 4, differences between baseline values and post-treatment values for each parameter (APD

90, APD 50 and APA) were assumed to be normally distributed based on Shapiro-Wilk normality tests and graphical examination of residuals, and were compared using paired t-tests. Statistical significance was defined as $P < 0.05$. In order to address potential Type I error, it was mentioned whether or not statistically significant results would withstand Bonferroni's correction. Bonferroni's correction was applied to paired t-test results by dividing the alpha of 0.05 by 3, the number of variables tested within each treatment (APD 90, APD 50 and APA) to obtain a lower *P*-value of 0.0167.

Non-parametric Friedman tests were used for treatments 1b and 1c (In these cases assumptions for repeated measures ANOVA could not be met). Multiple comparisons were performed using Dunn's tests.

Because the experiments of treatment 1b were chronologically performed first, a power analysis based on the results of this treatment revealed that at least 4 experiments were necessary to detect a significant change ($P < 0.05$) in APD 90 with a power of 80% (G*Power, version 3.1.9.2, Heinrich Heine Universität, Düsseldorf). Based on these results, at least 4 experiments (4 different fish) were used for other treatments (1a, 2, 3 and 4).

For each parameter (APD 90, APD 50 and APA), treatments 1b, 3 and 4 were compared with treatment 1a using a one-way analysis of variance (ANOVA) with Dunnett's adjustments for multiple comparisons. Homogeneity of variance was first calculated as the ratio between largest and smallest group standard deviation, which should not exceed 2. Normal distribution of residuals was determined graphically.

4. Results

4.1. Treatments with acetylcholine (treatments 1a, 1b and 1c)

- Treatment 1a

A low concentration of ACh (1 μM) caused a significant reduction in APD 90 and in APD 50, but no significant reduction in APA in atrial myocytes (Table 6, Figure 18). These results did withstand Bonferroni's correction.

- Treatment 1b

A high concentration of ACh (10 μM) caused a significant reduction in APD 90, in APD 50, and in APA in atrial myocytes (Table 7, Figure 19). The effect of ACh persisted during the immediate washing period for three out of five experiments, while it appeared reversible in two experiments. No significant difference could be identified between exposure to ACh and washing with Tyrode's solution for any of the action potential parameters.

- Treatment 1c

The effect of ACh (10 μM) on APD 90 was reversed with atropine, suggesting an effect of ACh on muscarinic receptors (Table 8, Figure 20).

Table 6. Atrial action potential parameters before and after exposure to acetylcholine (1 µM) – treatment 1a (n = 5).

	Baseline	ACh 1 µM	*P*-value
APD 90 (ms)	142.5 ± 11.2 (128.1-157.9)	106.2 ± 17.5 (88.1-134.3)	0.0107*†
APD 50 (ms)	117.5 ± 8.9 (109.6-131.8)	78.4 ± 19.8 (61.3-112.1)	0.0099*†
APA (mV)	104.3 ± 4.4 (98.5-109.6)	95.9 ± 5.5 (90.9-105.3)	0.0531

ACh: acetylcholine; APD 90: action potential duration at 90% repolarization; APD 50: action potential duration at 50% repolarization; APA: action potential amplitude. Baseline heart rate: 100 ± 39 bpm (66-164). Results expressed as mean ± standard deviation (range); *: $P < 0.05$; †: $P < 0.0167$ (after Bonferroni's correction). t-values (degrees of freedom) for APD 90, APD 50 and APA: 4.52 (4), 4.61 (4), 2.71 (4), respectively.

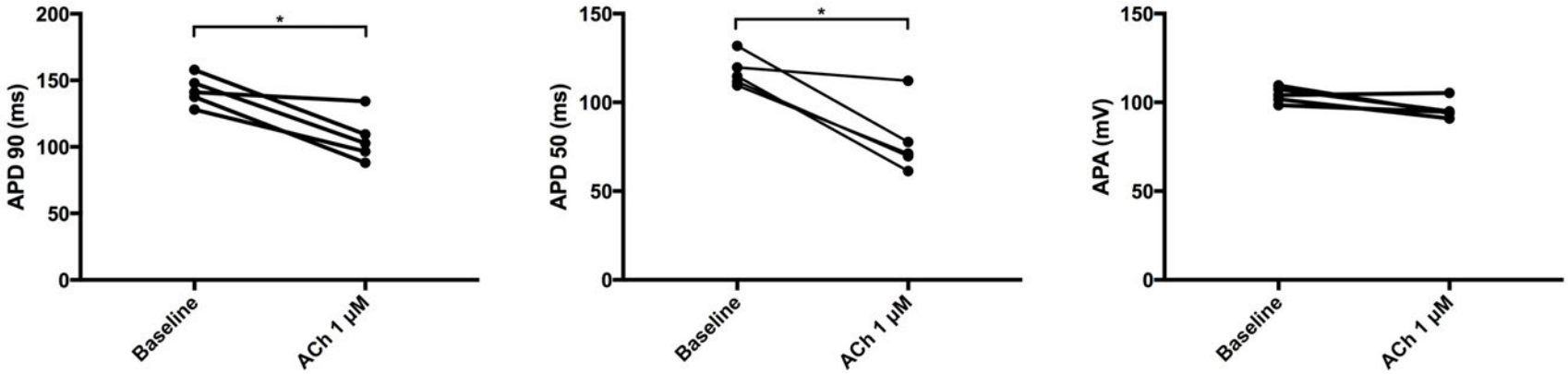

Figure 18. Atrial action potential parameters before and after exposure to acetylcholine (1 µM) – treatment 1a (n = 5). ACh: acetylcholine; APD 90: action potential duration at 90% repolarization; APD 50: action potential duration at 50% repolarization; APA: action potential amplitude; *: $P < 0.05$.

Table 7. Atrial action potential parameters before and after exposure to acetylcholine (10 µM) followed by a washing period – treatment 1b (n = 6).

	Baseline	ACh 10 µM	Washing	*Adjusted P*-value Baseline vs ACh	*Adjusted P*-value ACh vs Washing	*Adjusted P*-value Baseline vs Washing
APD 90 (ms)	114.7 ± 35.5 (69.9-176.0)	59.2 ± 41.3 (29.4-133.6)	75.6 ± 54.6 (32.6-157.6)	0.0045*	0.1299	0.7446
APD 50 (ms)	86.2 ± 21.5 (50.4-109.6)	29.7 ± 23.1 (12.6-71.3)	46.3 ± 43.9 (13.1-109.3)	0.0117*	0.4467	0.4467
APA (mV)	93.6 ± 10.4 (81.7-104.1)	71.8 ± 21.6 (46.6-96.8)	88.4 ± 12.4 (72.6-102.2)	0.0117*	0.0628	>0.9999

ACh: acetylcholine; APD 90: action potential duration at 90% repolarization; APD 50: action potential duration at 50% repolarization; APA: action potential amplitude. Baseline heart rate: 111 ± 19 bpm (74-125). Results expressed as mean ± standard deviation (range); vs: versus; *: $P < 0.05$. Friedman statistics for APD 90, APD 50 and APA: 10.33, 8.33, 9.33, respectively.

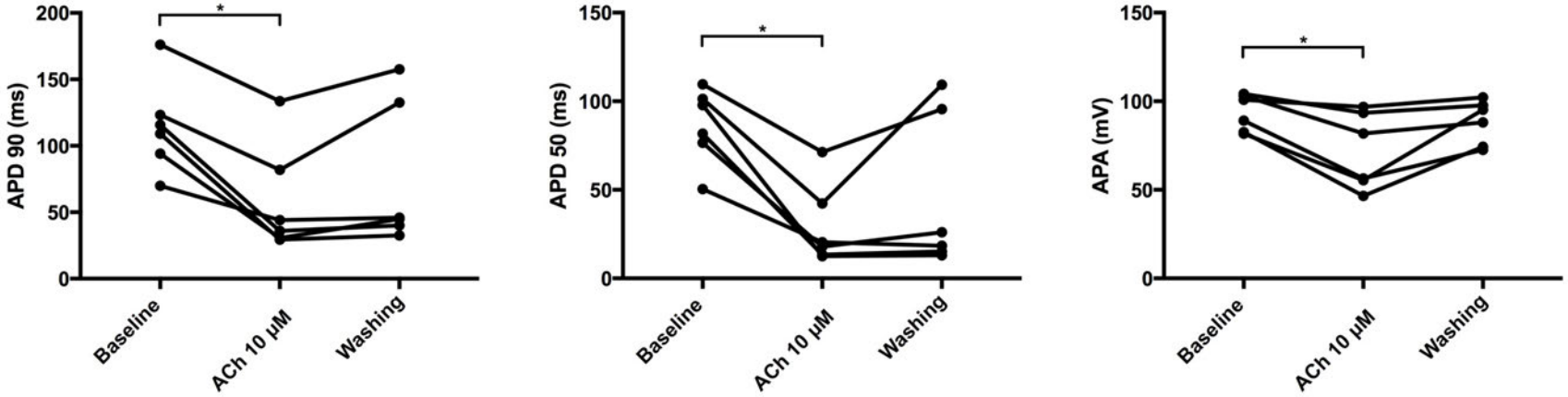

Figure 19. Atrial action potential parameters before and after exposure to acetylcholine (10 µM) followed by a washing period – treatment 1b (n = 6). ACh: acetylcholine; APD 90: action potential duration at 90% repolarization; APD 50: action potential duration at 50% repolarization; APA: action potential amplitude; *: $P < 0.05$.

Table 8. Atrial action potential parameters before and after exposure to acetylcholine (10 µM) followed by atropine (1 µM) – treatment 1c (n = 4).

	Baseline	ACh 10 µM	Atropine 1 µM + ACh 10 µM	*Adjusted P*-value Baseline vs ACh	*Adjusted P*-value Atropine + ACh vs ACh	*Adjusted P*-value Baseline vs Atropine + ACh
APD 90 (ms)	118.8 ± 24.6 (83.3-138.0)	75.83 ± 37.54 (31.8-121.3)	155.3 ± 26.84 (129.6-191.6)	0.4719	0.0140*	0.4719

ACh: acetylcholine; APD 90: action potential duration at 90% repolarization. Baseline heart rate: 109 ± 49 bpm (66-176). Results expressed as mean ± standard deviation (range); vs: versus; *: $P < 0.05$. Friedman statistic for APD 90: 8.

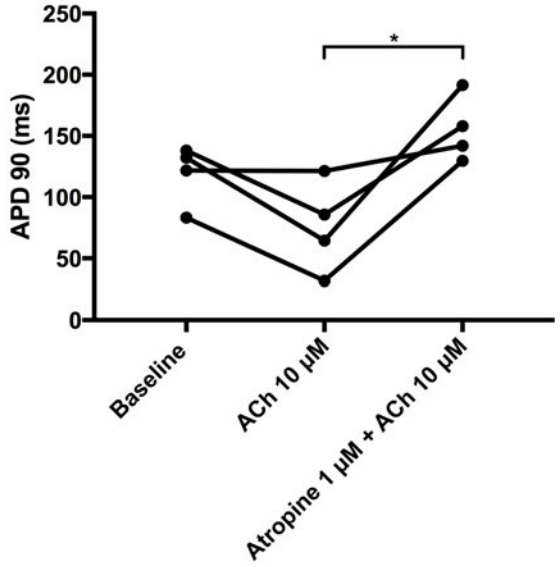

Figure 20. Atrial action potential parameters before and after exposure to acetylcholine (10 µM) followed by atropine (1 µM) – treatment 1c (n = 4). ACh: acetylcholine; APD 90: action potential duration at 90% repolarization; *: $P < 0.05$.

4.2. Treatment with physostigmine (treatment 2)

Physostigmine (50 μM), in presence of a low concentration of ACh (1 μM), caused near-complete suppression of electrical activity in atrial myocytes in all experiments (Figures 21 and 22). The very short and narrow atrial action potentials were not detectable by the program used for analysis. Baseline values are presented in Table 9.

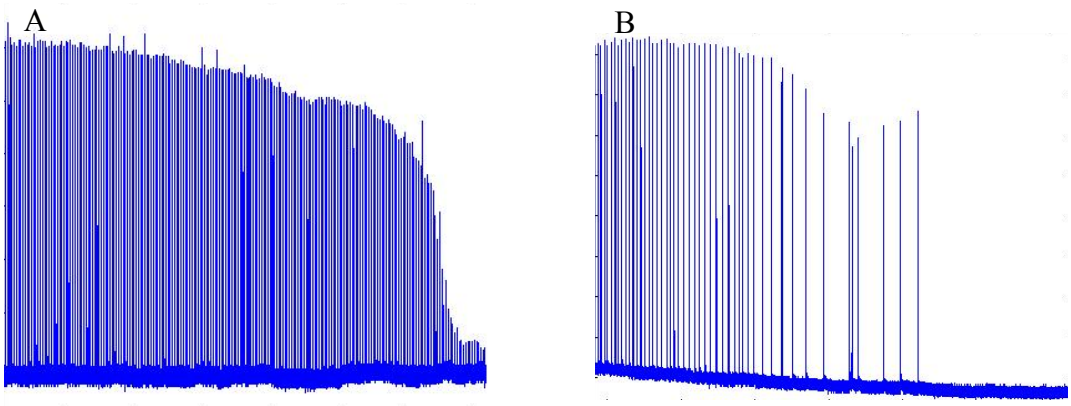

Figure 21. Suppression of atrial action potential induced by physostigmine (50 μM) in presence of a low concentration of acetylcholine (1 μM). A: Experiment 1 of treatment 2 (action potential parameters at baseline: APD 90: 133.1 ms, APD 50: 99.2 ms, APA: 85.8 ms); B: Experiment 3 of treatment 2 (action potential parameters at baseline: APD 90: 101.8 ms, APD 50: 80.9 ms, APA: 101.1 ms).

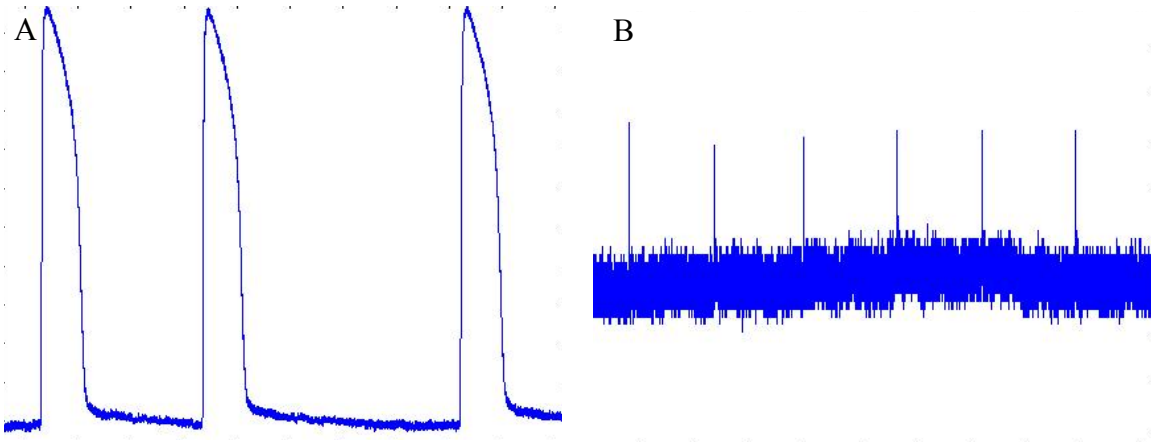

Figure 22. Change in action potential morphology induced by physostigmine (50 μM) in presence of a low concentration of acetylcholine (1 μM). A: Atrial action potential at baseline; B: Atrial action potential after exposure to physostigmine (50 μM) +ACh (1 μM). These recordings are magnified images of the experiment shown in figure 21A. Action potential parameters at baseline: APD 90: 133.1 ms, APD 50: 99.2 ms, APA: 85.8 ms.

Table 9. Atrial action potential parameters at baseline – treatment 2 (n = 5).

	Baseline
APD 90 (ms)	121.1 ± 24.7 (91.5-153.1)
APD 50 (ms)	92.7 ± 22.2 (66.9-126.2)
APA (mV)	89.1 ± 12.4 (76.5-103.1)

APD 90: action potential duration at 90% repolarization; APD 50: action potential duration at 50% repolarization; APA: action potential amplitude. Baseline heart rate: 103 ± 30 bpm (83-153). Results expressed as mean ± standard deviation (range).

4.3. Treatment with mancozeb (treatment 3)

Mancozeb (18.5 μM), in presence of a low concentration of ACh (1 μM), caused a significant reduction in APD 90 and in APD 50 in atrial myocytes (Table 10, Figure 23). This reduction was modest and statistical significance did not withstand Bonferroni's correction. No significant change in APA was observed.

4.4. Treatment with phorate (treatment 4)

Phorate (38.4 μM), in presence of a low concentration of ACh (1 μM), caused a significant reduction in APD 90, in APD 50, and in APA in atrial myocytes (Table 11, Figure 24). The reductions in APD 90 and APD 50 did withstand Bonferroni's correction. The reduction in APA was modest and statistical significance did not withstand Bonferroni's correction for this parameter.

Table 10. Atrial action potential parameters before and after exposure to mancozeb (18.5 µM) + acetylcholine (1 µM) – treatment 3 (n = 6).

	Baseline	Mancozeb 18.5 µM + ACh 1 µM	*P*-value
APD 90 (ms)	129.2 ± 20.4 (91.69-144.6)	99.8 ± 30.7 (63.0-137.9)	0.0493*
APD 50 (ms)	105.3 ± 17.4 (72.9-121.4)	75.7 ± 33.7 (34.0-116.5)	0.0374*
APA (mV)	96.3 ± 8.4 (88.4-107.3)	100.0 ± 8.8 (86.4-109.9)	0.4275

ACh: acetylcholine; APD 90: action potential duration at 90% repolarization; APD 50: action potential duration at 50% repolarization; APA: action potential amplitude. Baseline heart rate: 78 ± 23 bpm (45-99). Results expressed as mean ± standard deviation (range); *: $P < 0.05$; †: $P < 0.0167$ (after Bonferroni's correction). t-values (degrees of freedom) for APD 90, APD 50 and APA: 2.58 (5), 2.81 (5), 0.86 (5), respectively.

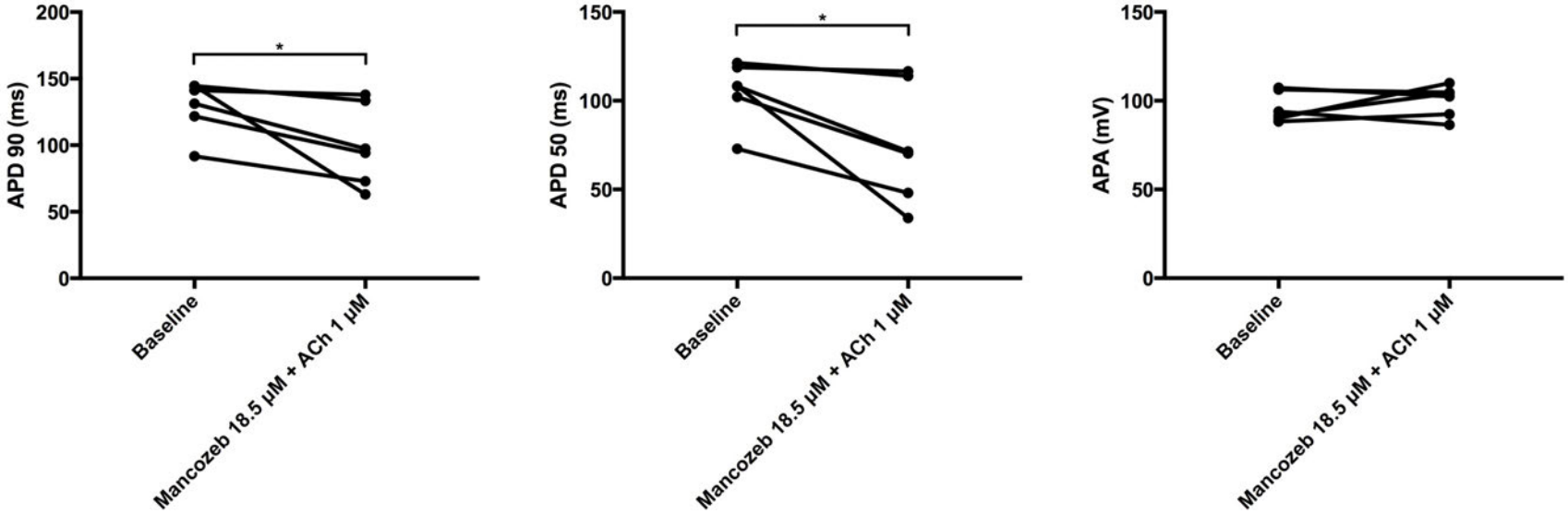

Figure 23. Atrial action potential parameters before and after exposure to mancozeb (18.5 µM) + acetylcholine (1 µM) – treatment 3 (n = 6). ACh: acetylcholine; APD 90: action potential duration at 90% repolarization; APD 50: action potential duration at 50% repolarization; APA: action potential amplitude; *: $P < 0.05$

Table 11. Atrial action potential parameters before and after exposure to phorate (38.4 µM) + acetylcholine (1 µM) – treatment 4 (n = 6).

	Baseline	Phorate 38.4 µM + ACh 1 µM	*P*-value
APD 90 (ms)	122.5 ± 5.7 (114.8-129.2)	75.8 ± 15.5 (57.1-96.6)	0.0010*†
APD 50 (ms)	99.6 ± 4.8 (93.2-106.8)	44.8 ± 16.4 (23.6-67.4)	0.0004*†
APA (mV)	94.6 ± 4.5 (88.0-98.8)	84.5 ± 10.6 (71.5-96.4)	0.0454*

ACh: acetylcholine; APD 90: action potential duration at 90% repolarization; APD 50: action potential duration at 50% repolarization; APA: action potential amplitude. Baseline heart rate: 94 ± 30 bpm (47-130). Results expressed as mean ± standard deviation (range); *: $P < 0.05$; †: $P < 0.0167$ (after Bonferroni's correction). t-values (degrees of freedom) for APD 90, APD 50 and APA: 6.91 (5), 8.31 (5), 2.65 (5), respectively.

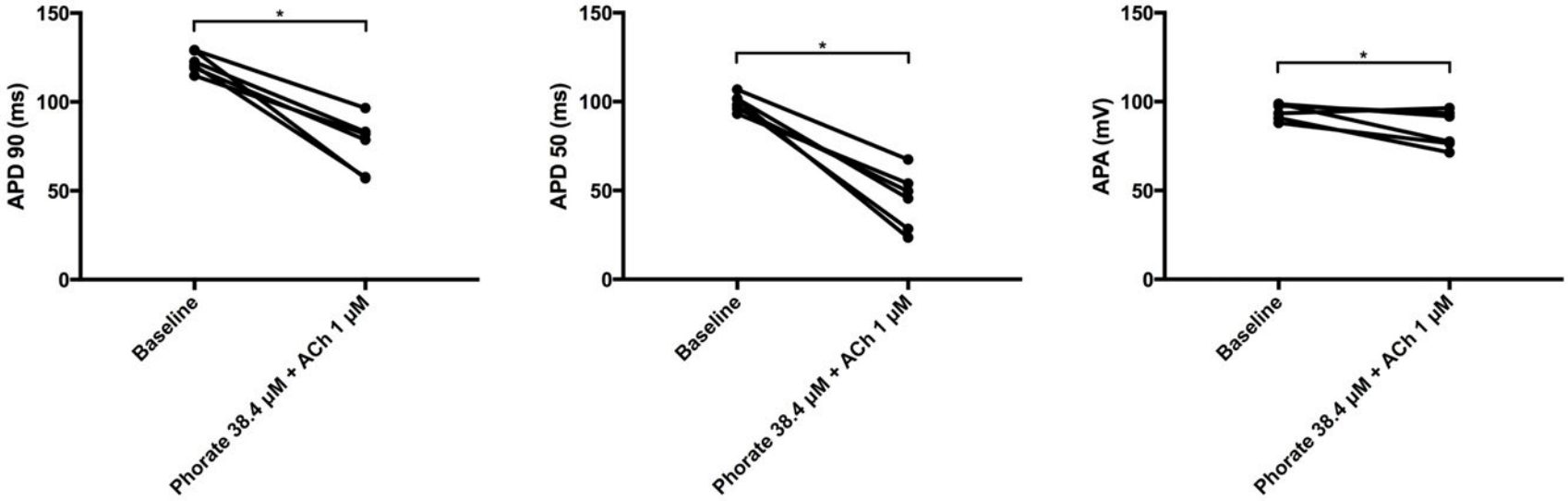

Figure 24. Atrial action potential parameters before and after exposure to phorate (38.4 µM) + acetylcholine (1 µM) – treatment 4 (n = 6). ACh: acetylcholine; APD 90: action potential duration at 90% repolarization; APD 50: action potential duration at 50% repolarization; APA: action potential amplitude; *: $P < 0.05$.

4.5. Between-group comparisons of atrial action potential parameters

The relative effects of treatments 1b, 3 and 4 were compared to the relative effect of treatment 1a on APD 90, APD 50 and APA. Physostigmine caused a dramatic effect on APD 90, APD 50 and APD with almost complete loss of electrical activity, and could not be included in the subsequent analysis.

- APD 90

All treatments caused a significant reduction in APD 90 (Figure 25). There was no significant effect of treatment on the relative change from baseline in APD 90 using a one-way ANOVA: $F(3,19) = 1.64$, $P = 0.21$.

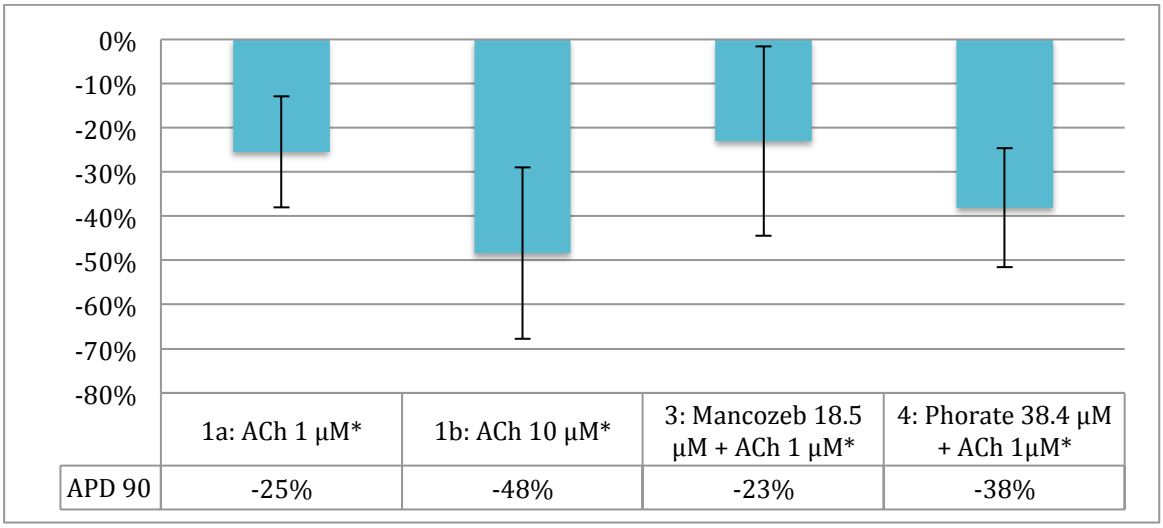

Figure 25. Relative change from baseline in action potential duration at 90% repolarization (APD 90). *: indicates significant change from baseline, $P < 0.05$.

- APD 50

All treatments caused a significant reduction in APD 50 (Figure 26). There was no significant effect of treatment on the relative change from baseline in APD 50 using a one-way ANOVA: $F(3,19) = 2.34$, $P = 0.11$.

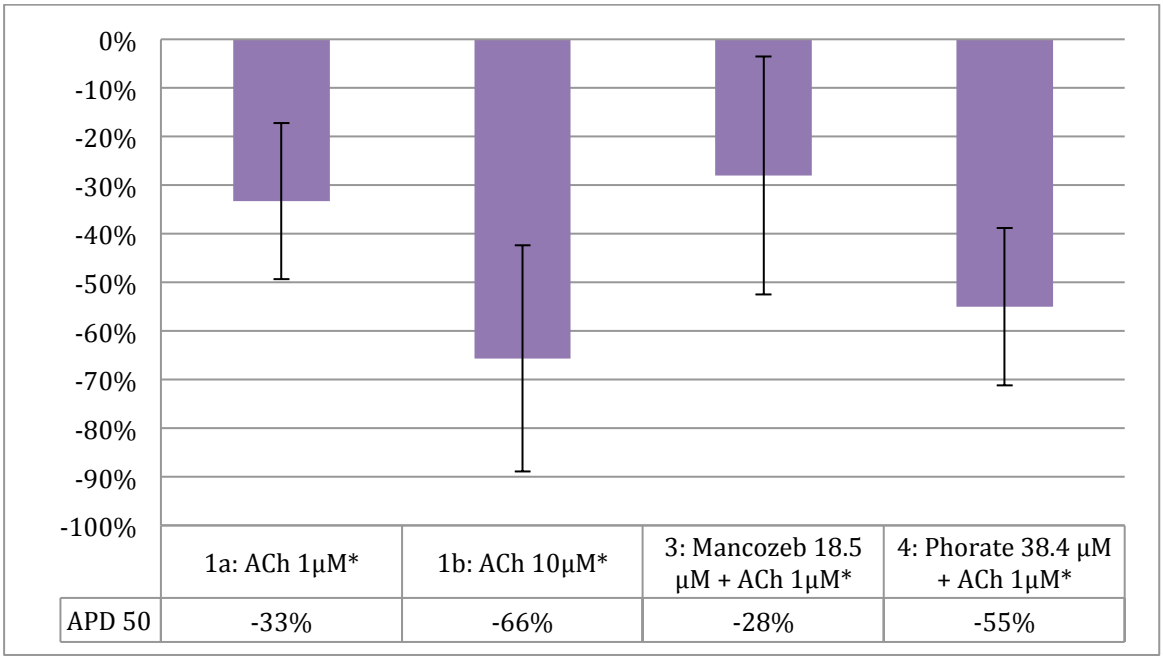

Figure 26. Relative change from baseline in action potential duration at 50% repolarization (APD 50). *: indicates significant change from baseline, $P < 0.05$.

- APA

Only treatments 1b (ACh 10 µM) and 4 (phorate 38.4 µM + ACh 10 µM) caused a significant decrease in APA (Figure 27). There was a significant effect of treatment on the relative change from baseline in APA using a one-way ANOVA: $F(3,19) = 6.37$, $P = 0.003$. However, there was no significant difference between the relative effects of treatment 1a (1 µM) and the relative effects of treatments 1b, 3 and 4 (1a-1b: $P = 0.10$; 1a-3: $P = 0.15$; 1a-4: $P = 0.99$).

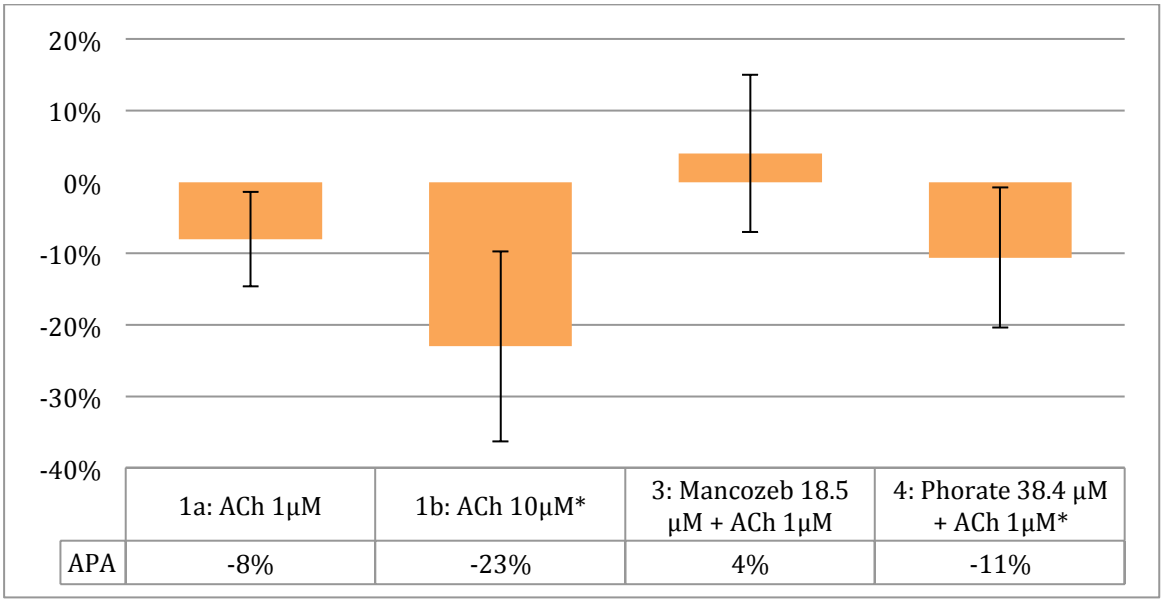

Figure 27. Relative change from baseline in action potential amplitude (APA). *: indicates significant change from baseline, $P < 0.05$.

5. Discussion

5.1. Overview of objectives

The primary goal of the present study was to test the hypothesis that selected environment toxicants lead to increased fish morbidity and mortality by depressing cardiac function, and more specifically by precipitating cardiac rhythm disturbances. To test this hypothesis, adult zebrafish hearts were used as models and exposed to selected toxicants *in vitro* in order to characterize their effects on action potential morphology.

Based on historical data on fish kills in PEI, pesticide sales statistics, and preliminary experiments, my work focused on evaluating the effects of cholinesterase-inhibiting pesticides, including the two main classes: organophosphates and carbamates. Due to the prominent cholinergic innervation of the zebrafish atrial myocardium, I used standard microelectrode techniques to record atrial action potentials exclusively. The effect of ACh on the atrial action potential morphology was described first. Although previous studies determined the effect of ACh on atrial action potential morphology in other fish species, this effect had not been previously evaluated in zebrafish and it is known that atrial cholinergic innervation varies among teleost species (Newton et al. 2013). Following these experiments, zebrafish hearts were exposed to AChEIs, including the documented AChEI physostigmine and pesticides commonly used in PEI: mancozeb and phorate. The results of my study are discussed below.

5.2. Effects of acetylcholine (treatments 1a, 1b and 1c)

In these experiments, I revealed the depressive effects of ACh on the atrial action potential in zebrafish. Indeed, exposure to low concentrations of ACh caused a significant reduction in atrial action potential duration (APD 90 and APD 50) and exposure to high concentrations of ACh also caused a significant reduction in APA. This phenomenon has been named cholinergic non-excitability and has been previously observed in the atrial myocardium of other teleosts including cod (*Gadus morhua*), carp (*Cyprinus carpio*), and trout (*Oncorhynchus mykiss*), as well as in frogs (*Rana temporaria* and *Rana cotesbeiana*) (Rozenshtraukh and Kholopov 1975; Giles and Noble 1976; Molina et al. 2007; Abramochkin et al. 2008; Abramochkin et al. 2009; Abramochkin et al. 2010). Cholinergic non-excitability appears to affect lower vertebrates only, because ACh has not been reported to alter APA in mammals or reptiles (Abramochkin et al. 2010). In dogs, for example, ACh only induces hyperpolarization of the resting membrane potential and shortening of APD (Calloe et al. 2013). It is worth mentioning that the graphs representing APD 90 and APD 50 followed the same pattern, suggesting that when APD 90 dramatically decreases APD 50 also dramatically decreases, and inversely.

The changes observed in atrial action potential morphology can lead to several deleterious consequences, including:

1) Reduced contractility caused by APD shortening, which in turn diminishes calcium influx during the plateau phase of the action potential (Ten Eick et al. 1976).

Although inotropy appeared subjectively depressed during experiments with ACh, the present study was not designed to quantitatively measure contractility.

2) Bradycardia or asystole. If a large proportion of the atrium becomes inexcitable, electrical conduction to the atrioventricular junction and ventricle may be interrupted and ventricular contraction may only rely on subsidiary ventricular pacemaker activity (escape rhythm). The heart rate generated by an escape focus is by definition slower than the sinus rate. Moreover, it has been demonstrated that ACh also reduces or even supresses the depolarization rate of cardiac pacemaker cells in fish, which can lead to asystole (Saito 1973). Optical mapping experiments revealed full cessation of electrical activity in approximately 60% of studied atrial zones after exposure to ACh (10 μM) in carp and frog (Abramochkin et al. 2010).

3) Initiation of reentry circuits and tachyarrhythmias. The effect of ACh is not uniform through the atrial myocardium, and this heterogeneity creates an arrhythmogenic substrate by facilitating the initiation and maintenance of reentry circuits (Abramochkin et al. 2010, Dobrev et al. 2014). Reentry is defined as continuous impulse propagation around a functional barrier (such as inexcitable areas of the atrial myocardium caused by ACh) or an anatomical obstacle. Moreover, one requirement for the maintenance of reentry is that the initially activated tissue regains excitability while the electrical impulse propagates around the reentry circuit. Recovery of excitability is more likely when the effective refractory period becomes shorter, as seen with a reduced APD duration (Dobrev et al. 2014). Lin et al. (2007) demonstrated the initiation of atrial tachyarrhythmias caused by ACh (1-10 μM) in tilapia fish. This mechanism has also

been demonstrated to initiate vagally induced atrial fibrillation in mammals and frogs (Dobrev et al. 2014; Abramochkin et al. 2010).

In mammals, ACh is known to alter action potential morphology via modulation of several ionic currents, including activation of the inwardly rectifying current $I_{K,ACh}$, suppression of I_{CaL}, and in pacemaker cell suppression of I_f (Ten Eick et al. 1976; Renaudon et al. 1997; Harvey and Belevych 2003; Dobrev et al. 2014). ACh modulates these currents via the activation of the muscarinic cholinoreceptors M_2R (Dobrev et al. 2014). Binding of ACh to M_2R leads to dissociation of G_i proteins and direct activation of the $I_{K,ACh}$ channels by $G_{\beta\gamma}$-subunits. The exact ionic mechanisms by which ACh alters atrial action potential morphology in fish are not fully understood yet, but several studies have suggested the presence of a strong inwardly rectifying current mediated by ACh in atrial myocardium (Molina et al. 2007, Nemtsas et al. 2010). Abramochkin et al. (2010) demonstrated that barium chloride ($BaCl_2$) completely prevented the onset of cholinergic non-excitability, including suppression of APA. Ba^{2+} is known to block channels responsible for $I_{K,ACh}$ and for the background inwardly rectifying current I_{K1} (Hassinen et al. 2008). Because ACh has not been shown to affect I_{K1} in fish, it is suspected that the suppression of APA is related to $I_{K,ACh}$ alterations (Harvey and Belevych 2003; Abramochkin et al. 2010). Furthermore, recent experiments in crucian carp (*Carassius carassisus*) and rainbow trout (*Oncorhynchus mykiss*) revealed the likely existence of a new cardiac inward rectifier current modulated by ACh, named $I_{K,ACh2}$. As opposed to $I_{K,ACh}$ and I_{K1}, $I_{K,ACh2}$ is mostly an outward current with only a small inward component (Abramochkin et al. 2014). $I_{K,ACh2}$ also was shown to be activated by M_2R stimulation. This newly discovered current might contribute to the decrease in APA observed in

some fish and amphibians. In the present study, the cholinergic non-excitability phenomenon on atrial myocardium was demonstrated for the first time in zebrafish. The effect of ACh was reversed by atropine, suggesting activation of M_2R receptors. Based on the recent findings from Abramochkin et al. (2014), I speculate that $I_{K,ACh2}$ may be present in zebrafish as well.

5.3. Effects of physostigmine (treatment 2)

A large proportion of pesticides currently in use are AChEIs, including organophosphates and carbamates. Organophosphorus pesticides were first developed in Germany in the 1930s and were initially used as chemical weapons (nerve agents) (Fulton and Key 2001; King and Aaron 2015). They are potent insecticides and have become attractive because of their rapid degradation in the environment. They are now the most widely used classes of insecticides worldwide (Fulton and Key 2001; King and Aaron 2015). AChEIs act by inhibiting synaptic AChE, which normally prevents further downstream neurotransmission by hydrolyzing ACh to acetate and choline. The inactivation of AChE by the binding of organophosphates or carbamates leads to accumulation of ACh at the synapses of all autonomic ganglia, at many autonomically inervated organs, including the heart, at the neuromuscular junction, and at many synapses in the central nervous system (King and Aaron 2015).

Organophosphates and carbamates inhibit AChE by causing phosphorylation or carbamylation of the AChE protein catalytic site (King and Aaron 2015). However, carbamate-AChE bonds spontaneously hydrolyze more rapidly and their effects are

more readily reversible. Although AChEIs are rapidly degraded in the environment, they generally lack target specificity and can be acutely toxic to many nontarget vertebrate and invertebrate species (Fulton and Key 2001). In fish, AChEI pesticides have been shown to cause cardiac developmental abnormalities, as well as rhythm disturbances, including bradycardia and tachyarrhythmias (Lin et al. 2007; Jee et al. 2009; Tryfonos et al. 2009; Simoneschi et al. 2014; Watson et al. 2014; Du et al. 2015; Pamanji et al. 2015). Considering the effects caused by high concentrations of ACh on the atrial action potential (i.e., cholinergic non-excitability) I speculated that AChEIs, which lead to ACh accumulation, would produce comparable changes that may cause acute cardiac depression and subsequent death. Prior to the present study, only one publication reported the effect of an AChEI, paraoxon (5-50 μM), on the atrial action potential morphology of fish (cod, *Gadus morhua*) (Abramochkin et al. 2012). Paraoxon caused significant reduction in APD but did not alter APA, as opposed to high concentrations of ACh.

Before testing the effects of AChEIs commonly used in PEI, this series of experiments first involved investigating the effect of a known and documented AChEI, physostigmine also known as eserine. Physostigmine is the active ingredient of the ordeal bean of Old Calabar in Nigeria (*Physostigma venenosum Balfour*), which was used to determine if individuals were innocent or guilty of some serious misdemeanour in the mid-19th century. It also was the first carbamate isolated by Europeans (Fulton and Key 2001; Proudfoot 2006). The effect of physostigmine on the heart of fish has been documented since at least 1941, when physostigmine was shown to cause bradycardia in hearts of common carp (*Cyprinus carpius*) and tench (*Tinca vulgaris*) (Filippova 1941).

Jullien and Ripplinger (1949) demonstrated that intracoelomic injections of physostigmine in smoothhounds (*Mustelus laevis,* now called *Mustelus mustelus,* which is a type of shark) and blackscorpion fish (*Scorpaena porcus,* which is a teleost) caused a significant increase in acetylcholine concentration in cardiac tissues (as high as six-fold). Physostigmine at a concentration of 50 μM significantly reduced AChE activity in zebrafish embryos (Küster 2005). However, the effect of physostigmine on the atrial action potential of fish had not been investigated prior to my study. My results showed a dramatic suppression of atrial action potentials in all experiments using physostigmine (50 μM) in the presence of a low concentration of ACh (1 μM) acting as a substrate. All action potential parameters including APD 90, APD 50 and APA were suppressed, as seen with cholinergic non-excitability. These dramatic effects were attributed to physostigmine, because a low concentration of ACh (1 μM) only reduced APD 90 and APD 50 and its relative effects on these parameters were smaller (approximately 30% reduction in APD 90 and APD 50).

5.4. Effects of mancozeb and phorate (treatments 3 and 4)

The last step in this series of experiments consisted of testing the effects of acute exposure to two commonly used AChEIs in PEI, mancozeb and phorate at high concentrations (10mg/L or 18.5 μM for mancozeb; 10mg/L or 38.4 μM for phorate). No previous studies were available in adult zebrafish, but concentrations causing 50% mortality (LC_{50}) in zebrafish embryos or other species of fish were reported to be lower than the concentrations used in the present study. For mancozeb, reported 20h LC_{50} in zebrafish embryos was 0.4 mg/L, reported 48h LC_{50} in carp (*Cyprinus carpio*) was 4-24

mg/L, and reported 48h LC_{50} in rainbow trout (*Oncorhynchus mykiss*) was1.9 mg/L (NIH 2017). Reported 96h LC_{50} for phorate included 13 μg/L in rainbow trout (*Oncorhynchus mykiss*), 5 μg/L in largemouth bass (*Micropterus salmoides*) or 280 μg/L in channel catfish (*Ictalarus punctatus*) (NIH 2017). Despite the high concentrations used, the present experiments failed to demonstrate a significant cardiotoxic effect of mancozeb or phorate in zebrafish compared with the effect of ACh at a low concentration (1 μM) alone. However, one could argue that phorate caused a significant reduction in APA compared with baseline (- 11%), which was not observed with ACh (1 μM) alone (- 8%). This slightly greater effect of phorate over ACh is likely not relevant biologically and the effect of phorate is by far not as robust as the effect seen with physostigmine. Moreover the statistically significant reduction in APA observed with phorate did not withstand Bonferroni's correction. I suspect that although mancozeb and phorate have AChE inhibitory properties, they may not be as potent as physostigmine, at least on the atrial myocardium of zebrafish.

5.5. Limitations of the study

The present series of experiments had several limitations, mainly due to technical difficulties and its *in vitro* nature. It was highly challenging to maintain stable atrial impalements during an extended period of time to allow all necessary recordings. Zebrafish cardiomyocytes are small and narrow, and motion due to superfusion or cardiac contractions causes the microelectrode to move out of the cells easily. Attempts to reduce motion were made by using the excitation-contraction uncoupler blebbistatin (10 μM) in order to inhibit cardiac contraction without altering action potentials (Jou et

al. 2010). However, blebbistatin needed to be dissolved in dimethylsulfoxide (DMSO), which caused changes in atrial action potential morphology. The solution I chose for the present work consisted of using a formulation of Tyrode's solution with a minimal calcium concentration in an attempt to decrease contractility and avoid excessive motion.

Our experiments were performed at room temperature (approximately 20 °C) and Tyrode's solution was not continuously gassed. The room temperature, pH and oxygen content of the Tyrode's solution may have varied slightly from one experiment to another, which may have affected action potential parameters as previously demonstrated in fish (Vornanen 2016). However, to limit this problem, Tyrode's solution was always made fresh and action potential parameters obtained after exposure to selected drugs were compared to their own baseline values recorded within an hour prior.

The use of TMS for euthanasia may also have influenced action potential morphology (Ryan et al. 1993). This problem was limited by washing explanted hearts with Tyrode solution for at least 15 min before starting experiments and by comparing action potential parameters to their own baseline values (Roberts and Syme 2016).

All experiments were performed *in vitro* on explanted hearts, removing extrinsic sources of cardiac control (nervous or hormonal). The effects of the pesticides that were used in this work may be modulated by these extrinsic sources of cardiac control and are likely influenced by the bioconcentration and bioaccumulation properties of each

toxicant. The bioconcentration factors (BCFs) of the pesticides we used have not been determined experimentally, but modeled BCFs suggest that physostigmine (average BCF: 35.2) and phorate (average BCF: 183) do not bioaccumulate substantially, whereas mancozeb appears to be very bioaccumulative (average BCF: 49000) (EPA 2017). *In vivo* studies may involve performing electrocardiograms on live and immobilized fish exposed to various pesticides, which raises ethical questions. One option may be to perform electrophysiological studies in euthanized zebrafish while keeping their hearts *in situ* to maintain extrinsic cardiac innervation; however, this approach is a technically difficult one considering the challenges encountered with explanted hearts.

Finally, although zebrafish have many advantages as research models, fish kills in PEI involve other species of fish, which may have different sensitivities to environmental toxicants including AChEIs. A logical approach would be to use zebrafish as research models to identify possible electrophysiological mechanisms to explain fish kills, and then to test whether or not these findings are reproducible in species of fish commonly found in PEI's rivers.

6. Conclusion and future directions

Fish kills are a common phenomenon in PEI and agricultural pesticides are suspected to be responsible for many events. However, a causal relationship is often impossible to demonstrate retrospectively. The present series of experiments aimed to investigate the possible cardiac effects of commonly used pesticides, focusing on the effects of AChEIs including mancozeb and phorate. While I was able to demonstrate the cholinergic non-excitability phenomenon, including suppression of atrial action potential duration and amplitude, for the first time in isolated adult zebrafish hearts exposed to the known AChEI physostigmine, similar toxic effects could not be observed after exposure to high concentrations of mancozeb and phorate.

Future investigations may include testing the effects of mancozeb and phorate on atrioventricular conduction by performing simultaneous recordings of atrial and ventricular actions potentials. Indeed, the atrioventricular junction may be more sensitive to the AChE inhibiting effects of these two pesticides. Because no substantial acute effects were found with these pesticides in the present study, their chronic effects on electrophysiological parameters may be evaluated as well. Other types of AChEIs or other classes of pesticides also may be tested.

Further experiments could also involve characterizing selected Na^+, Ca^{2+} and K^+ currents in isolated zebrafish atrial and ventricular myocytes using patch clamp techniques, before and after exposure to AChEIs or other pesticides. Isolation of cardiomyocytes could be performed using enzymatic dissociation (Brette et al. 2008;

Sander 2013). These experiments could explore the precise ionic basis for the changes in action potential morphology previously identified, such as cholinergic non-excitability. They also could provide further evidence for the mechanisms responsible for the development of cardiac arrhythmogenesis in this context.

7. References

Abramochkin DV, Suris MA, Sukhova GS, Rozenshtraukh LV. 2008. Acetylcholine-induced suppression of electric activity of working myocardium of the cod atrium. Dokl Biol Sci 419:73–76.

Abramochkin DV, Kuz'min VS, Sukhova GS, Rozenshtraukh LV. 2009. The cholinergic non-excitability phenomenon in the atrial myocardium of lower vertebrates. Ross Fiziol Zh Im I M Sechenova 95:573–582.

Abramochkin DV, Kuzmin VS, Sukhova GS, Rosenshtraukh LV. 2010. Cholinergic modulation of activation sequence in the atrial myocardium of non-mammalian vertebrates. Comp Biochem Physiol Part A: Mol Integr Physiol 155:231–236.

Abramochkin DV, Borodinova AA, Rosenshtraukh LV. 2012. Effects of acetylcholinesterase inhibitor paraoxon denote the possibility of non-quantal acetylcholine release in myocardium of different vertebrates. J Comp Physiol B 182:101–108.

Abramochkin DV, Tapilina SV, Vornanen M. 2014. A new potassium ion current induced by stimulation of M2 cholinoreceptors in fish atrial myocytes. J Exp Biol 217:1745–1751.

Antkiewicz DS, Peterson RE, Heideman W. 2006. Blocking expression of AHR2 and ARNT1 in zebrafish larvae protects against cardiac toxicity of 2,3,7,8 tetrachlorodibenzo-*p*-dioxin. Toxicol Sci 94:175–182.

Alday A, Alonso H, Gallego M, Urrutia J, Letamendia A, Callol C, Casis O. 2014. Ionic channels underlying the ventricular action potential in zebrafish embryo. Pharmacol Res 84:26–31.

Arnaout R, Ferrer T, Huisken J, Spitzer K, Stainier DYR, Tristani-Firouzi M, Chi NC. 2007. Zebrafish model for human long QT syndrome. Proc Natl Acad Sci USA 104:11316–11321.

Baker K, Warren KS, Yellen G, Fishman MC. 1997. Defective "pacemaker" current (Ih) in a zebrafish mutant with a slow heart rate. Proc Natl Acad Sci USA 94:4554–4559.

Bauer M, Greenwood SJ, Clark KF, Jackman P, Fairchild W. 2013. Analysis of gene expression in *Homarus americanus* larvae exposed to sublethal concentrations of endosulfan during metamorphosis. Comp Biochem Physiol Part D Genomics Proteomics 8:300–308.

Birt K. 2007. Runoff from potato farms blamed for fish kills on Canadian island. Journal of Soil and Water Conservation 62:136–136.

Bournele D, Beis D. 2016. Zebrafish models of cardiovascular disease. Heart Fail Rev 21:803–813.

Bovo E, Dvornikov AV, Mazurek SR, de Tombe PP, Zima AV. 2013. Mechanisms of Ca^{2+} handling in zebrafish ventricular myocytes. Pflugers Arch - Eur J Physiol 465:1775–1784.

Brette F, Luxan G, Cros C, Dixey H, Wilson C, Shiels HA. 2008. Characterization of isolated ventricular myocytes from adult zebrafish (*Danio rerio*). Biochem Biophys Res Commun 374:143–146.

Brette F, Ben Machado, Cros C, Incardona JP, Scholz NL, Block BA. 2014. Crude oil impairs cardiac excitation-contraction coupling in fish. Science 343:772–776.

Brown DR, Clark BW, Garner LVT, Di Giulio RT. 2015. Zebrafish cardiotoxicity: the effects of CYP1A inhibition and AHR2 knockdown following exposure to weak aryl hydrocarbon receptor agonists. Environ Sci Pollut Res Int 22:8329–8338.

Brown DR, Clark BW, Garner LVT, Di Giulio RT. 2016a. Embryonic cardiotoxicity of weak aryl hydrocarbon receptor agonists and CYP1A inhibitor fluoranthene in the Atlantic killifish (*Fundulus heteroclitus*). Comp Biochem Physiol Part C Toxicol Pharmacol 188:45–51.

Brown DR, Samsa LA, Qian L, Liu J. 2016b. Advances in the study of heart development and disease using zebrafish. J Cardiovasc Dev Dis 3:13.

Campbell K. 2016 Jun 06. Environmentalists, Opposition take aim at Health PEI appointments. CBC News [Internet]. [Updated 2016 Jun 06; accessed 2016 Aug 27]. http://www.cbc.ca/news/canada/prince-edward-island/environmentalists-opposition-take-aim-at-health-pei-appointments-1.3618590

Calloe K, Goodrow R, Olesen S-P, Antzelevitch C, Cordeiro JM. 2013. Tissue-specific effects of acetylcholine in the canine heart. Am J Physiol Heart Circ Physiol 305:66–75.

Chakraborty C, Sharma AR, Sharma G, Lee S-S. 2016. Zebrafish: A complete animal model to enumerate the nanoparticle toxicity. J Nanobiotechnology 14:65.

Chopra SS, Stroud DM, Watanabe H, Bennett JS, Burns CG, Wells KS, Yang T, Zhong TP, Roden DM. 2010. Voltage-gated sodium channels are required for heart development in zebrafish. Circ Res 106:1342–1350.

Chow TL, Daigle JL, Ghanem I, Cormier H. 1990. Effects of potato cropping practices on water runoff and soil erosion. Canadian Journal of Soil Science 70:137–148.

DAF – Department of Agriculture and Fisheries. 2015. Agriculture on Prince Edward Island. Prince Edward Island: Canada. [Updated 2015 Jul; accessed 2016 Aug 27]. http://www.gov.pe.ca/agriculture/AgonPEI

DCLE – Department of Communities, Land and Environment. 2011a. PEI fish kill map. Prince Edward Island: Canada. [Updated 2015 Apr 09; accessed 2016 Jul 31]. https://www.gov.pe.ca/photos/original/2011fshkllMAp.jpg

DCLE – Department of Communities, Land and Environment. 2011b. 1962 to 2011: Island fish kill summary report. Prince Edward Island: Canada. [Updated 2015 Apr 09; accessed 2016 Jul 31]. http://www.gov.pe.ca/photos/original/FWfishkll2011.pdf

DCLE – Department of Communities, Land and Environment. 2015a. 1993-2008 non-domestic pesticide sales. Prince Edward Island: Canada. [Updated 2015 Sept 22; accessed 2016 Aug 27]. https://www.princeedwardisland.ca/sites/default/files/publications/pei_annual_sales_figures_for_non-domestic_pesticides_1993-2008.pdf

DCLE – Department of Communities, Land and Environment. 2015b. 2013-2014 retail (domestic and non-domestic) pesticide sales, summary report. Prince Edward Island: Canada. [Updated 2015 Sept 21; accessed 2016 Aug 27]. https://www.princeedwardisland.ca/sites/default/files/publications/retail_pesticide_sales_report_september_21_2015.pdf

DCLE – Department of Communities, Land and Environment. 2015c. 2013-2014 retail (domestic and non-domestic) pesticide sales, sales data. Prince Edward Island: Canada. [Updated 2015 Sept 22; accessed 2016 Aug 27]. https://www.princeedwardisland.ca/sites/default/files/publications/20132014_retail_pesticide_sales_sales_data.pdf

DCLE – Department of Communities, Land and Environment. 2015d. 2013 Trout River fish kill: preliminary report. Prince Edward Island: Canada. [Updated 2015 Apr 09; accessed 2016 Aug 27]. http://www.gov.pe.ca/photos/original/2013TRfishkillr.pdf

DCLE – Department of Communities, Land and Environment. 2015e. 2014 North River fish kill: preliminary report. Prince Edward Island: Canada. [Updated 2015 Apr 09; accessed 2016 Aug 27]. http://www.gov.pe.ca/photos/original/2014Nriverfishk.pdf

Dlugos CA, Rabin RA. 2010. Structural and functional effects of developmental exposure to ethanol on the zebrafish heart. Alcohol Clin Exp Res 34:1013–1021.

Dobrev D, Voigt N, Nattel S. 2014. Cholinergic and constitutive regulation of atrial potassium channels. In: Zipes DP, Jalife J, editors. Cardiac electrophysiology: from cell to bedside, 6th ed. Philadelphia: Elsevier Saunders. p. 383–391.

Du Z, Wang G, Gao S, Wang Z. 2015. Aryl organophosphate flame retardants induced cardiotoxicity during zebrafish embryogenesis: By disturbing expression of the

transcriptional regulators. Aquat Toxicol 161:25–32.

Dunn AM, Julien G, Ernst WR, Cook A, Doe KG, Jackman PM. 2011. Evaluation of buffer zone effectiveness in mitigating the risks associated with agricultural runoff in Prince Edward Island. Sci Tot Environ 409:868–882.

Edmunds RC, Gill JA, Baldwin DH, Linbo TL, French BL, Brown TL, Esbaugh AJ, Mager EM, Stieglitz J, Hoenig R, Benetti D, Grosell M, Scholtz NL, Incardona JP. 2015. Corresponding morphological and molecular indicators of crude oil toxicity to the developing hearts of mahi mahi. Sci Rep 5:1–18.

Edwards L, Burney JR, Richer G, MacRae AH, 2000. Evaluation of compost and straw mulching on soil-loss characteristics in erosion plots of potatoes in Prince Edward Island, Canada. Agriculture, Ecosystems & Environment 81:217–222.

Ellis LD, Soo EC, Achenbach JC, Morash MG, Soanes KH. 2014. Use of the zebrafish larvae as a model to study cigarette smoke condensate toxicity. PLoS one 9:e115305.

Environment Canada. 2014. Prince Edward Island farmer pleads guilty to federal *Fisheries Act* offences - Court hands down $72,355 penalty. Canada. [Updated 2014 Nov 11; accessed 2016 Aug 27].
https://www.ec.gc.ca/alef-ewe/default.asp?lang=En&n=445E9A39-1

EPA. 2017. United States environmental protection agency. [Accessed 2017 Jan 01].
https://comptox.epa.gov/dashboard/

Farrell AP, Pieperhoff S. 2011. Cardiac anatomy in fishes. In: Farrel AP, editor. Encyclopedia of fish physiology: from genome to environment, volume 2. London: Academic press. p. 998–1005.

Fillipova AG. Action of eserine on the heart of fish. 1941. Byulleten Eksperimental'noi Biologii i Meditsiny 11:428–431.

Fulton MH, Key PB. 2001. Acetylcholinesterase inhibition in estuarine fish and invertebrates as an indicator of organophosphorus insecticide exposure and effects. Environ Toxicol Chem 20:37–45.

Galli GLJ. 2011. Cellular ultrastructure of cardiac cells in fishes. In: Farrel AP, editor. Encyclopedia of fish physiology: from genome to environment, volume 2. London: Academic press. p. 1006–1014.

Genge CE, Lin E, Lee L, Sheng X, Rayani K, Gunawan M, Stevens CM, Li AY, Talab SS, Claydon TW, Hove-Madsen L, Tibbits GF. 2016. The zebrafish heart as a model of mammalian cardiac function. Rev Physiol Biochem Pharmacol 171:99–136.

Gerger CJ, Weber LP. 2015. Comparison of the acute effects of benzo-*a*-pyrene on adult zebrafish (*Danio rerio*) cardiorespiratory function following intraperitoneal injection

versus aqueous exposure. Aquat Toxicol 165:19–30.

Giles W, Noble SJ. 1976. Changes in membrane currents in bullfrog atrium produced by acetylcholine. Journal Physiol 261:103–123.

Gillis TE. 2011. Cardiac excitation-contraction coupling: calcium and the contractile element. In: Farrel AP, editor. Encyclopedia of fish physiology: from genome to environment, volume 2. London: Academic press. p. 1054–1059.

Gilmour RF. Electrophysiology of the heart. 2015. In: Reece WO, editor. Duke's physiology of domestic animals, 13th ed. Ames: Wiley Blackwell.
p. 304–315.

Guardian, The. 2016 Aug 17. Stop fish kills, group urging P.E.I. government. The Guardian [Internet]. [Updated 2016 Aug 23; accessed 2016 Aug 27]. http://www.theguardian.pe.ca/News/Local/2016-08-17/article-4618069/Stop-fish-kills,-group-urging-P.E.I.-government/1

Gordon AM, Regnier M, Homsher E. 2001. Skeletal and cardiac muscle contractile activation: tropomyosin "rocks and rolls". News Physiol Sci 16:49–55.

Gordon RJ, VanderZaag AC, Dekker PA, De Haan R, Madani A. 2011. Impact of modified tillage on runoff and nutrient loads from potato fields in Prince Edward Island. Agricultural Water Management 98:1782–1788.

Gormley KL, Teather KL, Guignion DL. 2005. Changes in salmonid communities associated with pesticide runoff events. Ecotoxicology 14:671–678.

Guignion DL, Dupuis T, Teather KL, MacFarlane R. 2010. Distribution and abundance of salmonids in Prince Edward Island streams. Northeastern Naturalist 17:313–324.

Harvey RD, Belevych AE. 2003. Muscarinic regulation of cardiac ion channels. Br J Pharmacol 139:1074–1084.

Hassinen M, Paajanen V, Vornanen M. 2008. A novel inwardly rectifying K+ channel, Kir2.5, is upregulated under chronic cold stress in fish cardiac myocytes. J Expl Biol 211:2162–2171.

Hassinen M, Laulaja S, Paajanen V, Haverinen J, Vornanen M. 2011. Thermal adaptation of the crucian carp (*Carassius carassius*) cardiac delayed rectifier current, IKs, by homomeric assembly of Kv7.1 subunits without MinK. Am J Physiol Regul Integr Comp Physiol 301:255–265.

Hassinen M, Haverinen J, Hardy ME, Shiels HA, Vornanen M. 2015. Inward rectifier potassium current (I_{K1}) and Kir2 composition of the zebrafish (*Danio rerio*) heart. Pflugers Arch - Eur J Physiol 467:2437–2446.

Haustein M, Hannes T, Trieschmann J, Verhaegh R, Köster A, Hescheler J, Brockmeier K, Adelmann R, Khalil M. 2015. Excitation-contraction coupling in zebrafish ventricular myocardium is regulated by trans-sarcolemmal Ca^{2+} influx and sarcoplasmic reticulum Ca^{2+} release. PLoS One 10:e0125654.

Hicken CE, Linbo TL, Baldwin DH. 2011. Sublethal exposure to crude oil during embryonic development alters cardiac morphology and reduces aerobic capacity in adult fish. Proc Natl Acad Sci USA 108:7086–7090.
Holck AR, Estep JE, Childress TA.1993. Fish and other aquatic animal kills: causes and relevance to public health for military health care professionals. Mil Med 158: 587–590.

Howe K, Clark MD, Torroja CF, Torrance J, Berthelot C, Muffato M, Collins JE, Humphray S, McLaren K, Matthews L, et al. 2013. The zebrafish reference genome sequence and its relationship to the human genome. Nature 496:498–503.

Hu N, Sedmera D, Yost HJ, Clark EB. 2000. Structure and function of the developing zebrafish heart. Anat Rec 260:148–157.

Hu N, Yost HJ, Clark EB. 2001. Cardiac morphology and blood pressure in the adult zebrafish. Anat Rec 264:1–12.

Incardona JP, Collier TK, Scholz NL. 2004. Defects in cardiac function precede morphological abnormalities in fish embryos exposed to polycyclic aromatic hydrocarbons. Toxicol Appl Pharmacol 196:191–205.

Incardona JP, Carls MG, Teraoka H, Sloan CA, Collier TK, Scholz NL. 2005. Aryl hydrocarbon receptor-independent toxicity of weathered crude oil during fish development. Environ Health Perspect 113:1755–1762.

Incardona JP, Carls MG, Day HL, Sloan CA, Bolton JL, Collier TK, Scholz NL. 2009. Cardiac arrhythmia is the primary response of embryonic pacific herring (*Clupea pallasi*) exposed to crude oil during weathering. Environ Sci Technol 43:201–207.

Incardona JP, Gardner LD, Linbo TL, Brown TL, Esbaugh AJ, Mager EM, Stieglitz JD, French BL, Labenia JS, Laetz CA, Tagal M, Sloan CA, Elizur A, Benetti DD, Grosell M, Block BA, Scholtz NL. 2014. Deepwater Horizon crude oil impacts the developing hearts of large predatory pelagic fish. Proc Natl Acad Sci USA 111:1510–1518.

Incardona JP, Carls MG, Holland L, Linbo TL, Baldwin DH, Myers MS, Peck KA, Tagal M, Rice SD, Scholz NL. 2015. Very low embryonic crude oil exposures cause lasting cardiac defects in salmon and herring. Sci Rep 5:13499.

INERIS. 2017. Institut National de l'Environement Insustriel et des Risques. Portail substances chimiques. [Accessed 2017 Feb 12].
http://www.ineris.fr/substances/fr/search/result

Jatoe JBD, Yiridoe EK, Weersink A, Stephen Clark J. 2008. Economic and

environmental impacts of introducing land use policies and rotations on Prince Edward Island potato farms. Land Use Policy 25:309–319.

Jee JH, Koo JG, Keum YH, Park KH. 2009. Effects of dibutyl phthalate and di-ethylhexyl phthalate on acetylcholinesterase activity in bagrid catfish, Pseudobagrus fulvidraco (Richardson). J Appl Ichthyol 25 :771–775.

Johnston CE, Cheverie JC. 1980. Repopulation of a coastal stream by brook trout and rainbow trout after endosulfan poisoning. The Progressive Fish-Culturist 42:107–110.

Jost N. 2005. Restricting excessive cardiac action potential and QT prolongation: A vital role for I_{Ks} in human ventricular muscle. Circulation 112:1392–1399.

Jou CJ, Spitzer KW, Tristani-Firouzi M. 2010. Blebbistatin effectively uncouples the excitation-contraction process in zebrafish embryonic heart. Cell Physiol Biochem 25:419–424.

Jullien A, Ripplinger J. 1949. L'acétylcholine chez quelques poisons marins. Ses variations par l'emploi des cholinestérases. Ann Scient et Litt de Franche Comté.

Jung J-H, Hicken CE, Boyd D, Anulacion BF, Carls MG, Shim WJ, Incardona JP. 2013. Geologically distinct crude oils cause a common cardiotoxicity syndrome in developing zebrafish. Chemosphere 91:1146–1155.

Kepplinger KJ, Kahr H, Förstner G, Sonnleitner M, Schindler H, Schmidt T, Groschner K, Soldatov NM, Romanin C. 2000. A sequence in the carboxy-terminus of the alpha(1C) subunit important for targeting, conductance and open probability of L-type Ca(2+) channels. FEBS Lett 477:161–169.

Kikuchi K. 2014. Advances in understanding the mechanism of zebrafish heart regeneration. Stem Cell Res 13:542–555.

Kikuchi K. 2015. Dedifferentiation, transdifferentiation, and proliferation: mechanisms underlying cardiac muscle regeneration in zebrafish. Curr Pathobiol Rep 3:81–88.

King AM, Aaron CK. 2015. Organophosphate and carbamate poisoning. Emerg Med Clin North Am 33:133–151.

Küster E. 2005. Cholin- and carboxylesterase activities in developing zebrafish embryos (*Danio rerio*) and their potential use for insecticide hazard assessment. Aquat Toxicol 75:76–85.

La VT, Cooke SJ. 2011. Advancing the science and practice of fish kill investigations. Reviews in Fisheries Science 19:21–33.

Langheinrich U, Vacun G, Wagner T. 2003. Zebrafish embryos express an orthologue of

HERG and are sensitive toward a range of QT-prolonging drugs inducing severe arrhythmia. Toxicol Appl Pharmacol 193:370–382.

Lema SC, Schultz IR, Scholz NL, Incardona JP, Swanson P. 2007. Neural defects and cardiac arrhythmia in fish larvae following embryonic exposure to 2,2',4,4'-tetrabromodiphenyl ether (PBDE 47). Aquat Toxicol 82:296–307.

Leary S, Underwood W, Anthony R, Cartner S, Corey D, Grandin T, Greenacre C, Gwaltney-Brant S, McCrackin M, Meyer R, Miller D, Shearer J, Yanong R. 2013. AVMA guidelines for the euthanasia of Animals: 2013 edition.

Leong IUS, Skinner JR, Shelling AN, Love DR. 2010. Zebrafish as a model for long QT syndrome: the evidence and the means of manipulating zebrafish gene expression. Acta Physiol 199 :257–276.

Lin CC, Hui MNY, Cheng SH. 2007. Toxicity and cardiac effects of carbaryl in early developing zebrafish (*Danio rerio*) embryos. Toxicol Appl Pharmacol 222:159–168.

López-Olmeda JF, Sánchez-Vázquez FJ. 2011. Thermal biology of zebrafish (*Danio rerio*). Journal of Thermal Biology 36:91–104.

Macphail Woods Ecological Forestry Project. 2013. Overview of fish kills on PEI 1962-2011. Charlottetown: Canada. [Updated 2013 Feb 14; accessed 2016 Jul 31]. http://www.macphailwoods.org/wp-content/uploads/2013/02/History-of-Fish-Kills-PEI-.pdf

Matthews M, Varga ZM. 2012. Anesthesia and euthanasia in zebrafish. ILAR J 53: 192-204.

McCarthy E. 2016a Aug 23. Fish kill. The Guardian [Internet]. [Updated 2016 Aug 23; accessed 2016 Aug 27]. http://www.theguardian.pe.ca/photo/Fish-kill-3138124

McCarthy E. 2016b Aug 22. Officials investigating fish kill in Roseville, P.E.I. The Guardian [Internet]. [Updated 2016 Aug 22; accessed 2016 Aug 27]. http://www.theguardian.pe.ca/News/Local/2016-08-22/article-4621586/Officials-investigating-fish-kill-in-Roseville,-P.E.I./1

Mersereau EJ, Poitra SL, Espinoza A, Crossley DA, Darland T. 2015. The effects of cocaine on heart rate and electrocardiogram in zebrafish (*Danio rerio*). Comp Biochem Physiol Part C Toxicol Pharmacol 172-173:1–6.

Meyer FP, Barclay LA. 1990. Field manual for the investigation of fish kills. In: Resource Publication 177. Washington D.C.: U.S. Fish and Wildlife Service. p. 1-120.

Molina CE, Gesser H, Llach A, Tort L, Hove-Madsen L. 2007. Modulation of membrane potential by an acetylcholine-activated potassium current in trout atrial

myocytes. Am J Physiol Regul Interg Comp Physiol 292:388–395.

Muñoz MJ, Castaño A, Blazquez T, Vega M, Carbonell G, Ortiz JA, Carballo M, Tarazona JV. 1994. Toxicity identification evaluations for the investigation of fish kills: A case study. Chemosphere 29:55–61.

Mutch JP. Savard MA, Julien GRJ, MacLean B, Raymond BG, Doull J. 2002. Pesticide monitoring and fish kill investigations on Prince Edward Island, 1994–1999. In: D.K. Cairns (ed). Effects of land use practices on fish, shellfish, and their habitats on Prince Edward Island. Canadian Technical Report of Fisheries and Aquatic Sciences 2408:94–115.

NCBI. 2017. National Center for Biotechnology Information. Pubchem database. [Accessed 2017 Feb 10].
https://pubchem.ncbi.nlm.nih.gov

NDP PEI. 2013. Time to end fish kills. Prince Edward Island: Canada. [Updated 2013 Aug 13; accessed 2016 Jan 26].
http://www.ndppei.ca/time-to-end-fish-kills/

Nemtsas P, Wettwer E, Christ T, Weidinger G, Ravens U. 2010. Adult zebrafish heart as a model for human heart? An electrophysiological study. J Mol Cell Cardiol 48:161–171.

Newton CM. 2010. Cardiac innervation in Goldfish (*Carassius Auratus*) and Zebrafish (*Danio Rerio*) (dissertation). Dalhousie University. 185 p.

Newton CM, Stoyek MR, Croll RP, Smith FM. 2013. Regional innervation of the heart in the goldfish, Carassius auratus: A confocal microscopy study. J Comp Neurol 522:456–478.

NIH. 2017. U.S. National Library of Medicine. Toxnet toxicology data network. [Accessed 2017 Jan 01].
https://toxnet.nlm.nih.gov

Nilsson S. 2011. Autonomic nervous system in fishes. In: Farrel AP, editor. Encyclopedia of fish physiology: from genome to environment, volume 1. London: Academic press. p. 80–88.

Novak AE, Taylor AD, Pineda RH, Lasda EL, Wright MA, Ribera AB. 2006.

Embryonic and larval expression of zebrafish voltage-gated sodium channel α-subunit genes. Dev Dyn 235:1962–1973.

Opie LH, Bers DM. 2004. Excitation-contraction coupling and calcium. In: Opie LH. Heart physiology: from cell to circulation, 4th edition. Philadelphia: Lippincott Williams & Wilkins. p. 159-185.

Panáková D, Werdich AA, MacRae CA. 2010. Wnt11 patterns a myocardial electrical gradient through regulation of the L-type Ca^{2+} channel. Nature 466:874–878.

Pamanji R, Bethu MS, Yashwanth B, Leelavathi S, Venkateswara Rao J. 2015. Developmental toxic effects of monocrotophos, an organophosphorous pesticide, on zebrafish (*Danio rerio*) embryos. Environ Sci Pollut Res 22:7744–7753.

Plavicki J, Hofsteen P, Peterson RE, Heideman W. 2013. Dioxin inhibits zebrafish epicardium and proepicardium development. Toxicol Sci 131:558–567.

Post G, Leasure RA. 1974. Sublethal effect of malathion to three salmonid species. Bull. Environ Toxicol Chem 12:312–319.

Postlethwait JH, Yan YL, Gates MA, Horne S, Amores A, Brownlie A, Donovan A, Egan ES, Force A, Gong Z, Coutel C, Fritz A, Kelsh R, Knapic E, Liao E, Paw B, Ransom D, Singer A, Thomson M, Abduljabbar TS, Yelick P, Beier D, Joly JS, Larhammar D, Rosa F, Westerfield M, Zon LI, Johnson SL, Talbot WS. 1998. Vertebrate genome evolution and the zebrafish gene map. Nat Genet 18:345–349.

Proudfoot A. 2006. The early toxicology of physostigmine: a tale of beans, great men and egos. Toxicol Rev 25:99–138.

Purcell LA, Giberson DJ. 2007. Effects of an azinphos-methyl runoff event on macroinvertebrates in the Wilmot River, Prince Edward Island, Canada. Can Entomol 139:523–533.

Raimondo S, Jackson CR, Krzykwa J, Hemmer BL, Awkerman JA, Barron MG. 2014. Developmental toxicity of Louisiana crude oil-spiked sediment to zebrafish. Ecotoxicol Environ Saf 108:265–272.

Renaudon B, Bois P, Bescond J, Lenfant J. 1997. Acetylcholine modulates I(f) and IK(ACh) via different pathways in rabbit sino-atrial node cells. J Mol Cell Cardiol 29:969–975.

Roberts JR, Reigart JR. 2013. Recognition and management of pesticide poisonnings, 6th ed. Washington: EPA. 272 p.

Roberts JC, Syme DA. 2016. Effects of using tricaine methanesulfonate and metomidate before euthanasia on the contractile properties of rainbow trout (*Oncorhynchus mykiss*) myocardium. J Am Assoc Lab Anim Sci 55:565–569.

Rozenshtraukh LV, Kholopov AV. 1975. Role of the vagus nerves in the origin and cessation of atrial tachyarrhythmias. Kardiologiya 15:38–48.

Ryan SN, Davie PS, Gesser H, Wells R. 1993. The effect of MS-222 on paced ventricle strips and the perfused heart of rainbow trout, *Oncorhyncus mykiss*. Comp Biochem

Physiol 106C: 549–553.

Saito T. 1973. Effects of vagal stimulation on the pacemaker action potentials of carp heart. Comp Biochem Physiol A Comp Physiol 44:191–199.

Sander V, Suñe G, Jopling C, Morera C. 2013. Isolation and in vitro culture of primary cardiomyocytes from adult zebrafish hearts. Nat Protoc 8:800–809.

Santer RM. 1985. Morphology and innervation of the fish heart. Adv Anat Embryol Cell Biol 89:1–102.

Saunders JW. 1969. Mass mortalities and behaviour of brook trout and juvenile Atlantic salmon in a stream polluted by agricultural pesticides. J Fish Res Bd Canada 26:695–699.

Sarmah S, Marrs JA. 2016. Zebrafish as a vertebrate model system to evaluate effects of environmental toxicants on cardiac development and function. Int J Mol Sci 17.

Scholz EP, Niemer N, Hassel D, Zitron E, Bürgers HF, Bloehs R, Seyler C, Scherer D, Thomas D, Kathöfer S, et al. 2009. Biophysical properties of zebrafish ether-à-go-go related gene potassium channels. Biochem Biophys Res Commun 381:159–164.

Scott JA, Incardona JP, Pelkki K, Shepardson S, Hodson PV. 2011. AhR2-mediated, CYP1A-independent cardiovascular toxicity in zebrafish (*Danio rerio*) embryos exposed to retene. Aquat Toxicol 101:165–174.

Shiels HA. 2011. Cardiac excitation-contraction coupling: routes of cellular calcium flux. In: Farrel AP, editor. Encyclopedia of fish physiology: from genome to environment, volume 2. London: Academic press. p. 1045–1053.

Sidi S, Busch-Nentwich E, Friedrich R, Schoenberger U, Nicolson T. 2004. *gemini* encodes a zebrafish L-type calcium channel that localizes at sensory hair cell ribbon synapses. J Neurosci 24:4213–4223.

Singleman C, Holtzman NG. 2012. Analysis of postembryonic heart development and maturation in the zebrafish, *Danio rerio*. Dev Dyn 241:1993–2004.

Simoneschi D, Simoneschi F, Todd NE. 2014. Assessment of cardiotoxicity and effects of malathion on the early development of zebrafish (Danio rerio) using computer vision for heart rate quantification. Zebrafish 11:275–280.

Spears J, Kamunde C, Stevens ED. 2014. Effect of TRIS and bicarbonate as buffers on anesthetic efficacy of tricaine methane sulfonate in zebrafish (*Danio rerio*). Zebrafish 11:590–596.

Stoyek MR, Croll RP, Smith FM. 2015. Intrinsic and extrinsic innervation of the heart in zebrafish (*Danio rerio*). J Comp Neurol 523:1683–1700.

Stoyek MR, Quinn TA, Croll RP, Smith FM. Zebrafish heart as a model to study the integrative autonomic control of pacemaker function. Am J Physiol Heart Circ Physiol. *In press*.

Ten Eick R, Nawrath H, McDonald TF, Trautwein W. 1976. On the mechanism of the negative inotropic effect of acetylcholine. Pflugers Arch - Eur J Physiol 361:207–213.

Tessadori F, van Weerd JH, Burkhard SB, Verkerk AO, de Pater E, Boukens BJ, Vink A, Christoffels VM, Bakkers J. 2012. Identification and functional characterization of cardiac pacemaker cells in zebrafish. PLoS one 7:e47644.

Tryfonos M, Papaefthimiou C, Antonopoulou E, Theophilidis G. 2009. Comparing the inhibitory effects of five protoxicant organophosphates (azinphos-methyl, parathion-methyl, chlorpyriphos-methyl, methamidophos and diazinon) on the spontaneously beating auricle of *Sparus aurata*: An in vitro study. Aquat Toxicol 94:211–218.

Tsai CT, Wu CK, Chiang FT, Tseng CD, Lee JK, Yu CC, Wang YC, Lai LP, Lin JL, Hwang JJ. 2011. In-vitro recording of adult zebrafish heart electrocardiogram - a platform for pharmacological testing. Clin Chim Acta 412:1963–1967.

Van Scoy AR, Tjeerdema RS. 2014. Environmental fate and toxicology of chlorothalonil. Rev Environ Contam Toxicol 232:89–105.

Van Leeuwen CJ, Griffioen PS, Vergouw WHA, Maas-Diepeveen JL. 1985. Differences in susceptibility of early life stages of rainbow trout (*Salmo gairdneri*) to environmental pollutants. Aquat Toxicol 7:59–78.

Verkerk AO, Remme CA. 2012. Zebrafish: a novel research tool for cardiac (patho)electrophysiology and ion channel disorders. Front Physiol 3:255.

Vornanen M. 2016. The temperature dependence of electrical excitability in fish hearts. J Exp Biol 219:1941–1952.

Vornanen M, Hassinen M. 2016. Zebrafish heart as a model for human cardiac electrophysiology. Channels (Austin) 10:101–110.

Warren KS, Baker K, Fishman MC. 2001. The *slow mo* mutation reduces pacemaker current and heart rate in adult zebrafish. Am J Physiol Heart Circ Physiol 281:1711–1719.

Watson FL, Schmidt H, Turman ZK, Hole N, Garcia H, Gregg J, Tilghman J, Fradinger EA. 2014. Organophosphate pesticides induce morphological abnormalities and decrease locomotor activity and heart rate in *Danio rerio* and *Xenopus laevis*. Environ Toxicol Chem 33:1337–1345.

White R, Rose K, Zon L. 2013. Zebrafish cancer: the state of the art and the path forward. Nat Rev Cancer 13:624–636.

Wythe JD, Jurynec MJ, Urness LD, Jones CA, Sabeh MK, Werdich AA, Sato M, Yost HJ, Grunwald DJ, MacRae CA, et al. 2011. Hadp1, a newly identified pleckstrin homology domain protein, is required for cardiac contractility in zebrafish. Dis Model Mech 4:607–621.

WHO – World Health Organization. The top 10 causes of death. [Updated 2017 Jan; accessed 2017 Feb 08].

Wu C, Sharma K, Laster K, Hersi M, Torres C, Lukas TJ, Moore EJ. 2014. Kcnq1-5 (Kv7.1-5) potassium channel expression in the adult zebrafish. BMC Physiol 14:1.

Yarr K. 2016 Aug 26. More than 900 dead fish collected after fish kill. CBC News [Internet]. [Updated 2016 Aug 26; accessed 2016 Aug 27]. http://www.cbc.ca/news/canada/prince-edward-island/miminegash-fish-kill-pei-1.3736644

Zaccone G, Marino F, Zaccone D. 2011. Intracardiac neurons and neurotransmitters in fish. In: Farrel AP, editor. Encyclopedia of fish physiology: from genome to environment, volume 2. London: Academic press. p. 1067–1072.

Zhang C, Miki T, Shibasaki T, Yokokura M, Saraya A, Seino S. 2006. Identification and characterization of a novel member of the ATP-sensitive K^+ channel subunit family, Kir6.3, in zebrafish. Physiol Genomics 24:290–297.

Zhang P-C, Llach A, Sheng XY, Hove-Madsen L, Tibbits GF. 2011. Calcium handling in zebrafish ventricular myocytes. Am J Physiol Regul Integr Comp Physiol. 300:56–66.

8. Annexes: raw data tables

	Baseline										ACh 1 µM									
Exp 1	108,24	110,82	110,82	109,53	109,53	109,21	109,21	109,21	109,53	109,53	93,421	93,421	94,71	94,71	93,099	93,421	94,065	94,388	94,065	94,388
Exp 2	98,575	98,575	98,575	97,931	98,575	98,253	97,931	98,253	98,575	99,22	94,387	94,71	94,71	94,065	94,387	94,71	94,71	94,387	94,71	95,032
Exp 3	107,27	107,6	107,6	107,6	107,6	107,6	107,6	107,27	107,27	107,27	94,71	94,71	95,032	95,032	95,354	95,354	94,71	94,388	94,065	95,676
Exp 4	101,8	101,8	101,47	101,8	101,8	101,8	102,12	102,12	101,8	101,47	90,844	90,844	90,522	90,844	90,844	91,166	91,166	91,166	90,522	90,844
Exp 5	102,76	103,41	103,41	103,73	103,73	105,02	105,66	105,02	104,05	103,73	105,34	105,66	105,34	105,02	105,34	105,34	105,02	105,34	105,02	105,34

APA Treatment 1a

	Baseline										ACh 1 µM									
Exp 1	140,5	141,0	141,1	140,7	140,9	141,9	141,8	141,0	141,4	141,1	133,6	131,5	134,5	135,7	131,6	134,7	134,7	135,1	135,4	136,0
Exp 2	148,4	146,6	147,6	146,3	149,9	149,0	148,8	147,6	148,3	146,4	101,9	102,1	102,9	102,1	103,5	103,4	103,3	102,0	103,2	102,6
Exp 3	158,0	158,2	159,8	157,0	158,2	158,0	157,8	157,3	157,6	157,1	109,4	108,5	110,9	109,0	110,2	108,7	110,4	110,1	106,2	110,1
Exp 4	136,7	138,3	138,3	137,5	137,6	138,0	138,1	137,2	137,6	136,6	87,9	89,4	87,4	87,5	88,4	88,7	89,4	88,1	86,6	88,0
Exp 5	128,1	127,6	127,5	128,3	128,1	128,6	128,7	128,4	127,6	128,3	96,8	97,3	96,8	96,8	96,4	96,0	96,6	97,0	96,1	96,6

APD 90 Treatment 1a

	Baseline										ACh 1 µM									
Exp 1	119,9	119,1	119,9	119,5	119,1	119,9	119,9	119,9	119,8	119,7	112,1	109,7	112,1	112,4	110,2	112,5	113,0	112,7	113,2	113,7
Exp 2	112,4	111,6	112,1	111,5	111,1	112,1	111,1	112,3	112,0	111,5	69,5	69,2	69,5	69,4	69,9	70,0	69,6	69,9	69,9	69,7
Exp 3	132,3	131,8	133,6	131,6	131,8	131,7	131,4	131,4	131,6	131,2	78,2	78,2	78,2	77,0	78,3	76,9	78,5	77,9	75,9	77,8
Exp 4	114,5	115,1	114,8	114,8	114,8	114,6	114,6	114,6	114,6	114,6	60,9	61,7	61,2	61,2	62,1	61,5	61,6	61,7	61,0	59,9
Exp 5	109,4	109,5	109,5	109,7	109,6	109,8	109,3	109,9	109,5	109,8	71,4	71,3	71,2	71,1	71,0	71,1	71,2	71,2	71,0	71,5

APD 50 Treatment 1a

	Baseline										ACh 10 µM										Washing									
Exp 1	90,8	84,7	84,1	88,6	89,2	84,1	92,5	92,5	92,1	92,1	57,3	46,7	54,4	55,7	59,0	56,7	57,0	58,0	58,0	61,5	73,1	68,3	74,1	74,1	73,4	73,4	68,9	74,4	74,4	71,8
Exp 2	102,8	103,1	102,4	103,1	102,4	103,4	103,4	102,8	103,4	103,4	81,2	82,1	82,1	81,5	81,5	81,8	82,1	81,8	81,8	82,1	87,6	87,6	87,9	87,9	88,3	88,3	87,6	88,6	88,6	87,9
Exp 3	104,4	104,4	103,7	97,9	108,9	108,9	103,1	104,1	103,7	102,4	87,3	92,1	92,8	93,7	93,4	97,9	98,6	87,9	95,0	95,0	97,3	97,9	92,1	98,6	98,6	99,5	97,3	97,6	98,3	100,2
Exp 4	81,5	80,9	81,2	79,2	84,1	84,1	82,1	83,1	80,2	80,5	54,1	57,3	57,3	53,2	52,5	55,1	57,7	56,1	57,3	54,1	94,1	96,0	96,6	94,4	94,4	93,4	95,0	96,3	96,3	95,0
Exp 5	101,2	101,2	101,8	101,5	100,5	101,2	102,1	98,3	100,5	100,5	96,0	97,9	98,6	96,3	97,6	97,0	95,0	96,3	96,3	97,0	101,8	102,1	102,1	101,8	101,5	103,1	102,8	102,4	102,4	102,1
Exp 6	83,8	82,5	83,4	82,1	82,5	83,1	82,5	81,5	82,8	81,2	46,1	46,4	48,3	48,3	45,7	45,7	45,1	47,0	46,4	46,4	71,5	71,5	70,9	71,5	75,4	74,7	70,2	70,2	68,9	98,7

APA Treatment 1b

	Baseline										ACh 10 µM										Washing									
Exp 1	95,3	92,5	92,1	95,6	93,9	92,1	93,3	93,0	96,8	96,7	31,4	24,2	28,8	28,1	32,3	30,9	32,2	30,3	32,0	35,0	45,6	39,6	48,0	41,7	46,8	43,5	44,0	48,2	46,5	45,8
Exp 2	115,4	115,4	114,3	115,3	115,9	115,2	119,2	114,9	116,0	116,4	37,1	36,1	35,3	35,8	34,4	35,0	36,0	35,9	36,5	37,2	39,3	39,2	39,6	39,3	39,6	39,4	39,4	41,3	42,2	41,4
Exp 3	74,4	73,5	72,2	66,4	70,1	69,2	69,2	68,8	69,2	66,5	38,3	42,7	42,7	43,8	43,7	50,3	50,7	38,9	45,2	44,2	47,1	45,9	38,5	47,8	46,2	47,5	45,0	46,1	45,5	49,0
Exp 4	127,2	124,6	123,1	121,9	121,2	128,9	120,4	119,8	121,1	124,6	81,0	98,3	87,0	81,6	73,7	78,5	81,9	86,3	78,9	72,2	129,6	128,7	138,2	132,2	132,0	132,1	134,6	134,9	131,4	132,2
Exp 5	107,9	109,2	108,4	109,6	109,9	109,6	108,7	105,6	115,6	107,1	28,3	28,3	29,5	29,9	31,4	29,9	29,5	29,2	28,7	29,1	32,5	36,4	31,9	31,6	32,1	32,0	32,0	33,9	32,6	30,9
Exp 6	176,5	169,4	172,6	172,0	173,2	183,2	181,2	175,1	183,9	173,0	136,9	134,7	129,9	141,3	132,9	130,0	134,8	135,8	123,4	136,4	157,3	156,0	156,2	159,8	149,0	153,5	161,5	159,6	159,5	163,3

APD 90 Treatment 1b

	Baseline									ACh 10 µM										Washing									
Exp 1	77,1	76,0	75,2	78,1	76,5	76,4	74,2	76,0	78,0	78,1	18,4	15,7	17,8	18,1	18,0	17,7	18,5	17,8	18,6	18,8	26,4	24,3	27,2	23,4	26,9	25,0	26,2	27,1	26,8	27,1
Exp 2	98,1	97,6	97,2	97,7	98,2	97,4	97,5	97,9	98,2	98,3	13,0	12,5	12,4	12,7	12,8	12,3	12,5	12,7	12,6	12,6	12,7	13,0	12,8	12,9	13,3	12,9	13,5	12,9	13,5	13,5
Exp 3	51,6	51,2	51,3	50,3	50,5	49,1	50,6	50,3	50,2	49,3	18,9	20,1	20,8	20,7	21,2	21,6	21,6	19,2	20,4	20,4	18,8	18,3	17,4	18,9	18,7	18,7	18,3	18,4	18,7	18,5
Exp 4	100,2	101,8	102,5	101,4	100,8	103,2	100,0	99,5	102,0	102,1	42,4	45,5	41,9	43,4	39,5	43,2	41,9	42,5	38,7	43,6	108,1	106,5	110,2	109,5	109,5	108,4	110,0	111,7	108,6	110,4
Exp 5	81,8	80,8	81,6	81,3	83,9	82,1	81,6	80,8	81,6	80,9	13,6	13,4	13,1	13,4	13,6	13,7	13,2	13,5	13,2	13,4	15,2	15,5	15,2	15,0	15,6	15,2	15,1	15,3	15,2	15,2
Exp 6	109,6	109,6	108,3	108,2	110,1	111,4	108,3	109,9	110,8	109,3	72,1	71,5	67,3	71,4	72,8	69,8	72,9	71,6	71,2	72,4	93,5	94,4	95,7	97,3	95,7	91,5	98,4	94,3	95,7	98,7

APD 50 Treatment 1b

	Baseline										ACh 10 µM										Atropine 1 µM + ACh 10 µM									
Exp 1	120,7	124,3	123,1	119,1	158,9	118,6	120,3	159,5	120,9	157,0	66,4	66,9	67,3	76,7	61,7	68,8	65,8	64,9	53,3	53,7	195,3	194,0	185,8	191,0	193,7	194,1	192,0	195,6	190,6	183,6
Exp 2	120,2	126,8	119,4	122,6	118,3	120,0	123,5	120,6	126,1	119,8	120,6	120,6	121,2	119,9	119,6	121,5	122,3	122,7	122,5	122,0	140,6	179,6	120,6	147,4	142,7	129,5	142,6	141,9	125,3	149,5
Exp 3	137,5	139,2	140,3	138,0	139,1	137,1	136,0	138,0	137,3	137,8	85,0	86,8	85,3	84,4	89,9	85,1	84,8	85,2	86,1	83,8	158,5	159,5	158,5	158,9	159,0	157,8	158,8	158,6	158,7	151,6
Exp 4	83,3	83,6	84,2	83,8	83,0	84,0	83,5	82,5	82,2	82,6	30,9	33,4	30,8	31,6	30,2	31,6	32,3	32,8	32,2	32,2	127,7	130,7	130,6	129,8	130,2	129,3	128,8	128,6	129,6	130,4

APD 90 Treatment 1c

	Baseline									
Exp 1	85,4	84,4	85	85	87	87	85,7	83,4	87,6	87,9
Exp 2	101,8	102,8	102,8	103,1	102,8	102,4	102,8	103,7	104,4	104,4
Exp 3	102,8	102,8	99,5	99,2	99,5	102,1	102,4	100,2	100,8	101,8
Exp 4	78,9	78,9	79,2	78,9	78,6	79,9	79,2	78,9	79,2	78,3
Exp 5	75,7	74,7	74,7	76	76,7	76,3	78,6	78,6	76,3	77

APA Treatment 2

	Baseline									
Exp 1	134,5	131	132	132	132,4	133,2	133,9	135,3	134,3	132,2
Exp 2	152,7	153	153,6	153,7	153,5	152,5	153,3	151,7	153,8	153,5
Exp 3	103,9	101,2	100,8	100,8	100,8	103,2	100,2	102	102,2	102,8
Exp 4	126,3	127,9	126,7	128,1	125,8	126,5	126,2	124,7	125,2	124,5
Exp 5	90,1	90,4	90,3	90,8	91	91,4	95,8	93	90,3	92

APD 90 Treatment 2

	Baseline									
Exp 1	98,0	97,9	98,8	98,2	100,7	99,5	98,9	99,8	102,2	98,2
Exp 2	126,5	126,5	126,4	126,2	126	126,1	125,7	126,1	126,5	126,1
Exp 3	82,9	80,1	79,5	79,6	80,5	83	79,9	80,2	81	82,3
Exp 4	90,9	91,2	89,7	91,4	90,9	91,7	91,2	90,1	90	87,9
Exp 5	65,5	65,7	66,2	67,4	66,6	67,6	67,2	68,2	66,7	67,4

APD 50 treatment 2

	Baseline										Phorate 38.4 µM + ACh 1 µM									
Exp 1	96,3	96,6	96,6	97,3	97,3	98,3	98,6	98,3	98,6	98,6	92,8	93,4	93,7	93,4	93,7	93,7	93,4	93,4	93,7	93,7
Exp 2	88,3	88,3	88,3	88,3	88,3	88,3	87,6	87,9	87,6	87,3	76,7	76,7	77,0	77,0	76,0	76,3	76,7	76,7	76,0	76,0
Exp 3	93,1	93,1	92,8	93,7	92,8	93,7	94,1	94,1	94,1	92,8	95,0	96,0	97,0	97,0	96,3	96,3	96,3	96,6	96,6	97,0
Exp 4	89,9	90,2	91,8	91,8	90,5	90,8	91,5	90,8	89,9	90,5	71,5	72,2	73,1	71,8	71,8	72,2	69,3	70,9	69,6	72,2
Exp 5	100,2	100,2	98,9	98,3	98,3	97,6	97,6	97,3	99,5	100,2	75,7	78,9	78,9	76,3	76,3	78,6	78,6	75,1	78,3	78,3
Exp 6	97,6	98,6	98,9	99,2	98,9	98,3	98,3	98,6	98,9	99,2	91,8	91,8	91,2	91,2	92,1	92,5	92,1	91,5	91,5	91,5

APA Treatment 3

	Baseline										Phorate 38.4 µM + ACh 1 µM									
Exp 1	119,5	119,3	118,2	119,1	119,0	119,5	118,6	120,1	119,4	119,3	77,8	78,5	78,6	78,4	78,4	78,8	78,7	78,7	79,5	79,0
Exp 2	121,0	120,9	122,0	123,5	123,9	124,7	123,3	122,8	121,1	122,4	83,0	82,4	83,1	83,7	82,3	83,0	83,9	84,1	82,8	83,1
Exp 3	116,0	115,0	114,2	115,0	114,7	114,6	115,0	113,6	115,4	114,4	81,4	82,0	81,3	81,9	82,6	81,5	82,2	82,2	82,4	81,9
Exp 4	131,4	130,6	128,0	127,5	126,8	128,6	129,8	130,3	127,0	129,2	56,1	55,0	54,0	57,1	55,9	57,6	55,1	59,7	63,3	57,0
Exp 5	123,3	122,2	119,9	119,4	118,6	119,1	118,7	117,7	123,7	122,2	57,5	57,2	57,0	56,3	56,3	56,5	60,8	59,9	57,2	58,5
Exp 6	127,9	129,6	128,9	129,4	129,6	129,2	128,4	129,4	129,1	130,7	95,8	96,2	96,4	96,0	97,2	96,8	95,9	97,3	96,1	97,9

APD 90 Treatment 3

	Baseline										Phorate 38.4 µM + ACh 1 µM									
Exp 1	102,1	102,1	100,5	102,1	101,7	102,0	100,6	102,7	101,7	102,0	45,7	45,7	45,6	45,8	45,2	45,8	45,6	45,7	45,9	45,4
Exp 2	95,9	96,0	96,3	96,4	96,5	96,3	96,4	96,2	95,8	96,2	49,1	49,5	49,8	49,8	49,3	49,3	50,1	49,9	50,1	49,5
Exp 3	93,0	93,2	93,3	93,3	93,4	93,2	93,2	93,0	93,5	93,1	53,9	53,6	54,1	53,4	54,0	54,2	53,7	54,4	53,9	54,3
Exp 4	98,5	99,0	98,7	98,0	97,5	99,2	97,0	98,5	97,0	98,7	28,0	27,9	27,8	28,8	28,6	27,8	28,6	28,8	29,2	28,9
Exp 5	104,7	103,3	100,5	100,3	99,5	99,8	99,0	98,7	105,0	103,5	24,5	22,7	22,9	24,1	23,1	22,9	24,6	23,6	23,4	23,8
Exp 6	106,0	106,8	106,9	107,0	106,2	106,9	106,6	107,5	106,6	107,1	66,5	67,3	67,2	67,2	67,4	68,0	67,4	67,0	68,2	68,0

APD 50 Treatment 3

	Baseline										Mancozeb 18.5 µM + ACh 1 µM									
Exp 1	87,6	88,6	88,6	87,9	87,9	87,9	87,9	89,2	89,2	88,6	93,1	93,1	92,8	92,5	92,1	92,1	92,1	92,1	92,5	92,5
Exp 2	105,0	106,0	106,6	106,6	107,0	107,0	106,0	105,7	106,6	106,6	103,7	103,4	104,1	104,7	105,0	105,3	105,3	104,7	105,3	105,3
Exp 3	91,8	92,1	92,1	91,5	91,5	91,2	91,2	91,2	91,2	91,8	102,8	104,1	104,1	104,1	104,4	104,4	104,1	104,4	105,0	104,4
Exp 4	107,6	107,6	107,6	107,3	107,6	107,6	107,0	107,3	107,0	107,0	102,4	103,1	103,1	103,1	102,1	102,1	102,1	102,1	102,1	102,1
Exp 5	87,3	89,9	90,5	89,9	90,8	90,5	90,5	91,2	90,8	90,8	109,5	110,2	109,9	109,5	110,2	110,2	109,9	109,9	109,9	109,9
Exp 6	93,4	94,1	94,1	93,7	94,4	94,1	93,7	93,7	93,7	94,1	86,3	86,3	86,7	86,7	86,7	86,3	86,7	86,7	86,3	85,7

APA Treatment 4

	Baseline										Mancozeb 18.5 µM + ACh 1 µM									
Exp 1	90,3	92,9	91,0	91,7	91,3	91,6	91,5	94,6	91,2	90,8	73,2	72,8	73,5	72,7	73,0	72,1	72,4	72,9	72,7	73,3
Exp 2	138,9	143,3	141,4	138,7	145,8	142,2	140,8	142,5	137,4	141,0	136,8	134,1	137,6	136,5	137,4	139,0	139,6	139,3	140,5	138,0
Exp 3	121,6	123,0	123,1	123,0	122,7	121,4	120,6	121,0	120,9	120,6	95,2	93,7	93,6	94,6	94,1	93,6	94,6	93,8	94,7	94,3
Exp 4	131,5	131,7	131,3	130,8	131,8	131,1	130,4	131,4	130,9	130,9	98,5	98,1	98,3	98,4	97,5	95,7	95,9	96,4	97,7	97,7
Exp 5	143,5	146,2	143,7	144,3	143,5	143,6	145,0	144,6	145,5	145,4	134,0	133,8	133,6	133,4	133,7	133,5	133,2	133,3	133,3	133,4
Exp 6	147,4	141,1	146,0	145,5	145,1	143,6	145,8	144,7	143,8	142,6	63,2	63,2	63,6	63,5	63,4	63,0	63,3	63,0	62,6	61,3

APD 90 Treatment 4

	Baseline										Mancozeb 18.5 µM + ACh 1 µM									
Exp 1	71,8	74,6	72,4	72,7	72,3	72,2	72,4	75,5	73,0	72,5	48,2	47,8	48,5	47,9	48,3	47,9	48,1	48,3	47,9	48,1
Exp 2	118,5	121,2	119,9	114,5	122,1	119,1	119,8	120,9	115,2	117,5	115,6	113,2	116,4	115,6	116,2	117,5	118,2	117,8	119,1	115,9
Exp 3	101,8	102,7	102,7	102,8	103,3	101,9	101,3	101,9	101,6	101,5	70,7	70,0	70,0	70,3	70,4	70,4	70,1	70,3	70,6	70,2
Exp 4	108,3	108,3	108,2	108,2	108,7	108,6	108,0	108,1	108,1	108,0	72,7	72,2	72,0	71,9	71,4	70,6	70,5	70,9	71,4	71,3
Exp 5	120,4	122,5	120,6	120,9	120,9	120,8	122,4	120,7	122,2	122,3	114,4	114,3	114,0	113,5	114,2	114,1	113,8	113,7	113,8	114,0
Exp 6	108,8	109,4	108,2	110,4	106,9	107,6	108,5	107,9	107,6	107,6	34,5	34,6	34,4	34,0	33,9	34,2	33,7	34,0	33,4	33,1

APD 50 Treatment 4